UNIVERSITY OF PISA
Dpt. Crop Plant Biology

UNIVERSITY OF TUSCIA
Dpt. Geology and Mechanics, Naturalistic and Hydraulic Engineering for Land

DOCTORATE IN HORTICULTURE
XXII COURSE

Physiological and molecular aspects of flower senescence in *Lilium Longiflorum*

(BIO/04)

COORDINATOR:
Prof. Alberto Graifenberg

SUPERVISORS:
Prof. Nello Ceccarelli
Prof. Piero Picciarelli
Dr. Hilary Rogers

CANDIDATE:
Riccardo Battelli

SUMMARY

ABSTRACT

The flower is the organ involved in plant reproduction and is removed once pollinated or after a given period of time depending from the species. Flower senescence allows resource allocation to developing ovary or to other plant organs. Understanding the underling mechanisms of flower senescence would be extremely useful for improving post-harvest flower quality and longevity. Senescence is certainly an irreversible and programmed event which culminates with cell death and several indications point to this process as a form of programmed cell death (PCD). Physiological and biochemical changes occurring during lily senescence were described. The process of senescence starts three days after flowering, before visible signs of wilting. Mesophyll cell degradation accompanies the appearance of visible signs of senescence and is associated with vacuole permeabilization and rupture. Changes in protein content are accompanied by the increase in total protease activity, caspase-like protease activation, DNA degradation and alteration of the endogenous hormone levels. cDNAs encoding cysteine proteases were isolated from lily tepals and sequenced. The genes codify for KDEL-proteases of 356 aa (LlCyp9 and LlCyp20) belonging to the papain-like family and VPEs of 480 aa (LlVPE4 and LlVPE5) belonging to the legumain family. The expression of LlCyp9 increased during tepal senescence and decreased in completely wilted tissues. Western blotting with an antibody raised against a tomato KDEL-cysteine protease identified homologous proteins in lily tepals. Transient expression of LlCyp9 fused with YFP reporter localized the protease within the ER. LlVPE4 expression was high in tepals form flower bud and opening flower, while decreased during flower senescence. Moreover, VPE activity was detected in crude extracts from lily tepals using a fluorogenic substrate.

ABBREVIATIONS

1-MCP	1-methylcyclopropene
3-AT	3-amino-1,2,4-triazole
3,3-DMCP	3,3-dimethylcyclopropene
ABA	abscisic acid
AEBSF	4-(2-aminoethyl)-benzene-sulfonyl fluoride
APX	ascorbate peroxidase
BSA	bovine serum albumine
CAD	caspase-activated DNase
CAT	catalase
CHAPS	.3-[(3-cholamidopropyl)dimethyllammonio]-1-propanesulfonate
CKs	cytokinins
CP	cyclopropene
CTAB	cetyl trimethyl ammonium bromide
DAPI	4, 6-diamidino-2-25 phenylindole
DFP	diisopropylfluorophosphate
DMSO	dimethyl sulfoxide
DTT	dithiothreitol
ER	endoplasmic reticulum
GAs	gibberellins
GC/MS	gas chromatography/mass spectrometry
GR	glutathione reductase
HEPES	4-2-idroxyethil-1-piperazinil-ethanesulfonic acid
HR	hypersensitive response
IAA	indolacetic acid
IPTG	isopropyl β-D-1thiogalactopyranoside
KV	KDEL-vesicles
LOX	lipoxygenase
L-NAME	NG-nitro-L-arginine mrthyl ester
LRW	London Resin White
PCD	programmed cell death
PSV	protein storage vacuole
ROS	reactive oxygen species
SAG	senescence associated gene

SDS	sodium dodecyl sulfate
SDW	sterile distilled water
SOD	superoxide dismutase
STS	silver thiosulfate
TBARS	thiobarbituric acid reactive substance
TCA	trichloroacetic acid
TEMED	N,N,N',N', tetramethylethylenediamine
TMV	tobacco mosaic virus
TUNEL	TdT-mediated dUTP-biotin nick end labelling
VPE	vacuolar processing enzyme

1. INTRODUCTION

Senescence is a tightly regulated process affecting single cells, organs or the whole plant and eventually leading to death within a developmental program, which allows the plant or the species to survive (Leopold, 1961; Quirino *et al.,* 2000; Lim *et al.,* 2007). During senescence nutrients are recovered through the degradation of macromolecules and transported to other plant parts working like a sink. This recycling mechanism plays a relevant role in determining yield and quality of crop plants.

The limited life span and the existence of an irreversible program largely independent of environmental factors make the flower a useful system for studying the senescence process in plant (Rogers, 2006). Senescence in flower organs has been pointed out as a form of programmed cell death (PCD), a genetically controlled cell death involving a suicide pathway regulated at different levels and associated with well defined and characteristic events (Danon *et al.,* 2000; Rubinstein, 2000; Zhou *et al.,* 2005). Flower senescence is certainly programmed and irreversibly leads to cell death making the distinction between senescence and PCD unnecessary for this system (van Doorn and Woltering, 2004a; Rogers, 2006).

Flowers are the structures responsible for sexual reproduction, and thus play a relevant role in the perpetuation of the earth's most dominant group of plants (Rubinstein, 2000). Plants have often showy and gaudy flowers and produce scents to attract insects and other animals. Most insect-pollinated plants pay their pollinators in energy rich nectar whilst others, including the early spider orchid (*Ophrys sphegodes*), mimic females and promise their pollinators a sexual partner (Ledford, 2007). Despite its irreplaceable ecological role the flower is energetically expensive to maintain beyond its useful life (Ashman and Schoen, 1994). Flower senescence allows the removal of the structures no longer necessary and the redistribution of the nutrients to the growing ovary or to other plant organs. The length of time a flower remains open and functional varies among species from one day to several weeks depending on ecological adaptations. In several species the flowers are long-lived when not pollinated, but show petal wilting, withering or petal abscission soon after pollination. The effect of pollination in promoting senescence doesn't occur in all species and floral longevity can even be increased following pollination-induced flower closure or a pollination-induced change in colour (van Doorn, 1997). The pollination effect seems to be mediated by ethylene. Moreover, ethylene was shown to be involved in senescence of many flowers, which therefore are classified as ethylene-sensitive (Woltering and van Doorn, 1988; van Doorn, 2001). Studies on flower senescence have been often carried out using species like *Petunia*

hybrida, *Dianthus caryophyllus*, and *Mirabilis jalapa* in which flower wilting, withering or abscission are regulated by ethylene (Xu *et al.*, 2007; Hoeberichts *et al.*, 2007; O'Donoghue *et al.*, 2009). However, in several species senescence is not associated with the production of this hormone and ethylene sensitivity is null or very low (Woltering and van Doorn, 1988; van Doorn, 2001). Ethylene-insensitive species include important bulb plants such as *Lilium*, *Narcissus*, *Tulipa*, *Iris*, and *Hemerocallis*. The regulation of flower senescence in ethylene-insensitive flowers has not been clearly understood so far and a role for hormones other than ethylene has been hypothesized but not yet fully demonstrated (Panavas *et al.*, 1998; van der Kop *et al.*, 2003; Hunter *et al.*, 2004).

Although the signals and the translation pathway leading to flower senescence have not been well understood, the events associated with the progression of flower degeneration have been at least partially elucidated in both ethylene-sensitive and ethylene-insensitive species. During senescence of both ethylene-sensitive and -insensitive flowers, marked changes occur in the biochemical and biophysical properties of the cell membranes (Leverenz *et al.*, 2002). Loss of membrane permeability is a typical feature used to determine the onset of senescence through the measurement of the ion leakage (Panavas *et al.*, 1998; Stephenson and Rubinstein, 1998; Hossain *et al.*, 2006). The loss of cellular organization, the degradation of cytoplasm and organelles were observed in several species (Smith *et al*., 1992; O'Donoghue *et al*., 2002; Wagstaff *et al*., 2003). Ultrastructural studies of senescing petals showed the presence of vesicles, cytoplasm, organelles and electron dense structures within the vacuole leading to the conclusion that the autophagic machinery could be implicated (Matile and Winkenbach, 1971; Phillips and Kende, 1980; Smith *et al*., 1992). Recent work strengthens the hypothesis that autophagy may be involved in petal senescence (Shibuya *et al*., 2009a; Shibuya *et al*., 2009b).

Numerous mRNAs are produced during senescence and such production requires intact mechanisms of both translation and post-translational RNA modification (van Doorn and Woltering, 2008). As shown by several molecular studies, the up-regulation of genes involved in cell death regulation and cell dismantling is essential for senescence to occur (Buchanan-Wollaston, 1997). In spite of the key role for mRNA synthesis during developmental cell death and senescence, both RNA and DNA are degraded during these processes. The breakdown of the nucleic acids can take place within the nucleus, mitochondria and plastids by localised enzymes. Nuclear DNA fragmentation in plant cells was observed in nuclei during physiological senescence of seed tissues (Kladnik *et al*., 2004; Lombardi *et al*., 2007a), leaves (Gunawardena *et al*., 2004; Lee and Chen, 2002), flowers

(Orzaez and Granell, 1997; Langson *et al*., 2005; Hoeberichts *et al*., 2005) and other plant organs (Groover *et al*., 1997; Gladish *et al*., 2006). In particular, the appearance of a DNA ladder, due to the internucleosomal fragmentation of nuclear DNA, is considered a typical hallmark of programmed cell death both in animals and plants, even if, in some cases, it may not be detectable in cells showing characteristic apoptotic features. It was reported to occur in petals (Orzaez and Granell, 1997; Yamada *et al*. 2003; Wagstaff *et al*. 2003) and in other plant parts or cultured cells during natural or induced death (Chen and Dickman, 2004; Lombardi *et al*., 2007b; Yakimova *et al*., 2007).

By analogy with animal system, where proteases play an important role in the onset of PCD, it is suggested that the strong up-regulation of a variety of proteases that occur during flower senescence may play a regulatory role (Reid and Chen, 2007). Proteases are also involved in cell dismantling and in the massive remobilization of nutrients. The decrease in protein level in petals has been reported for several plant species and it can be due to a decrease in synthesis as well as an increase in degradation (Stephenson and Rubinstein, 1998; Wagstaff *et al*., 2002; Jones *et al*., 2005; van Doorn and Woltering, 2008). Protein degradation has often been reported to be followed by an increase in protease activity which has been characterized using protease inhibitors (Stephenson and Rubinstein, 1998; Wagstaff *et al*., 2002; Jones *et al*., 2005; Pak and van Doorn, 2005; Lerslerwong *et al*., 2009), leading to the conclusion that newly translated proteinases or proteinase activators could determine the proteolytic activity and that several classes of proteases are active during flower senescence.

In animals, caspases, a class of cysteine protease with specificity towards aspartate, play a prominent role in the initiation as well as in the execution of apoptosis and PCD (Hengartener, 2000; Sanmartin *et al*., 2005; Bonneau *et al*., 2008). In plants, homologues of caspase genes have not been found so far, even if accumulating evidence in recent years suggests the existence of caspase-like activities in tissues undergoing PCD, and protease inhibitors to various mammalian caspases can suppress caspase-like activity and plant cell death (Lam and del Pozo, 2000; De Jong *et al*., 2000; Bozhkov *et al*., 2004; Chichkova *et al*., 2004; Lombardi *et al*., 2007b; Zhang *et al*., 2009). These findings strongly suggest that a true caspase-like activity exists in plants and that it plays a key role within the machinery leading to cell death. Vacuolar processing enzymes (VPEs) and metacaspases are suggested to have a regulatory role, while other proteases such as papain-like cysteine proteases seem to be involved in protein degradation and cell dismantling. Most of these proteases have an optimum activity at an acidic pH pointing to the vacuole as a key player in plant senescence.

Because the balance between import and export of nutrients and the content of macromolecules within the tissue seems to be important in the regulation of senescence, several studies have been made to understand the role of sugars in flower senescence (Yamada *et al*., 2003; Azad *et al*., 2008; Ranwala and Miller, 2009). In fact, for some authors petal senescence may also be due to sugar starvation or sugar accumulation. Sugar starvation may be involved because application of sugars to cut flowers generally delays visible senescence (van Doorn, 2004). Sugar treatments also prevent up-regulation of senescence-associated genes in flowers (Hoeberichts *et al*., 2007). The effect of sugars on senescence has to be elucidated to understand to what extent it is due to a nutritional action rather than to a regulatory and signalling role.

The impact of characterizing programmed cell death in petals allows an understanding of a process crucial to the survival of plants and other plant organs as well as providing economic benefits (Rubinstein, 2000). Elucidating the mechanism underling flower senescence could provide new tools to improve flower vase life and quality.

1.2. EVENTS ASSOCIATED WITH SENESCENCE

1.2.1. Structural and biophysical changes

The maintenance of the cellular organization and compartmentalization is an essential prerequisite so that the cell can survive and carry out its metabolic functions. During senescence cells undergo structural and biochemical changes and gene regulation. The activation of the catalytic machinery allows the recovery of the nutrients accumulated during the growth phase. The earliest and most significant change in leaf cell structure is the breakdown of the chloroplast, the organelle that contains up to 70% of the leaf proteins (Lim *et al*., 2007). What may not be immediately apparent is that the senescence of leaves is not simply concerned with death, but that leaf senescence represents a key developmental phase in the life of both annual and perennial plants which is as ordered and complex as any other phase of development (Buchanan-Wollaston, 1997). The roles of petals and leaves are very different, as are their development and the signalling mechanisms that trigger their senescence (Price *et al*., 2008). However, leaf and flower senescence share several structural and biophysical features. Moreover, a large proportion of remobilization-related genes are up-regulated in both leaf and petals (Price *et al*., 2008).

The petal has a complex structure including different cell types and tissues in which the senescence process is not spatially homogeneous. In several species, mesophyll cells die well

before epidermal cells and visible signs of petal senescence have been associated with mesophyll collapse (O'Donoghue *et al.*, 2002; van Doorn *et al.*, 2003; Wagstaff *et al.*, 2003). In *Gypsophila paniculata* there was no difference in the timing of cell death between mesophyll and epidermal cells, but visible senescence closely correlates with collapse of epidermal cells (Hoeberichts *et al.*, 2005). In *Alstroemeria*, petal senescence starts in the petal margin (Wagstaff *et al.*, 2003), while in tobacco flowers it begins in the proximal part where the abscission will eventually take place (Serafini-Fracassini *et al.*, 2002). In carnation the ultrastructural changes were shown to be asynchronous in the mesophyll tissue as well as in the parenchyma surrounding the vascular tissues (Smith *et al.*, 1992). In some flowers it has been reported that the vascular tissues are the very last to degrade (Matile and Winkenbach, 1971; Wagstaff *et al.*, 2003). This is probably correlated with the need to recover and reallocate nutrients until the late stage of flower senescence. The difference in timing of cell death and degradation makes the understanding of the mechanisms underling flower senescence difficult. Several genes have been shown to be up-regulated during flower senescence, but we do not know in which cells transcription and eventually translation occur.

When plant tissues undergo senescence, cellular membranes progressively lose their organization and changes in the bilayer structure occur leading to impairment of functions. At a biochemical level, loss of membrane lipid phosphate is one of the best documented indices of membrane lipid metabolism during senescence (Thompson *et al,*. 1998). The increasing activity of phospholipases and acyl hydrolases leads to the replacement of phospholipids with neutral lipids. Although the release of electrolytes from senescing tissues is considered a hallmark of membrane degradation and senescence, changes in lipid content and membrane structure occur before the leakage of nutrients is evident (Thompson *et al.*, 1998; Leverentz *et al,*. 2002). The decline of the phospholipids/neutral lipids ratio accompanies the increase in sterol/phospholipids ratio contributing to the reduction of membrane fluidity. Another senescence-associated event that leads to a loss of membrane permeability is the oxidation of existing membrane components (Rubinstein, 2000). The oxidation of membrane fatty acids takes place through two distinct mechanisms: the enzymatic oxidation mediated by lipoxygenase (LOX) and the non-enzymatic autoxidation. In several species an increase of LOX activity was detected during flower senescence. Lipid peroxidation is generally measured as thiobarbituric acid reactive substance (TBARS). In daylily, a short living ethylene-insensitive flower, lipid peroxidation increases from 24 hours before flower opening reaching a peak at 18 hours after flower opening. Lipid peroxidation is followed by an increase in LOX activity before flower opening (Panavas and Rubinstein, 1998b). The

increase in lipid peroxidation and LOX activity was estimated also in ethylene-sensitive species such as rose and carnation (Fobel *et al*., 1987; Bartoli *et al*., 1995; Fukuchi-Mizutani *et al*., 2000). On the contrary, in *Alstroemeria peruviana* LOX activity declined during senescence and loss of membrane function was not related to LOX activity or accumulation of lipid hydroperoxyde (Leverentz *et al*., 2002).

Examples of apoptotic-like morphology are reported to occur during PCD of reproductive cells, in the self-incompatible response, the hypersensitive response (HR), seed development and senescence (Reape and McCabe, 2008). During cell dismantling the nucleus is one of the last organelles to be degraded, even if it undergoes ultrastructural changes (van Doorn and Woltering, 2008). In senescing petals of carnation the nuclei were small, sometimes horseshoe shaped, and with compact nucleoli (Smith *et al*., 1992). Wagstaff *et al*., (2003) reported a reduction of nuclear size in *Alstroemeria* petals and sepals from just before flower opening until the oldest stage, when the nucleus was the only recognizable structure in the cell. These data were confirmed by the reduction of nuclear size observed in *Argyranthemum*, *Petunia* and *Ipomea* (Yamada *et al*., 2006a, b). Blebbing of nuclei, a typical feature often observed in animal cells undergoing PCD, was observed in tobacco senescing petals stained with DAPI or toluidine blue (Serafini-Fracassini *et al*., 2002). Changes in nucleus include also chromatin condensation and fragmentation. If fragmentation results in the formation of DNA masses that do not stay inside the same nuclear envelope, it may be referred to as nuclear fragmentation (Yamada *et al*., 2006b). In *Argyranthemum*, *Petunia* and *Ipomea* petals an increase in the number of DNA masses was observed and was mainly due to nuclear fragmentation (Yamada *et al*., 2006a, b). Conversely, in *Antirrhinum* chromatin clumping into spherical bodies was reported to take place inside the nuclear membrane, therefore a true nuclear fragmentation during senescence was lacking (Yamada *et al*., 2006a).

Several cellular ultrastructural changes have been observed during flower senescence and the role of the vacuole as a lytic compartment has been often emphasized (Matile and Winkenbach, 1970; Phillips and Kende, 1980; Smith *et al*., 1992; Wagstaff *et al*., 2003). Decaying mitochondria, ribosomes and membranes have been found in the vacuole of senescing cells. In *Ipomea purpurea* invaginations of the tonoplast were reported, resulting in the sequestration of cytoplasmic material into the vacuole. Moreover, the invaginations of the tonoplast were connected with the formation of membrane whorls originating from the ER (Matile and Winkenbach, 1970). Numerous small vesicles were found in the cytosol and associated to the forming central vacuole (Matile and Winkenbach, 1970; Phillips and Kende, 1980; Smith *et al*., 1992; van Doorn *et al*., 2003). In *Ipomea* (Matile and Winkenbach, 1970),

carnation (Smith *et al*., 1992) and *Iris* (van Doorn *et al*., 2003) the decrease in the number of small vesicles was associated with the increase in vacuole size. It has been hypothesized that vacuolar space may be generated by small vesicles presumably derived from the swelling of dictyosomes and ER or by the invaginations of cytoplasm (Matile and Winkenbach, 1970; and Kende, 1980; van Doorn *et al*., 2003). The increase in vacuolar size is accompanied by the reduction of cytoplasm to a thin layer and by a decrease in organelle content. Also the amount of rough ER and ribosomes was reported to be considerably reduced (Phillips and Kende, 1980; van Doorn *et al*., 2003). In carnation and *Ipomea*, as the cells approached autolysis the vacuole shrank and the cytoplasm assumed a dilute appearance. The de-compartmentalization was accompanied by the accumulation of a variety of different membranous structures probably due to the enlargement of ER, mitochondria and dictyosomes (Matile and Winkenbach, 1970; Smith *et al*., 1992). Mitochondria, ER cisterns, plastids and nuclei may be observed during various stages of senescence and cell degradation, but at the end of the cellular dismantling the cytoplasm has completely disappeared and the cells are completely collapsed (Matile and Winkenbach, 1970; Phillips and Kende, 1980; Smith *et al*., 1992; Wagstaff *et al*., 2003; van Doorn *et al*., 2003). One of the last events in senescing cells is vacuole rupture, which is probably the direct cause of cellular death (van Doorn and Woltering, 2008). Cell depletion and the loss of wall functions promote the cellular crushing and lead to visible signs of petal senescence. Reduction of wall thickness was reported during flower senescence in *Ipomea tricolor* (Phillips and Kende, 1980). Conversely, in *Alstroemeria* wall thickness was reported to increase, even in the oldest flower (Wagstaff *et al*., 2003), and in Iris tepals it exhibited extensive swelling leading to cell collapse (van Doorn *et al*., 2003). Moreover, in advanced stages of senescence cellular material appeared to be accumulated in the intercellular spaces of *Alstroemeria* and carnation flowers suggesting the disruption of the cells (Smith *et al*., 1980; Wagstaff *et al*., 2003).

1.2.2. Oxidative events

ROS is a collective term that includes both oxygen radicals and certain non-radicals that are oxidizing agents and/or are easily converted into radicals (HOCl, HOBr, O_3, $ONOO^-$, $^1O_2$, and H_2O_2) (Halliwell, 2006). ROS have been shown to have a role in stress-induced and normal senescence in animals and plants and are possible determinants of membrane degradation (Panavas and Rubinstein, 1998). Cells have evolved strategies to utilise ROS as biological signals that control various genetic stress programs (Laloi *et al*., 2004). As H_2O_2 is both an important signalling molecule and a toxic by-product of cell metabolism, its cellular

levels are under tight control (Gechev and Hille, 2005). During flower senescence of *Gladiolus* the level of H_2O_2 increased along with lipid peroxidation (Hossain *et al.*, 2006). A similar pattern was found in natural senescing daylily petals and a bigger increase in H_2O_2 level was reported in petals after treatments that accelerate senescence (Panavas and Rubinstein, 1998). Because of the signalling role and the oxidative stress possibly arising from an imbalance in generation and metabolism of ROS, the plant possesses a defence system in which several enzymes are involved in the protection against deleterious effects. Under normal conditions, ROS are rapidly metabolised with the help of constitutive antioxidant enzymes and other metabolites via non-enzymatic pathways such as antioxidant vitamins, proteins and non-protein thiols (Kotchoni and Gachomo, 2006). Following the observation that high levels of H_2O_2 may be correlated with flower ageing, several studies were made in order to analyze the level and the activity of such scavenging enzymes during flower senescence (Bartoli *et al.*, 1995; Panavas and Rubinstein, 1998; Bailly *et al.*, 2001; Hossain *et al.*, 2006). H_2O_2 is reduced by ascorbate peroxidase (APX) with the consequent oxidation of ascorbate to dehydroascorbate while catalase converts H_2O_2 into H_2O and O_2. Glutathione reductase (GR) reduces glutathione, one of the most important antioxidants. Superoxide dismutase (SOD) is effective in ROS scavenging but produces H_2O_2 which has to be degraded to avoid cell damage. In *Iris* APX and SOD activity decreased by the time the tepals showed wilting, whilst CAT activity increased and GR activity exhibited no change (Bailly *et al.*, 2001). In *Gladiolus* tepals the decrease in APX activity was assumed to be the prerequisite for flower senescence resulting in an increase of the endogenous H_2O_2 level. The increase in SOD activity over the senescing period could be due to the over-expression of genes induced by H_2O_2 accumulation (Hossain *et al.*, 2006). In daylily the decline in APX and CAT activity along with LOX action resulted in high H_2O_2 endogenous levels during senescence (Panavas and Rubinstein, 1998). Natural antioxidants, such as ascorbate, glutathione and α-tocopherol, are also present in flower petals (Rubinstein, 2000). In chrysanthemum petals the activity of antioxidant enzymes increased during the early stage of senescence. The content of α-tocopherol and total thiols increased at the onset of flower senescence and decreased in browning petals (Bartoli *et al.*, 1997). In daylily, the level of ascorbate decreased by 6 h before flower opening. The limiting amount of this reductant could be an important factor in the ability of the remaining APX to reduce H_2O_2 (Panavas and Rubinstein, 1998). In petals, the activity of anti-oxidative enzymes and the level of non-enzymatic antioxidant has been assessed only in vitro and in whole petals, but should be determined in various cells and cell compartments. However, there is at present no conclusive

evidence that ROS are either an early signal or a direct cause of cellular death during petal senescence (van Doorn and Woltering, 2008).

1.2.3. Nucleic acid synthesis and breakdown

Numerous mRNAs are produced during senescence and such production requires intact mechanisms of both translation and post-translational RNA modification (van Doorn and Woltering, 2008). As shown by several molecular studies, the up-regulation of genes involved in cell death and cell dismantling is essential for senescence to occur. It has been postulated for some time that the senescence process may depend on de novo transcription of nuclear genes and molecular studies have shown that this is the case (Buchanan-Wollaston, 1997). Using suppressive subtractive hybridization and microarray analysis, Breeze *et al.* (2004) found that in *Alstroemeria* petals both cell wall related genes and genes involved in metabolism were present in higher proportions in the earlier stages, while genes encoding metal binding proteins were the major component of senescence enhanced libraries. In senescing wallflower petals a large proportion of up-regulated genes were related to the remobilization process (Price *et al.*, 2008). A limiting factor in understanding the mechanism underling flower senescence could be the heterogeneity of the petal tissues with different cells dying at different times. The up-regulation or down-regulation of genes cannot be ascribed to cells at a specific stage of development or senescence but only to the petal tissue.

In spite of the key role of mRNA synthesis during developmental cell death and senescence, both RNA and DNA are degraded during these processes. The breakdown of the nucleic acids can take place within the nucleus, mitochondria and plastids by localised enzymes. In animal cells caspase-activated DNase (CAD) pre-exists in living cells as an inactive complex with an inhibitory subunit. The cleavage of the inhibitory subunit mediated by caspase-3 results in the release and activation of the catalytic subunit responsible of the characteristic DNA laddering (Hengartner, 2000). Although in plants there is no evidence for a protease activated DNase, the degradation of DNA and RNA is also a common feature of the dying cells. In *Petunia inflata* the increase in corolla size and fresh/dry weight ratio until 24 hours after pollination was coupled with the continuous decrease in RNA content (Xu and Hanson, 2000). Molecular changes, therefore, follow compatible pollination despite a healthy appearance of the petal.

TdT-mediated dUTP-biotin nick end labelling (TUNEL) has been a widely used method to assess DNA fragmentation in plants (Orzaez and Granell, 1997; Lee and Chen, 2002; Gunawardena *et al.*, 2004; Hoeberichts *et al.*, 2005; Lombardi *et al.*, 2007). In *Pisum sativum*

petals DNA fragmentation was observed during normal senescence and TUNEL positive nuclei were not detected in cells treated with inhibitors of ethylene (Orzaez and Granell, 1997). In *Gypsophyla paniculata* the DNA degradation became apparent well before visible signs of petal senescence and TUNEL positive nuclei appeared before the increase in ethylene production. The occurrence of TUNEL positive nuclei was stimulated by ethylene treatments but was not prevented by silver thiosulphate (Hoberichts *et al*., 2005). Nuclease activity results in DNA degradation and sometimes in the appearance of the nucleosomal ladder. Often the first step of DNA degradation leads to the formation of high molecular weight fragments (50 – 300 kb) (Nagata *et al*., 2003). Afterwards, through the activation of specific DNase, the internucleosomal cleavage produces 180 bp multiple fragments that look like a ladder when placed on a gel. However, DNA fragmentation into oligonucleosomal units should not be considered as an indicator of PCD without parallel evaluation of morphological changes especially in quickly dying cells. DNA fragmentation can occur in tissues killed by quickly freezing with liquid nitrogen or following homogenization or treatment with Triton-X100 (Kuthanova *et al*., 2008). However, DNA laddering has been detected in several plant tissues and cells undergoing natural or induced death. In *Arabidopsis* roots and maize suspension-cultured cells the exposure to D-Mannose resulted in the characteristic DNA laddering associated with cytochrome c release from mitochondria and with the activation of a DNase in maize cytosolic extract (Stein and Hansen, 1999). Balk *et al*. (2003) identified two different mitochondrially associated pathways for DNA degradation in *Arabidopsis*. One was reported to be associated with the formation of high molecular weight DNA fragments and chromatin condensation. The second one appeared to mediate DNA laddering. This double mechanism resembles the DNA degradation pathway during apoptosis in animals in which the intermembrane- space protein AIF mediates high molecular weight fragmentation and chromatin condensation while the caspase activated DNase CAD leads to DNA laddering. In petals, the oligonucleosomal fragmentation of DNA has been reported in several species while in many others such fragmentation was not observed. This leads to the conclusion that DNA laddering is not a good indicator of programmed cell death and senescence in petals. However, a clear DNA laddering was evident in *Gladiolus hybrid*, *Alstroemeria peruviensis* and *Pisum sativum* (Yamada *et al*. 2003; Wagstaff *et al*. 2003; Orzaez and Granell, 1997). In *Alstroemeria* it was detected from two days after flower opening and increased during the final stages of senescence (Wagstaff *et al*. 2003). In Gladiolus the ladder-like DNA banding was not detected in flowers showing no signs of

senescence, but it became clear in wilting petals 1-3 days after flower opening (Yamada *et al.* 2003).

Several authors focused their attention on the study and characterization of the enzymes responsible for DNA and RNA degradation both in flowers and other tissues. In barley aleurone cells the activity of three nucleases is regulated by gibberellic acid (GA) and abscisic acid (ABA). GA induced and ABA repressed DNA degradation in accordance with programmed cell death progression (Fath *et al*., 1999). Tobacco mosaic virus (TMV) infection triggers a HR leading to cell death. An increase in nuclease activity appeared to occur at a late stage during the cell death process, but nuclear DNA degradation did not involve ladder-like band formation (Mittler and Lam, 1995). *BFN1*, a senescence-associated gene encoding a bifunctional nuclease I enzyme, was cloned and characterized in *Arabidopsis*. High BFN1 mRNA levels were detected in flowers and during leaf and stem senescence (Pérez-Amador *et al*., 2000). The *BFN1* senescence specificity was demonstrated in *Arabidopsis* and tomato plants transformed with *BFN1*-GUS in which a very good association between *BFN1* promoter activation and senescence was observed (Farage-Barhom *et al*., 2008). In daylily petals a cDNA encoding a putative 298 amino acid (aa) nuclease with similarity to P-type endonuclease from *Penicillium* sp. and S1-type nucleases from *Aspergillus oryzae* was isolated. The mRNA level was almost undetectable until flower opening and started to accumulate exponentially during senescence (Panavas *et al*., 1999). Total nuclease activity increased 6 h before flower opening as demonstrated by single strand and double strand DNase activities. The increase in nuclease activity was inhibited by cycloheximide and occurred prematurely after ABA treatments (Panavas *et al*., 2000). These findings suggest a role for ABA during flower senescence and show that nucleases are translated de novo or that a newly synthesized protein regulator is essential for the increase of nuclease activity. RNase activity assays showed that several RNase activities increase in senescing *Petunia inflata* flowers and accompany the decrease of the RNA level. Both single strand and double strand DNase activities were also demonstrated to increase during petal senescence (Xu and Hanson, 2000). PhNUC1 nuclease activity in *Petunia x hybrida* was detected at the last stages of flower senescence. The neutral pH optimum and the activity detected in the nuclear enriched protein fraction suggested that PhNUC1 might be localized within the nucleus (Langston *et al*., 2005).

The increase in RNase and DNase activity is a common feature in senescing petals and is correlated with the extensive degradation of RNA and DNA. The increase in activity is probably due to the activation of pre-existing enzymes but also to the increase in newly

synthesized nucleases or regulator genes as demonstrated by the inhibitor effect of cycloheximide and the increase of the mRNA level of specific enzymes.

1.2.4. Protein degradation and protease activity

Protein degradation plays a crucial role in recycling intracellular damaged proteins or proteins that are no longer necessary and to ensure a constant turnover of macromolecules. Selective protein breakdown takes place in the proteasome, plastids, mitochondria, nucleus, and vacuole and carries out a number of different roles during plant development. At a cellular level it prevents deleterious effects due to the presence of abnormal and non-functional proteins, regulates the activity of metabolic pathways through the modulation of key enzymes and regulates the levels of receptors (Callis, 1995).

During the striking autumnal leaf yellowing of perennial species, the degradation of proteins supplies the woody tissues with nitrogen and amino acids. In annual plans the proteins coming from senescing leaves are imported into the newly formed fruits and seeds. Leaf senescence is accompanied by a change in leaf colour due to chlorophyll loss and results in the death or abscission of the leaf (Yoshida, 2003). Up to 75% of total cellular nitrogen may be located in the chloroplasts of mesophyll cells of C3 plants. Proteolysis of chloroplast proteins begins at an early stage of senescence and the amino acids are exported to growing parts of the plant (Hörtensteiner and Feller, 2002). Autophagy is a recycling system used by eukaryotic cells that utilizes small vesicles to deliver cytosolic proteins and organelles to the vacuole for breakdown. A null mutant for the ATG10 enzyme, an enzyme involved in autophagy, was hypersensitive to nitrogen and carbon starvation and underwent programmed cell death and senescence more quickly than wild type (Phillips *et al.*, 2008). This demonstrates that protein and organelle turnover is essential for the timely progression of senescence in plants.

In flowers the transition from sink to source involves the activation of catabolic pathways allowing the recovery of organic and inorganic compounds. A study on the physiological nature of macromolecule remobilization and its function in *Hemerocallis* flowers showed that vascular tissues remain fully functional after the parenchyma was completely inactive. Furthermore, sucrose was demonstrated to be the main sugar in the phloem exudate and hydroxyproline and glutamine the main amino acids (Bielesky, 1995). During the remobilization processes proteins are involved as executioners, regulators or substrates. The role of protein synthesis and breakdown during flower senescence has been widely studied (Lay-Yee *et al.*, 1992; Jones *et al.*, 1994; Stephenson and Rubinstein, 1998; Wagstaff *et al.*,

2002). The decrease in protein level has been reported for several plant species and it can be due to a decrease in synthesis as well as an increase in degradation (van Doorn and Woltering, 2008). The decrease in protein content may begin before flower opening (Wagstaff *et al.*, 2002; Azeez *et al.*, 2007) or after flower opening (Stephenson and Rubinstein, 1998; Pak and van Doorn, 2005). A rapid decrease in protein level was reported after compatible pollination in *Petunia inflata* (Xu and Hanson, 2000). In *Petunia x hybrida* protein content decreased starting from 4 d after flower opening (Jones *et al.*, 2005). Protein degradation has often been reported to be followed by an increase in protease activity. In daylily the level of proteins in soluble and plastid-enriched fractions was shown to decrease as soon as the flower opened while in the microsomal-enriched fraction it decreased 10 h before flower opening. A sharp increase in protease activity was also observed, reaching a maximum 36 h after flower opening. The inhibition of protease activity using cycloheximide and class-specific protease inhibitors supported the hypothesis that newly translated proteases or protease activators could determine the proteolytic activity and that cysteine, serine and metalloproteinases are active during senescence in daylily (Stephenson and Rubinstein, 1998). A similar increase of protease activity was observed in *Alstroemeria* after flower opening and zymograms conducted with specific inhibitors revealed a major role for cysteine proteases in protein degradation (Wagstaff *et al.*, 2002). Analogous results were obtained in senescing flowers of *Petunia x hybrida* in which the majority of protease activity was due to cysteine proteases (Jones *et al.*, 2005). In *Iris* tepals endoprotease activity increased after flower opening and was drastically reduced by treating the flowers with AEBSF [4-(2-aminoethyl)-benzene-sulfonylfluoride] and DFP (diisopropylfluorophosphate). The reduction was less evident using $ZnCl_2$ and E-64d and null with other protease inhibitors. It was concluded that cysteine, serine proteases and probably metalloproteases are involved close to the maximum of endoprotease activity (Pak and van Doorn, 2005). All these results suggest that several classes of proteolytic enzymes could be involved during flower senescence as executioners and regulators. Moreover, differences in the timing of proteolysis increase and in specific protease activities occur in senescing flowers of different species. Nevertheless, protease activity in vitro does not necessary reflect the in vivo situation. The diversity of intracellular spaces in which proteolysis occurs, the diversity of proteolytic activities and pathways present in cells, and the relatively low level of proteinase activities complicates the elucidation of the mechanisms degrading proteins (Callis, 1995).

Subtractive hybridization and microarray technology have been used to identify the genes involved in flower senescence. Data derived from the use of these techniques are in

accordance with the predominant role of the catabolic metabolism and confirm that protein degradation is an important event during the senescence programme. Genes putatively associated with signal transduction, remobilization of phospholipids, proteins and cell wall compounds were found to be related to the final stage of senescence in *Iris* tepals (van Doorn *et al*., 2003). Likewise, in *Alstroemeria*, *Mirabilis jalapa* and *Dianthus caryophyllus* genes related to signalling, transport, carbohydrate metabolism, defence and protein degradation were reported to be up-regulated in senescing flowers (Breeze *et al*., 2004; Xu *et al*., 2007). In *Ipomea nil* three cysteine protease genes were up-regulated during senescence together with other senescence associated genes (SAGs).

1.2.5. Ubiquitin-proteasome pathway

The ubiquitin-proteasome pathway is used by all eukaryotes for protein degradation in the cytoplasm and nucleus. This degradation system ensures the turnover of misfolded and damaged proteins and controls numerous regulatory proteins involved in several biosynthetic pathways (Vierstra, 2003; Moon *et al*., 2004). Ubiquitin-mediated proteolysis can regulate hormone biosynthesis, transport and perception. Targeted degradation of proteins may also affect downstream transcriptional regulation of hormone-responsive genes in the auxin, gibberellin, abscisic acid, ethylene and jasmonate signalling pathways (Dreher and Callis, 2007).

The activation of ubiquitin's C-terminal Gly by linkage to a Cys residue of ubiquitin activating enzyme (E1) is the first step for ubiquitination of substrate proteins. Afterwards, the activated ubiquitin is transferred to a Cys residue of a ubiquitin-conjugating enzyme (E2) and then to the substrate to form an isopeptide bond to a Lys residue with the help of another factor, a ubiquitin-protein ligase (E3) (Bachmair *et al*., 2001). Ubiquitination may lead to different consequences for the substrate protein depending on the form of ubiquitin modification. The most common fate for ubiquitinated protein is degradation by means of the proteasome pathway. Ubiquitination may also remodel proteins affecting their properties such as activity and stability and may promote interactions with other proteins and influence subcellular localization (Mukhopadhyay and Riezman, 2007).

Protein ubiquitination has been linked to senescence of plant organs and ubiquitin genes were demonstrated to be expressed during senescence (Courtney at al., 1994; Belknap and Garbarino, 1996; Buchanan-Wollaston, 1997; Bhalerao *et al*., 2003). The ubiquitin system is likely to be involved not only in the bulk degradation of proteins but also in regulating the activity of specific biosynthetic pathway. The ORE9 protein of *Arabidopsis* limits leaf

longevity by degrading target proteins that are implicated in delaying leaf senescence program, through the ubiquitin pathway. The *ore9* mutant displayed delayed senescence symptoms in natural and hormone-modulated senescence (Woo *et al*., 2001).

Ubiquitin-mediated protein degradation has been presumed to occur during flower senescence. In daylily petals, ubiquitinated proteins were detected using western blotting. Affinity purified antibody to ubiquitin detected masses that whether increased or decreased in amount during flower senescence (Courtney *et al*., 1994). Analysis of components of the ubiquitin pathway in daylily through western blotting showed that the system is present during senescence even if it is not up-regulated (Stephenson and Rubinstein, 1998). The decrease in ion leakage following treatments with two inhibitors of the 26S proteasome indicates that flower senescence is associated with the proteasome route. Moreover, the increase in the mRNA level of genes related to the ubiquitin-proteasome pathway has been reported for several species (Breeze *et al*., 2004; Hoeberichts *et al*., 2007; Yamada *et al*., 2007; Xu *et al*., 2007). *MjXB3*, a putative E3 ubiquitin ligase gene of *Mirabilis jalapa*, and its *Petunia* homologue *PhXB3* were strongly up regulated during flower senescence, but not in flower buds or open flowers. Virus-induced gene silencing increased significantly flower longevity in *Petunia* (Xu *et al*., 2007), indicating that the ubiquitin system is involved in protein regulation and/or degradation during senescence.

1.2.6. Non-proteasomal pathway

The ubiquitin-proteasome pathway is not the only route used for the control of the key aspects of plant growth, development and defence. Besides the 1300 genes belonging to the ubiquitin-proteasome pathway, more than 600 protease genes have been annotated in the *Arabidopsis* genome that may be involved in the control of protein turnover as well as in protein trafficking and regulation of protein activity (Schaller, 2004). Proteases may act in the bulk degradation of proteins and are also responsible for the maturation of enzymes, protein assembly and subcellular targeting by means of the post-translational modification of proteins by removing selectively specific amino acid sequences (Schaller, 2004).

Proteolytic enzymes can be classified as endopeptidases or exopeptidases. The first group includes enzymes that act internally in polypeptide chains while the second one includes enzymes that act near the terminus of polypeptide chains (Barrett, 1994). While the exopeptidases can be classified on the bases of substrate specificity as amino or carboxypeptidases, classification of the endopeptidases into serine, cysteine, aspartic, metallo and threonine endopeptidases is made according to the catalytic mechanism (Schaller, 2004).

Just a few peptidases remain with an unknown catalytic type. Rawlings *et al*. (2008) used a hierarchical, structure-based classification of the peptidases and created the MEROPS peptidase database (http://merops.sanger.ac.uk). In this classification, each peptidase is assigned to a family according to the statistically significant similarities in amino acid sequence. The families that are thought to be homologous are grouped in a clan.

Much of the initial work on plant proteolytic enzymes was focused on cysteine proteases (Schaller, 2004). They have been extensively studied and have been reported to be involved in a number of developmental processes in plants (Beers *et al*., 2000 and references therein). The involvement of cysteine proteases in developmental or stress-induced PCD and senescence has been widely demonstrated and suggests that these enzymes may play a critical regulatory role (Trobacher *et al*., 2006). Moreover, vacuolar processing enzymes (VPEs) belonging to the legumain family (C13 family) and metacaspases belonging to the caspase family (C14 family) have been proposed as candidates for caspase-like activity in plants (Woltering *et al*., 2002; Sanmartin *et al*., 2005).

1.2.6.1. Papain-like cysteine proteases

Peptidases belonging to the C1 family (papain-like) have been widely studied in plants and have been pointed out as key enzymes in regulating developmental processes as well as cell death programs (Beers *et al*., 2000; Beers *et al*., 2004; Schaller, 2004; Trobacher *et al*., 2006). Papain was first identified and isolated from the latex and fruit of papaya and is used as a model for the C1 family (Trobacher *et al*., 2006).

Plant papain-like proteases are synthesized as pre-pro-enzymes (40-50 KDa) that are processed in a multi-step fashion through the removal of the pre- and pro-sequences to yield the mature and fully active form (22-35 KDa) (Beers *et al*., 2000; Trobacher *et al*., 2006). The N-terminal pre-sequence is a hydrophobic chain of 10-26 aa that directs co-translational delivery to the lumen of the endoplasmic reticulum. The 38-150 aa papain-type prodomain serves for proper protein folding, to block the catalytic site of the enzyme, inhibiting its activity, and is also important for targeting of the enzyme (Beers *et al*., 2000; Trobacher *et al*., 2006).

The 210-260 aa active enzyme includes the Cys25 and His159 (papain numbering) residues forming the catalytic dyad and two other residues, Gln and either Asn or Asp, all of which are important for catalysis (Beers *et al*., 2000; Trobacher *et al*., 2006). The catalytic sites in the papain-like family are quite large allowing for a broad substrate specificity (Trobacher *et al*., 2006). However, papain-like peptidases prefer substrates containing a bulky non-polar side-

chains at the P2 position (Beers *et al*., 2000) and even have the rare ability to accept proline at the P1 and P1' position of the cleavage site (Than *et al*., 2004).

The C1 family proteases may be also classified based on the amino acid sequence of the prodomain. The first sub-group, similar to animal cathepsins H and L, includes the **E**X3**R**X3**F**X2**N**X3**I**X3**N** (ERFNIN) motif which is strongly conserved and acts as an inhibitory domain. The second sub-group, similar to cathepsin B, lacks the ERFININ motif and has a shorter pro-peptide (Karrer *et al*., 1993; Beers *et al*., 2000; Beers *et al*., 2004).

In some cases, papain-like proteases possess a C-terminal HDEL, RDEL, TDEL, KDEL tetrapeptide sequence which acts as an ER retention signal (Valpuesta *et al*., 1995; Kuo *et al*., 1996; Guerrero *et al*., 1998, Eason *et al*., 2002). The tetrapeptide is recognized by a receptor on the Golgi complex, resulting in retrieval of H/KDEL proteins from this compartment back into the ER (Okamoto *et al*., 2003). In addition to protein localized into the ER, the KDEL tetrapeptide is also present in protein or protein precursors that absolve their function in other cell compartments (Frigerio *et al*., 2001). In *Vigna mungo* it has been demonstrated that a KDEL-tailed cysteine peptidase (SH-EP) is first synthesized and accumulated in the ER, and subsequently packed into 200-500 nm KDEL-vesicles (KV) that bud from the ER bypassing the Golgi apparatus. The KVs were shown to fuse with protein storage vacuoles (PSV) where SH-EP is released and converted into the active enzyme (Toyooka *et al*., 2000; Okamoto *et al*., 2003). In this system, the KDEL tetrapeptide was demonstrated to be involved in the formation of KV and in the efficient transport of the proteins to vacuoles through KV (Okamoto *et al*., 2003). Similarly, in *Ricinus communis* a 45 KDa cysteine endoprotease precursor (CysEP) accumulates within small vesicles, called ricinosomes, that bud directly from the ER (Schmid *et al*., 2001). Unlike KDEL-vesicles containing SH-EP, it has been proposed that ricinosomes do not fuse with the vacuole but release their content directly into the cytosol after cell acidification, presumably due to proton release or vacuole rupture. Cytosol acidification also triggers the activation of the CysEP by removing the N-terminal and C-terminal propeptide (Schmid *et al*., 2001). Ricinosome-like structures containing KDEL proteases were found in flower petals and more recently in tomato anthers (Schmid *et al*., 1999; Senatore *et al*., 2009). Despite the apparent difference in function, the KVs and ricinosomes are quite similar in terms of biogenesis and protein content, and they are similarly involved in protein degradation for the recovery of nitrogen resources (Schaller, 2004). The subcellular localization is a fundamental feature for understanding the in vivo functions of a given enzyme. Though most papain-like peptidases are vacuole localized,

some of them are located in other compartments as well including the cytosol, chloroplast, nucleus and cell wall (Cervantes *et al.*, 2001; Harrak *et al.*, 2001; Sheokand *et al.*, 2005).

So far, a number of papain-like enzymes have been identified as key elements in a variety of PCD events and plant tissues (Trobacher *et al.*, 2006). Studies on leaf, fruit and flower senescence have resulted in the discovery and cloning of cDNAs coding for papain-like peptidases (Huang *et al.*, 2001; Eason *et al.*, 2002; Hunter *et al.*, 2002; Wagstaff *et al.*, 2002; Eason *et al.*, 2005; Jones *et al.*, 2005). An aleurain-like protein (BoCP5) was up-regulated during post-harvest senescence of florets and leaves in broccoli. In transgenic broccoli where BoCP5 was down-regulated, floret yellowing was delayed and chlorophyll levels were higher than in wild-type plants (Eason *et al.*, 2005). The hydrophobic N-terminal sequence and the vacuolar sorting signal suggested that BoCP5 is localized in the vacuole (Eason *et al.*, 2005). In carnation the increase in the expression level of the cysteine peptidase DC-CP1 is coupled with decrease in the expression of the specific inhibitor DC-CPIn, homologous to cystatins. Cystatin data from multiple plant species has suggested that these inhibitors act as defence proteins against pests and pathogens and as regulators of protein turn-over (Martinez *et al.*, 2009), and in other systems were able to suppress PCD (Rojo *et al.*, 2003, 2004). The recombinant DC-CPIn protein was able to inhibit the protease activity of petal extracts and papain (Sugawara *et al.*, 2002). Nine papain-like proteases were detected in *Petunia* petals and six of them were up-regulated during petal senescence (Jones *et al.*, 2005). Several papain-like proteases expressed during flower senescence possess the C-terminal tetrapeptide KDEL or RDEL (Guerrero *et al.*, 1998; Eason *et al.*, 2002).

All these findings strongly suggest the involvement of papain-like cysteine peptidases in plant organ senescence, but the exact role for each peptidase is far from being understood.

1.2.6.2. Vacuolar processing enzymes

Vacuolar processing enzymes (VPEs) are cysteine proteases, found in various eukaryotic organisms including higher plants and mammals, that cleave the peptide bond at the carboxyl group of asparagine or aspartic acid and belong to the C13 legumain family (Yamada *et al.*, 2005). VPEs are vacuole-localized proteases responsible for maturation and activation of various vacuolar proteins both in seeds and vegetative tissues (Hara-Nishimura *et al.*, 1991; Kinoshita *et al.*, 1999). These enzymes are synthesized as inactive precursors with an N-terminal pro-sequence and a C-terminal pro-sequence. VPEs may be transported to the vacuole as an inactive precursor which is converted into the active enzyme by the removal of the C-terminal pro-peptide, and subsequently of the N-terminal pro-peptide (Kuroyanagi *et*

al., 2002). Hayashi *et al*. (2001) showed that two stress-inducible cysteine proteases, RD21 and γVPE, accumulated in long-shaped ER bodies derived from the endoplasmic reticulum. In stress conditions, the ER bodies started to fuse with each other and with the vacuole releasing the protease precursors.

A number of cDNAs of VPE homologues have been identified in seeds and vegetative tissues (Münz and Shutov, 2002; Hara-Nishimura *et al*., 2005 and references therein). They can be classified as vegetative-, seed- or uncharacterized-type (Yamada *et al*., 2005). VPEs have been demonstrated in detail to be involved in the proper processing of seed storage proteins (Shimada *et al*., 2003; Gruis *et al*., 2004). This is also supported by the evidence that VmPE-1, a VPE homologue isolated from *Vigna mungo*, can process the papain-like cysteine protease SH-EP (Okamoto and Minamikawa, 1999). Plants have been able to develop during evolution sophisticated mechanisms to counteract pathogen infections. It has been demonstrated that VPEs are involved in HR during tobacco mosaic virus (TMV) infection. The virus-induced silencing of VPE genes prevented lesion formation and HR in tobacco plants (Hatsugai *et al*., 2004). It has also been reported that VPEs may be involved during senescence of vegetative tissues. The fusion of αVPE and γVPE promoters with the GUS reporter directed the expression in senescing tissues and not in young tissues (Kinoshita *et al*. 1999). Furthermore, transcript level increased in senescing leaves.

The role of VPEs during flower senescence is still not clear and few homologous genes have been reported to be up-regulated in wilting petals. From microarray analysis, a cysteine protease gene, displaying homology to a tobacco VPE, was found to be up-regulated during flower senescence in carnation (Hoeberichts *et al*., 2007). Most recently, the expression of a VPE gene from *Ipomea nil* petals was shown to increase significantly, suggesting a function for VPE peptidases in flower senescence (Yamada *et al*., 2009).

1.2.6.3. Metacaspases

In animals, PCD is often associated, and depends on, the activation of caspases, a class of Cys –dependent Asp-specific peptidases. To date, homologues of caspase genes have not been found in plants, though caspase-like activities are easily detected using specific synthetic substrates and caspase specific inhibitors (Bonneau *et al*., 2008). In recent years, two families of caspase-like proteins were identified, one from animals and slime mold (paracaspases) and the other from plant, fungi and protozoa (metacaspases) (Uren *et al*., 2000). Metacaspases can be distinguished into type I and type II. Type I metacaspases have a proline- or glutamine-rich N-terminal domain similar to initiator or inflammatory caspases,

while type II metacaspases lack such a pro-domain and have a linker region between the large and small subunit (Vercammen *et al*., 2007). In plants both type I metacaspases and type II metacaspases have been found. In the *Arabidopsis thaliana* genome there are nine predicted metacaspase genes, three of which belong to the type I (AtMCP1a-1c) and the other six to the type II (AtMCP1a-2f) (Watanabe and Lam, 2005).

The role of metacaspases during plant senescence has not been yet clarified, although several metacaspase genes have been demonstrated to be strongly induced in senescing flowers, in response to pathogens and elicitors and during various abiotic stresses (Sanmartin *et al*, 2005; Vercammen *et al*., 2007). Moreover, a redundancy effect may exist between the various members of this family, and additional factors may be necessary to activate ectopically expressed metacaspases (Vercammen *et al*., 2007). Single metacaspases may carry out specific roles and could be involved in developmental processes other than PCD. Metacaspases may also have different pH optima and display different substrate specificity, in accordance with possible different functions (Vercammen *et al*., 2004; Watanabe and Lam, 2005). Therefore, in vivo activity assays and the identification of metacaspase substrates may be useful to understand the role of individual metacaspases in plant development and stress responses (Vercammen *et al*., 2007).

1.2.7. Caspase-like activities in plants

Apoptosis, a particular form of PCD characterized by a distinct morphology, the formation of apoptotic bodies, and caspase activation, does not occur in plants but apoptotic-like events may be recognized in plant cell death (Reape and McCabe, 2008). By contrast, autophagy seems to be common in plants and the role of the vacuole as a lytic compartment has been pointed out (van Doorn and Woltering, 2005). In some cases cell death follows different pathways and has been placed in the necrotic or non-lysosomal category. The fact that apoptosis-like PCD and autophagic PCD show a morphological overlap and that the same cell may undergo an apoptosis-like or autophagic PCD depending on the stimulus, indicates the existence of a common set of cell death regulators. It has been hypothesized that the nature of the cell death trigger determines the temporal path of plant PCD and thus the appropriate machinery to be activated (Love *et al*., 2008).

The key role of caspases in several forms of animal PCD and the similarity of plant and animal cell death stimulated the research on plant caspases. In animals, activation of caspases does not result in the bulk degradation of cellular proteins. Caspases selectively cleave a restricted number of target proteins, always after an aspartate residue. Caspase activity results

in activation of proteins by cutting off negative regulatory domains or by inactivating regulatory sub-units (Hengartner, 2000). In plants, different types of proteases are known to be involved during developmental, pathogen- or stress induced cell death. Moreover, likewise caspases, specific plant proteases which have functional and not structural similarity with caspases are expected to regulate plant PCD (Woltering *et al*., 2002; Reape and McCabe, 2008). In spite of the lack of orthologous caspase sequences in plants, as demonstrated by the analysis of *Arabidopsis* and rice genomes, caspase-like activities have been detected in plants using synthetic tetrapeptides for specific mammalian caspases. Data available in the literature are in support of up to eight distinct caspase-like activities in plants (Bonneau *et al*., 2008). However, these substrates have overlapping specificities with various caspases and other proteases. This makes them useful to characterize in vitro purified proteases but adds difficulty to interpret caspase-like activity in a complex milieu such as whole plant extracts (Timmer and Salvesen, 2007; Bonneau *et al*., 2008). In spite of the non complete substrate specificity, caspase-like activity assays have been used in plant research and caspase-like activities have been reported to occur in various species and tissues, and have been often correlated with PCD induction or progression (Bonneau *et al*., 2008). In order to assess if caspase-like activities are really required for completion of PCD, specific caspase inhibitors mimicking the caspase substrate recognition site are used. An increasing number of reports show that these inhibitors significantly suppress also plant cell death (Woltering *et al*., 2002; Bonneau *et al*., 2008). One of the first studies concerning the inhibitory effect of synthetic peptides on plant cell death related to the HR of tobacco leaves inoculated with *Pseudomonas syringe* pv. phaseolicola (del Pozo and Lam, 1998). The caspase-3-specific inhibitor Ac-DEVD-CHO and the caspase-1-specific inhibitor Ac-YVAD-CMK were able to suppress HR cell death and down-regulate the specific molecular markers *hsr203J* and *hin1*. Following this, the involvement of caspase-like activities during plant pathogen interaction has been demonstrated by several authors (Rojo *et al*., 2000; Chichkova *et al*., 2004). Recently it has been demonstrated that the *Alternaria alternaria* AT toxin induces programmed cell death in tobacco leaves leading to the increase of hydrogen peroxide, malondialdehyde, free proline and protease activity. Lesion development and the production of stress metabolites were suppressed by the infiltration with Ac-YVAD-CMK (caspase-1 inhibitor) and Z-Asp-CH_2-DCB (broad range caspase inhibitor) leading to the conclusion that caspase-like proteases play a prominent role in AT toxin-induced cell death (Yakimova *et al*., 2009).

Stress responses may also activate a cell death program resulting in activation of caspase-like proteases. Ultraviolet light is known to induce programmed cell death that may be modulated

by caspase-like proteases (Danon *et al.*, 2004; He *et al.*, 2008). Recently, the real time detection of caspase-3-like protease activation has been achieved by measuring the degree of fluorescence resonance energy transfer (FRET) in cells exposed to UV-C. A mutation in the tetrapeptide close to the cleavage site or the treatment of protoplasts with the caspase inhibitor Ac-DEVD-CHO prevented the increase in caspase-like activity detected through the decrease in fluorescence (Zhang *et al.*, 2009). In tomato fruits, PCD was induced by heat shock and caspase-like activity was detected using Ac-DEVD-AMC and Ac-LEHD-AMC substrates. The treatment with a broad spectrum caspase inhibitor (Z-VAD-FMK) suppressed cell death and decreased LEHDase and DEVDase activities (Gui-Qin *et al.*, 2009).

Moreover, activation of caspase-like enzymes has been associated with developmental PCD in different plant organs, suggesting their involvement as part of the core mechanism of plant cell death. In *Papaver rhoeas*, self incompatibility (SI) activated VEIDase, LEVDase and DEVDase activities. DEVDase and VEIDase activities could be detected 90 minutes after SI-induction and examining the timing of their activation led to the conclusion that they could be functionally involved in SI-induced PCD, while LEVDase activity increased less rapidly peaking later and was still increasing after DEVDase and VEIDase activity was significantly decreased. Using Ac-DEVD-CHO, Ac-VEID-CHO and Ac-LEVD-CHO inhibitors the increase of caspase-like activity was significantly reduced and SI-induced PCD was alleviated (Bosch and Franklin-Tong, 2007; Bosch *et al.*, 2008). The cleavage of caspase specific substrates was reported also in developing and germinating seeds (He and Kermode, 2003; Boren *et al.*, 2006). In the suspensor of *Phaseolus coccineus* the increase of YVADase and DEVDase activity was shown to correlate with PCD hallmarks. Furthermore, specific inhibitors were able to completely abolish or significantly reduce caspase-like activities in cell-free extracts obtained from suspensors undergoing cell death (Lombardi *et al.*, 2007).

The use of viral or cellular macromolecular inhibitors thought to interact directly with proteases is a useful tool to control caspase-like activity and to demonstrate the involvement of caspase-like proteases in plant cell death. The baculovirus protein p35 may inhibit caspases and is able to block cell death when ectopically expressed, as demonstrated in several experimental systems (Lincoln *et al.*, 2002; del Pozo and Lam, 2003; Danon *et al.*, 2004; Wijayanto *et al.*, 2009). Expression of p35 protein partially inhibited HR cell death, while different mutant versions of p35 protein, unable to block caspases, were ineffective in transgenic tobacco plants (del Pozo and Lam., 2003). Likewise, integration and expression of p35 protein in *Lupinus angustifolius* reduced fungal disease symptoms caused by necrotrophic fungal pathogens without affecting fecundity and nodulation (Wijayanto *et al.*,

2009). Inhibitors of apoptosis protein (IAP) family are conserved between various organisms and are involved in the regulation of caspase activity. Heterologous expression of IAPs was reported to reduce *Agrobacterium tumefaciens*-induced PCD and pathogen-induced PCD in maize and tobacco (Hansen, 2000; Dickman *et al*., 2001), strongly supporting the idea that caspase-like proteases do exist.

Up to date, there are no published data on caspase-like activity and on the effects of caspase inhibitors, and no evidence has been reported that may suggest a role for caspase-like proteases during leaf and petal senescence. However, regulation of senescence clearly involves the activation of cysteine proteases, some of which could be similar to caspases in terms of substrate specificity, structure and functions.

The presence of caspase-like activities in plants and the evidence supporting their involvement during induced and natural PCD events stimulated researchers to search for the enzymes responsible for such activities. Vacuolar processing enzymes and metacaspases have been proposed to be responsible for caspase-like activities in plants by virtue of their structure similarity with caspases and their function in regulating PCD (Bonneau *et al*., 2008). Moreover, a serine protease possibly involved in PCD has been identified in oat displaying caspase-like activity (Coffeen and Wolpert, 2004).

Metacaspases were expected to have caspase-like activity but several studies have demonstrated that they are not able to cleave caspase substrates. Recombinant metacaspases from Arabidopsis have been produced and all prefer tetrapeptides with an Arg in the P1 position (Vercammen *et al*., 2004; Watanabe and Lam, 2005; He *et al*., 2007). Likewise, a metacaspase from pine and metacaspase-9 from *Arabidopsis* do not cut caspase substrates (Vercammen *et al*., 2006; He *et al*. 2007). In addition, all these recombinant metacaspases are not sensitive to caspase inhibitors. Even if metacaspases have not been reported to cleave specific caspase substrates and thus can not be responsible for caspase-like activity detected in plants, there is strong support for a role of metacaspases in plant PCD (Hoeberichts *et al*., 2003; Bozhkov *et al*., 2005; Watanabe and Lam, 2005; He *et al*., 2008). The yeast metacaspase (YCA1) knock-out survives in the presence of H_2O_2, and the expression of AtMCP1b and AtMCP2b restored apoptosis-like cell death, suggesting that metacaspases from higher plants may serve similar functions (Watanabe and Lam, 2005). Metacaspase mcII-Pa was demonstrated to be involved in embryogenesis by promoting nuclear envelop disassembly and DNA fragmentation in cells that are destined for elimination (Bozhkov *et al*., 2005). Furthermore, some evidence pointed out metacaspases as key regulators during cell death following pathogen infection (Hoeberichts *et al*., 2003; van Baarlen *et al*., 2007).

Recently, it was demonstrated that TSN (Tudor staphylococcal nuclease) is a natural substrate cleaved in vivo by mcII-Pa. TSN has ribonuclease activity essential for plant viability that can be impaired by metacaspase-mediated cleavage during PCD (Sundström *et al*., 2009). In spite of these results, not always obvious correlations have been found between metacaspases and PCD (Watanabe and Lam, 2005; Vercammen *et al*., 2006; Belenghi *et al*., 2007).

VPE in Nicotiana benthamiana has been demonstrated to have YVADase activity and was involved in TMV-induced cell death (Hatsugai *et al*., 2004). The quadruple knock out *Arabidopsis* mutant for all VPE genes (α-VPE, β-VPE, γ-VPE, δ-VPE), showing no differences in developmental growth but with a reduction of lesion formation in response to the fumosin B1 micotoxin, did not display VPE or YVAD activity, suggesting that in *Arabidopsis* there are no other proteases with a similar activity (Kuroyanagi *et al*., 2005). Experiments using the biotinylated inhibitor biotin-YVAD-fmk suggested that also δ-VPE has caspase 1 activity (Nakaune *et al*., 2005).

Saspase, a serine protease of the subtilisin family, has caspase-like activity, is inhibited by caspase inhibitors and is involved indirectly in victorin-induced cleavage of Rubisco during PCD in *Avena sativa* leaves. Purified saspase was able to cut several caspase substrates showing maximal activity against VKMD, VEHD and VNLD substrates, while it did not cleave VEID, WEHD or DEVD tetrapeptides (Coeffeen and Wolpert, 2004).

Overall, caspase-like activities and inhibition of plant PCD by caspase inhibitors does not automatically imply that caspase functional homologous are present in plants, rather they suggest that PCD progression requires proteases that cleave caspase substrates and are inhibited by caspase inhibitors (Bonneau *et al*., 2008).

1.3. REGULATION OF SENESCENCE BY SUGARS

Metabolites play a crucial role in the regulation of developmental processes as well as in response to biotic and abiotic stresses in plants (Wingler and Roitsch, 2008). Senescence is regulated by carbon and nitrogen signals, and sugars control plant metabolism, growth, and development and are strictly correlated with light, stress and hormone signalling, having also important hormone-like functions as primary messengers in signal transduction (Rolland *et al*., 2002). Several lines of evidence support the idea that hexose accumulation could be involved as a signal for senescence initiation and regulation in leaves (Rolland *et al*., 2002; Yoshida, 2003; Wingler and Roitsch, 2008; Wingler *et al*., 2009). However, little is known

about the concentration of various sugars in different cells or cell compartments in relation to the senescence processes, and a causal relationship between sugars and senescence may not always be proved. In addition, there are several factors and more than one pathway leading to senescence, which makes it difficult to reach definitive conclusions (van Doorn, 2008).

In flowers, at present, there is no good reason to accept the hypothesis that either starvation or sugar accumulation are general signals for petal senescence in flowers of intact plants (van Doorn, 2004). Several studies have shown the effect of exogenous sugars on vase life and carbohydrate metabolism of many cut flowers, and sugars usually delay visible senescence in flowers. They may act by improving water relations, providing the energy for the maintenance of cellular homeostasis and influencing ethylene sensitivity (van Doorn and Woltering, 2008).

In ethylene sensitive species exogenous sugars considerably delay the increase in ethylene production and the onset of visible signs of senescence. The effect of sugars is greater in species in which detached flowers show much earlier visible senescence (van Doorn, 2004). In carnation flowers, sucrose delayed the expression of almost all senescence-associated genes, very similar to the effect of silver thiosulfate (STS), suggesting that sugars act as a repressor of ethylene signal transduction (Hoeberichts *et al*. 2007). However, it is not known how the sugar signal is translated into an anti-ethylene signal. In tulip, a decrease in ATP level was identified as a very early trigger for flower senescence, rather than ethylene production. Furthermore, sucrose supplementation to cut flowers maintained ATP levels and delayed senescence (Azad *et al*., 2008).

In ethylene-insensitive flowers, sugars can also delay senescence but the effect on the time to visible senescence is much smaller. In *Gladiolus* flowers, sucrose and trehalose reduced nuclear fragmentation and delayed petal wilting and browning by 2 days (Yamada *et al*, 2003). In *Sandersonia*, sugar feeding delayed flower senescence and the alteration in the pattern of senescence was reflected also on flower colour, firmness, protein content and gene expression (Eason *et al*., 1997; Eason *et al*., 2002). In *Alstroemeria*, inclusion of 1% sucrose in the vase solution also was effective in extending flower longevity (Chanasut *et al*., 2003). Overall, in ethylene-insensitive species it is not fully clear if sugars delay senescence by preventing a drop in the level of osmotic solutes or by delaying cell death, but the evidence supports a relationship to remobilization and cell death.

In many species, petal sugar levels remain rather high when senescence symptoms are already visible, in apparent contradiction with the effect of exogenous sugar application (van Doorn, 2004; van Doorn and Woltering, 2008). However, this could be explained because

different tissues in the petal are at different stages of development and the sugar distribution in the various cell compartments is an unequal. During flower senescence there is an accumulation of soluble sugars within the phloem that does not necessary reflect the situation within the mesophyll or epidermis. Often whole petals are sampled and the estimation of the sugar levels could be misleading (van Doorn, 2004; van Doorn and Woltering, 2008).

1.4. HORMONAL SIGNALS FOR SENESCENCE-ASSOCIATED EVENTS

1.4.1. Ethylene

In many species, the time to petal wilting or abscission is regulated by ethylene and the high sensitivity to applied ethylene in petals coincides with a regulatory role of the endogenous hormone (van Doorn, 2001). In ethylene-sensitive flowers, senescence is accompanied by a sudden and transient increase of respiration associated with an upsurge in ethylene production (van Doorn and Woltering, 2008). In many species pollination hastens the senescence-associated events inducing a rise of ethylene production (Llop-Tous *et al*., 2000; Xu and Hanson, 2000) and may lead to changes in nectar composition, flower structure and colour, and determine flower wilting or abscission (Stead, 1992).

After the discovery of S-adenosyl-methionine (SAM) and 1-aminocyclopropane-1-carboxylic acid (ACC) as ethylene precursors several enzymes and genes involved in the biosynthetic pathway have been characterized and it has been shown that ACC synthase and ACC oxidase are encoded by gene families (Wang *et al*., 2002). In *Dianthus caryophyllus*, exposure to ethylene resulted in premature petal senescence and increased or reduced the abundance of mRNA populations, suggesting that changes in petal physiology may be the result of rapid changes in gene expression (Woodson and Lawton, 1988). The pattern of ethylene production in carnation flowers during the vase life and in response to exogenous ethylene and the expression of one ACC oxidase gene and two ACC synthase genes were investigated. Increased expression of these genes was observed during natural senescence as well as a rapid induction by ethylene treatment. In the same species, the correlation between the increase in ethylene production and the increase in gene expression indicated ethylene as a main regulator of ACC oxidase and ACC synthase. A regulatory role for the ovary in carnation flower senescence was proposed and ethylene produced in the gynoecium was identified as a diffusible signal, which stimulates the expression of ethylene biosynthetic genes and the autocatalytic production of ethylene in other organs (ten Have and Woltering, 1997). The key role for the gynoecium in carnation petal senescence was confirmed by

successive studies (Shibuya *et al*, 2000; Nukui *et al*., 2004). An open question to answer is what signal triggers the rise in ethylene production in unpollinated petals of ethylene-sensitive flowers (van Doorn and Woltering, 2008).

The first prerequisite for any signalling molecule to be functional, is the existence of a detection system to precisely monitor its levels. The ability to easily diffuse through the membranes and the cytoplasm eliminates the need for an active transport system to deliver ethylene to its receptors on the ER (Alonso and Stepanova, 2004). The expression of genes encoding receptor proteins has been monitored in a few flower species. *DC-ERS2* and *DC-ETR1* mRNAs were present at considerable levels in carnation petals, ovaries and styles at full bloom. *DC-ERS2* mRNA decreased towards the later stages of petal senescence while *DC-ETR1* showed little or no change in level throughout senescence (Shibuya *et al*., 2002). In cut rose, flower opening is regulated by ethylene through the expression in petals of two receptors and two *CTR* genes, and the application of exogenous ethylene induced expression of *Rh-ETR* genes (Xue *et al*., 2008). Interestingly, two ethylene receptor genes homologues of *Arabidopsis ERS1* were isolated from the flowers of *Gladiolus*, an ethylene-insensitive species. *GgERS1b* mRNA level decreased in petals during flower development, while *GgERS1a* was constitutively expressed at high level suggesting a role in conferring ethylene insensitivity (Arora *et al*., 2006). The importance of ethylene biosynthesis and perception has been emphasized using transgenic plants with up- or down-regulation of key biosynthetic genes. *Petunia x hybrida* over-expressing the antisense *BoACS1* gene (ACC synthase) or the antisense *BoACO1* gene (ACC oxidase) from broccoli showed reduced ethylene biosynthesis and delay of flower senescence (Huang *et al*., 2007). The over-expression of the *Arabidopsis ETR1-1* gene delayed DNA fragmentation and nuclease *PhNUC1* gene expression in *Petunia* flowers (Langston *et al*., 2005), and delayed flower and leaf senescence and increased the flowering time in tobacco and *Campanula carpatica* respectively (Sriskandarajah *et al*., 2007; Yang *et al*., 2008).

1.4.2. Cytokinins

Cytokinins have been implicated in senescence and PCD processes in plant organs. Expressing the isopentenyl transferase (*IPT*) gene under the control of the *Arabidopsis thaliana SAG12* promoter delayed senescence in tobacco leaves, suggesting that cytokinins may regulate senescence (Gan and Amasino, 1995). In spite of the well known anti-senescence activity, in some cases cytokinins may also accelerate senescence. High levels of N-benzyladenine (BAP) induced PCD in carrot and *Arabidopsis* cell cultures. Moreover, the

application of BAP to *Arabidopsis* plants induced leaf yellowing and root mass reduction accompanied by DNA fragmentation (Carimi *et al*., 2003).

Several studies suggest a role for cytokinins during flower senescence and it has been hypothesized that they are implicated in the onset of the rise in ethylene production. *Petunia x hybrida* transformed with the IPT gene under the control of the *SAG12* promoter showed a strong delay in flower senescence. Furthermore, transgenic plants were less sensitive to applied ethylene and the increase in ethylene production following pollination and the up-regulation of a senescence-associated cysteine protease were significantly delayed in *IPT* plants (Chang *et al*, 2003). The effect of cytokinins as anti-senescence factors was reported to be related to their ability to reduce ethylene synthesis, by controlling ACC synthesis and the conversion of ACC to ethylene. The onset of senescence was correlated with a decrease in cytokinin activity (van Staden *et al*, 1987).

The importance of cytokinins also follows from the observation that treatments with cytokinins delayed carnation petal senescence and feeding carnation flowers with 6-methylpurine, an inhibitor of cytokinin oxidase/dehydrogenase, resulted in a much longer petal life span (Taverner *et al*., 2000). Treatments with kinetin or 6-methylpurine delayed senescence and abscission of petals in wallflower (Price *et al*., 2008). The up-regulation of genes encoding cytokinin oxidase/dehydrogenase in carnation (Hoeberichts *et al*., 2007) and wallflower (Price *et al*., 2008) may also suggest accelerated cytokinin breakdown.

1.4.3. Abscisic acid

The role of abscisic acid (ABA) in flower senescence is still not clear either in ethylene-sensitive or ethylene-insensitive flowers.

In carnation cut flowers, application of ABA stimulated ethylene production and hastened petal wilting, and it was proposed that ABA and indolacetic acid (IAA) may act through induction of ethylene production in the gynoecium. The produced ethylene would function as a diffusible signal perceived by the petals (Shibuya *et al*., 2000). Exogenous ABA was also able to induce ethylene production and petal senescence in the long-vase life carnation "White Candle" in which ethylene was below the detection level (Nukui *et al*., 2004). In transgenic P_{SAG12}-IPT petunia the ABA level was greatly reduced compared to the wild type suggesting that it could be implicated in flower senescence together with cytokinins and ethylene (Chang *et al*., 2003). In cocoa flowers, ABA seems to be essential for flower abscission and senescence and ethylene accelerates abscission only in the presence of ABA (Aneja *et al*., 1999). In miniature potted rose plants, exogenous application of ABA resulted

in hastened flower senescence but the effect was apparently mediated by ethylene (Müller *et al*., 1999). Daylily is an ethylene-insensitive species in which ABA may also play a role during flower senescence. Exogenous ABA application prematurely up-regulated events associated with natural flower senescence such as electrolyte leakage, increase in lipid peroxidation and induction of proteinases and RNase. Moreover, endogenous ABA levels increased before flower opening and continued to increase throughout the senescence process (Panavas *et al*., 1998). Further evidence supporting the involvement of ABA in senescence of ethylene-insensitive species came from *Narcissus pseudonarcissus* flowers in which exogenous application of ABA led to premature tepal wilting. An increase of endogenous ABA was also observed to coincide with visual signs of senescence. Senescence-associated transcripts accumulated prematurely following ABA application. However, in control flowers transcripts accumulated before the rise in endogenous ABA indicating that it was not an early regulator (Hunter *et al*., 2004).

1.4.4. Auxins

Auxins can in some cases reduce ethylene sensitivity such as is found in the abscission zone, while in other tissues they can induce ethylene production (van Doorn and Woltering, 2008). Exogenous application of indoleacetic acid was reported to induce senescence in isolated carnation petals, increasing the duration and amount of ethylene production (Wulster at al., 1982). IAA application has been reported to accelerate carnation flower senescence through the stimulation of ethylene biosynthesis. The removal of the gynoecium prevented ethylene production and petal wilting, indicating that the action of exogenous IAA was mediated by the gynoecium (Shibuya *et al*., 2000). The auxin response is dependent on the Aux/IAA family of transcriptional regulators: the proteasomal degradation of Aux/IAA proteins results in the expression of auxin-responsive genes (Quint and Gray, 2006). A transient increase in the mRNA abundance of an Aux/IAA gene was observed in senescing carnation petals (Hoeberichts *et al*., 2007), moreover, three genes relating to auxin signaling were up-regulated with age in flowers and leaves of wallflower and *Arabidobsis* (Price *et al*, 2008). In contrast, in *Mirabilis jalapa* flowers two Aux/IAA genes were reported to be down-regulated during ageing (Xu *et al*., 2007).

1.4.5. Gibberellins

The key role that gibberellins (GAs) play in plant growth and development is clearly evident from observing GA-deficient mutants that usually appear shorter than the wild type (Hedden

and Phillips, 2000). A role for GAs in flower ageing has been proposed observing the effects of exogenous application on the hallmarks and timing of senescence. Gibberellic acid delayed the senescence of carnation flowers and modified the climacteric ethylene rise (Saks *et al.*, 1992). The effect of delaying senescence hallmarks led to the hypothesis that a decline in endogenous GAs may be a correlative event associated with the onset of senescence in carnation (Saks and van Staden, 1993), but data on endogenous levels of GAs are lacking. In *Alstroemeria* leaves, endogenous levels of several GAs were quantified and the proportion of biologically active GA_1 and GA_4 was shown to decrease with senescence (Kappers *et al.*, 1997). Most recently, application of exogenous GA_4+GA_7 was reported to delay leaf senescence and petal fall in *Alstroemeria*, improving postharvest quality of cut stems and suggesting a role for GAs in the senescence of leaves and flowers (Mutui *et al.*, 2006). Moreover, a gene encoding a gibberellin induced protein was reported to be down-regulated during *Alstroemeria* post-harvest senescence (Breeze *et al.*, 2004). In daylily flowers, exogenous GA_3 extended the vase life and was able to counteract the senescing effect of ABA, supporting the anti-ageing role of GAs in plants (Hunter *et al.*, 2004). However, in contrast, Guerrero *et al.* (1998) reported that gibberellic acid application resulted in increased transcript abundance of two thiolprotease genes involved in natural flower senescence in daylily, suggesting an opposite role for GAs.

1.5. APPROACHES TO IMPROVE THE QUALITY OF POST-HARVEST ORNAMENTALS

Post-harvest quality of ornamental plants is a crucial aspect to be considered for successful commercialization. PCD is an important process during petal senescence and is associated with post-harvest quality. The knowledge obtained through the study of petal PCD may be applied to the objective of producing flowers with a longer vase life (Zhou *et al.*, 2005). This goal may be achieved by preserving flower freshness during their transport, by designing new holding solutions or by genetically modifying the flowers through the induction of useful target genes.

The rise in ethylene production and the effect of ethylene on flower senescence of many species resulted in the application of ethylene inhibitors for prolonging flower vase life. Molecules that appear to block ethylene receptors such as cyclopropene (CP), 1-methylcyclopropene (1-MCP), 3,3-dimethylcyclopropene (3,3-DMCP) have been used to prolong the vase life of ethylene-sensitive flowers (Sisler and Serek, 1997; Feng *et al.*, 2004).

Pulse treatments with STS usually prolongs flower longevity in species where ethylene is implicated (Serek *et al.*, 1995). STS had the same effect as sucrose treatment in delaying the expression of senescence associated genes (Hoeberichts *et al.*, 2007).

Because energy depletion or sugar starvation may trigger flower senescence, the application of sugars through the vase solution is a common practice to delay flower senescence both in ethylene-sensitive and -insensitive species (Azad *et al.*, 2008; van Doorn, 2004). Sucrose and trehalose were effective in delaying flower senescence of gladiolus and tulips (Yamada *et al.*, 2003; Ranwala and Miller, 2009) and sucrose delayed senescence and prevented the up-regulation of senescence-associated genes in carnation flowers (Hoeberichts *et al.*, 2007).

A biotechnological approach has been used to improve the vase life of several flower species. In carnation it has been successful. Over-expressing the Arabidopsis *etr1-1* allele under the control of a flower specific promoter increased the vase life of carnation up to 24 d (Bovy *et al.*, 1999). However the same approach did not have the same effect in roses, demonstrating that specific solutions need to be found for different species (Zhou *et al.*, 2005).

Advanced techniques can now be used to improve our knowledge on senescence. The use of the microarray technology may bring useful information about the genes involved in physiological or induced flower senescence (van Doorn *et al.*, 2003; Breeze *et al.*, 2003; Hoeberichts *et al.*, 2007; Price *et al.*, 2008). This will provide us with a range of genes putatively involved in the complicated pathways leading to flower ageing, that may be blocked or induced to modify the progression of senescence.

2. MATERIALS AND METHODS

2.1. Plant material

Plants of *Lilium longiflorum* cv. "White Heaven" were grown at CRA-VIV, Pescia or in commercial greenhouses. Only stems with one flower were used for the experiments. Stems were cut at the base two days before flower opening and immediately transferred to the laboratory where they were recut above the last leaf. Flowers were held in dH_2O (control) or $CaCl_2$ 1 mM, $ZnCl_2$ 1 mM, $LaCl_3$ 5 mM, 3-AT 2 nM, trehalose 300 or 30 mM, E-64 25 µM, L-NAME 300 µM, sucrose 300 mM (all from Sigma). Experiments were carried out in a climate-controlled room at 22°C and 50% relative humidity. Each flower was tagged when it reached the reference stage (T0) in which flower tips begin to separate and anthers begin dehisce. Samples were collected from closed flowers, from flowers at the reference stage and 2, 3, 4, 5, 7, and 10 days after the reference stage. For fresh weight and ion leakage measurements both inner and outer tepals were used while for all other analyses only outer tepals were sampled.

2.2. Ion leakage

For measurements of ion leakage, 7 mm discs were cut from the upper part of both outer and inner tepals avoiding the central midrib. The discs were placed in dH_2O and washed by shaking for one hour to remove ions from the surface and the cut section. Afterwards, 40 discs were placed in each Petri dish, 10 mL of bi-dH_2O were added and the dishes were placed in the growth chamber. Every 24 hours the aqueous solution was collected and the conductivity measured with a portable conductivity meter HI8733 (Hanna Instruments). After each measurement clean bi-dH_2O was added to the Petri dishes.

2.3. Agarose gel electrophoresis

For agarose gel electrophoresis 1% or 2% gels were used. For gel preparation 0.5 g or 1 g of agarose (Bioline or Sigma) were added to 50 ml of TAE buffer (50x: 242 g/L Tris, 100 mL/L 0.5 M NaEDTA pH 8.0, 57.1 mL/L glacial acetic acid), boiled in a microwave and 4 µL of 10 mg/mL EtBr was added after cooling the mix to approximately 50°C. The gel was poured and solidified in a tray. Samples were prepared by adding 10x loading buffer (50 mM Tris-HCl pH 7.6, 60% glycerol, bromophenol blue) and were loaded on the agarose gels. The latter were run in 1x TAE buffer at 100 V for 15 – 20 min or at 30 - 40 V for 3 – 4 hours in the case

of DNA, and 250 – 500 ng of 1 Kb or 100 bp ladder (Invitrogen) were used as marker. Afterwards the gels were analysed with UV light.

2.4. SDS-PAGE

For the analysis of proteins 12% acrylamide gels were used. The separating gel was made by mixing 3.3 mL 40% acrylamide/bis-acrylamide (37.5:1) (Melford Laboratories), 4.4 mL 2.5% separating buffer (1.875 M Tris-HCl pH 7.5, 0.25% SDS), 100 µL 10% ammonium persulfate (APS), 10 µL N,N,N',N'-tetramethyl-athylenediamine (TEMED) (Sigma) and 3.3 mL dH_2O. For each gel 3 mL of mix were poured between two glass plates, covered with dH_2O up to the top of the plates and let solidify. The stacking gel was made by mixing 0.56 mL 40% acrylamide/bis-acrylamide (37.5:1) (Melford Laboratories), 0.66 mL 2.5% stacking buffer (0.3 M Tris-HCl pH 6.7, 0.5% SDS), 30 µL 10% APS, 5 µL TEMED (Sigma) and 2 mL dH_2O. After removing the water layer the mix was poured between the glass plates onto the separating gel and after placing the comb, was let solidify.

For obtaining sufficient concentration of proteins, the samples were concentrated using 10% trichloriacetic acid (TCA) (BDH Limited Poole England). Briefly, the protein extract was mixed with 10% TCA (1:1 v/v) and centrifuged for 3 min at room temperature and 13000 rpm using a microcentrifuge (MiniSpin Eppendorf, UK). The supernatant was carefully discarded and the samples centrifuged again to completely remove the TCA. Proteins were resuspended in 20 µL of dH_2O, prepared by adding the appropriate amount of 5x loading buffer (250 mM Tris-HCl pH 6.8, 10% SDS, 30% glycerol, 0.5 M DTT, 0.02% bromophenol blue) and were placed in 95°C water bath for 5 min. Afterwards the samples were loaded on the gel and run in 1x running buffer (10x: 10 g/L SDS, 30.3 g/L Tris base, 144.1 g/L glycine) at 100 – 120 V. As marker 5 µL of PageRulerTM Prestained Protein Ladder (Fermentas) were used.

2.5. DNA extraction from tepals

For the isolation of DNA from tepals the cetyl trimethyl ammonium bromide (CTAB) method was used (Ausubel et al., 2002). Approximately 200 mg of floral tissue were ground in a mortar with liquid nitrogen and transferred to 1.5 mL Eppendorf tubes. Two volumes of extraction buffer (CTAB 2%, NaCl 1.4 M, EDTA 20 mM, Tris 100 mM pH 8, βMe 0.2%) were added and the mix was incubated at 65°C for 45 min. One volume of chloroform:isoamyl alcohol (24:1) was added and the tubes were mixed gently. After centrifugation at 3000 rpm, at room temperature, the aqueous supernatant was transferred to

clean Eppendorf tubes. For the precipitation of DNA one volume of isopropanol was added and after gently mixing, the tubes were centrifuged at 14000 rpm for 20 min at room temperature in a microcentrifuge (MiniSpin, Eppendorf Italia). The pellet was allowed to dry under a sterile hood and then was re-suspended in TE pH 8. The samples were treated with RNase A (100 µg/mL) at 37°C for 20 min. DNA concentration was determined by reading the absorbance at 260 nm with a spectrophotometer UV-1204 (Shimadzu Europe Gmbh) and the samples were stored at -80°C until use.

2.6. RNA extraction

For RNA extraction 200 mg of tissue from each stage were used. The samples were ground to a fine powder in a pre-cooled mortar with liquid nitrogen. 1 mL of TRI Reagent (Sigma) was added and after grinding for a further few minutes the liquid was split into 1.5 mL Eppendorf tubes. After vortexing, the tubes were allowed to stand at room temperature for 5 min. Then the samples were centrifuged at 12000 rpm, 4°C, for 15 min using a Beckman Coulter Allegra TM 21R centrifuge fitted with a F2402H rotor. The supernatant was transferred to fresh Eppendorf tubes, 0.2 mL of chloroform were added and after vortexing, the tubes were left at room temperature for 5 min. After centrifugation at 12000 rpm, 4°C, for 15 min the aqueous supernatant was transferred to fresh Eppendorf tubes and 0.5 mL of isopropanol was added. The samples were gently mixed and incubated on ice for 10 min before centrifugation at 12000 rpm, 4°C, for 10 min. The supernatant was removed and discarded, 1 mL of 75% EtOH was added to the pellet and the tubes were vortexed for 15 s. After centrifugation the supernatant was discarded and the pellet was allowed to air dry before re-suspending in 30 – 50 µL of sterile water and combining contents of the two tubes. Presence of RNA was checked by 1% gel electrophoresis of 10 µl of product and the remaining RNA was stored at -80°C.

2.7. DNase treatment and cDNA synthesis

For DNase treatment the DNase digestion reaction was set up mixing 2 µg of RNA with 2 µL of 10x RQ DNase buffer (400 mM Tris-HCl pH 8, 100 mM $MgSO_4$, 10 mM $CaCl_2$), 2µL of RQ1 DNase (Promega) and making up to 20 µL with sterile water. The mix was incubated at 37°C for 30 min before adding 2 µL of RQ1 DNase stop solution (20 mM EGTA pH 8.0) and incubating at 65°C for 10 min to inactivate the DNase. For cDNA synthesis 19 µL of treated RNA (2µg) were mixed with 500 ng of Oligo(dt)15 primer (Promega) in a final volume of 20 µL. The mix was incubated at 70°C for 10 min and then placed at 4°C for 10 min. Then 6 µL

5x M-MLV RT buffer (250 mM Tris-HCl pH 8.3, 375 mM KCl, 15 mM $MgCl_2$, 50 mM DTT), 2 µL 0,1 M DTT and 1 µL 10 mM dNTP mix were added and the samples were incubated at 42°C for 2 min. After the addition of 200 U of M-MLV Reverse Transcriptase (Promega) the mix was incubated at 42°C for 50 min and subsequently at 70°C for 15 min to inactivate the enzyme and to stop the reaction.

Alternatively, total RNA was subjected to DNase treatment using a TURBO DNA-free kit (Ambion). Then, two micrograms of each sample were reverse-transcribed into cDNA using a high-capacity cDNA archive kit (Applied Biosystems) following the manufacturer instructions.

For checking the presence of cDNA PUV2 and PUV4 primers, which bind to 18S rRNA, were used and the PCR reaction was set up by mixing 1 µL of cDNA, 0.5 µL dNTP 10 mM, 2.5 µL 10x PCR buffer (500 mM KCl, 100 mM Tris-HCl (pH 9 at 25°C), 15 mM MgCl2), 1 µL of each primer (10 µM), 0.125 µL of in house purified Taq polymerase and sterile water to a final volume of 25 µL. The reaction was cycled in a GeneAmp PCR system 2700 machine (Applied Biosystems) for 36 cycles of {95°C 1 min, 58°C 1 min, 72°C 1 min}. The remaining cDNA was stored at -80°C.

2.8. Cloning of KDEL cysteine protease and VPE

Degenerate primers were used according to Wagstaff *et al.* (2002). These were designed comparing conserved regions of cysteine protease genes from monocotyledonous species in the database (CYPF: GCATGASCWRSSAGGARTT and CYPR: AAYTSGAAYGCATARTCCAT). In the PCR reaction 2 µL of cDNA from flower sepals at stage T9 was used and mixed with 1 µL 10 mM dNTP, 2.5 PCR buffer (Tris-HCl, KCl, $(NH_4)_2SO_4$, 15 mM $MgCl_2$; pH 8.7), 1 µL each primer 100 µM, 0.125 µL Hot Start Taq (Qiagen), 1.5 µL 25 mM $MgCl_2$ and sterile dH_2O to a final volume of 25 µL. For the PCR reaction the following thermal profile was used: 95°C 15 min, 40 cycles {95°C 1 min, 50°C 1 min, 72°C 1 min}, 72°C 15 min. Products were run on a 1% agarose gel at ~100 V for 20 min for checking the presence of a partial cDNA.

For VPE isolation a combination of different degenerate primers was used, designed by comparing conserved regions of VPE genes from several species in the database (VegF1: C ATG TAT GAY GAY ATH GC; VegF2: GA GTT CCN AAG GAY TAY AC; VegR1: TGA TGC AGT NGT NGC RTA; VegR2: ATC TGC ATC NCK YTG RTT; SeedF1: TT ATG TAT GAY GAY ATH GC; SeedF2: T GTT TGC CAY GCN TAY CA; SeedR1: TGC CGT TGT NAC RTA DAT; SeedR2: CTC ACT RCT YTC CAT CCA; SeedR3: GCA ATC CCA

RTC RTC NAC). In the PCR reaction 2 µL of cDNA from flower sepals at stage T9 was used and mixed with 1 µL 10 mM dNTP, 2.5 PCR buffer (Tris-HCl, KCl, $(NH_4)_2SO_4$, 15 mM $MgCl_2$; pH 8.7), 1 µL each primer 100 µM, 0.125 µL Hot Start Taq (Qiagen), 1.5 µL 25 mM $MgCl_2$ and sterile dH_2O to a final volume of 25 µL. For the PCR reaction the following thermal profile was used: 95°C 15 min, 40 cycles {95°C 1 min, 50°C 1 min, 72°C 1 min}, 72°C 15 min

2.9. Purification of DNA

Gel extraction and purification of the partial cDNA were done using a QIAquick Gel Extraction Kit (Qiagen) according to the manufacturer's instructions. Presence of DNA was checked by electrophoresis of 5 µL of product on a 1% agarose gel.

2.10. Ligation

For the ligation reaction the pGEM-T Easy Vector System (Promega) was used. The ligation reaction was set up as follows: 1 µL 10x Rapid Ligation Buffer (Tris-HCl 60 mM pH 7.8, $MgCl_2$ 20mM, 20 mM DTT, 2 mM ATP, 10% polyethylene glycol), 1 µL 50 ng/µL pGEM-T Vector, 7 µL PCR products, 1 U T4 DNA Ligase. In order to check the efficiency of the ligation reaction, Control Insert DNA (4 ng/µL) was used in a separate ligation reaction. The reaction was incubated at 4°C overnight and then stored at -20°C.

2.11. Transformation

Competent *E. coli* DH5α cells were transformed with plasmid DNA by heat shock transformation and were used for cloning cDNA fragments. The cells, prepared in house and stored at -80^{o}C, were thawed on ice and 2 µl of ligation mixture were added to 70 µL *E. coli* in Eppendorf tubes. The mix was placed on ice for 20 min, incubated at 42°C for 45 sec in a water bath and then immediately transferred back on ice for 2 min. LB medium containing 100 µg/ml ampicillin (900 µL) were added to the transformation mix and was incubated at 37°C for 1.5 hour at 100 rpm in an orbital incubator. After this the mix was plated onto Petri dishes containing LB medium (1 g tryptone, 0.5 g yeast extract, 1 g NaCl, H_2O_2 up to 100 mL) plus 100 µg/ml ampicillin (200 µL of the mix per plate) and plates were incubated at 37°C overnight. After incubation 5-6 colonies were picked from the agar, placed in Eppendorf tubes containing 200 µL of LB medium plus 100 µg/ml ampicillin and incubated for 4-5 hours at 37°C on a shaker at 100 rpm. Then the colonies were selected by odour and 1 µL of cell culture was used in a PCR reaction for checking the presence of the cDNA insert

using M13 primers (M13F-GTTTTCCCAGTCACGACGTTG; M13R–TGAGCGGATAACAATTTCACACAG). The PCR reaction was performed as follows: 1 µL bacterial culture, 0.5 µL 10 mM dNTP, 2.5 µL PCR Buffer (100 mM Tris-HCl pH 8.8, 200 mM KCl, 15 mM $MgCl_2$), 1 µL each primer 10 µM, 0.125 µL in house purified Taq DNA polymerase, and sterile dH_2O to a final volume of 25 µL. The reaction was cycled in a GeneAmp PCR system 2700 machine (Applied Biosystems) for 36 cycles of {95°C 1 min, 50°C 1 min, 72°C 1 min}. After agarose gel electrophoresis the clones for sequencing were selected based on size and amount of the PCR product. 50 µL from selected cultures were used to inoculate 3 ml of LB plus 100 µL/ml ampicillin in 15 mL tubes and the culture was incubated overnight at 37°C in a Gallenkamp orbital shaker at 200 rpm.

2.12. Plasmid preparation

Plasmid DNA purification was performed using a QIAprep Spin Miniprep Kit (Qiagen) according to the QIAprep Miniprep Handbook (Qiagen). Purified plasmid (10 µL) was electrophoresed on an agarose gel to verify the quality and quantity of the extracted plasmid. The remaining amount of purified plasmid was used for the determination of the concentration by using 1.5 µL in a NanoDrop spectrophotometer (Thermo Scientific) or 4 µL in a spectrophotometer UV-1204 (Shimadzu Europe GmbH), and for sequencing through an ABI Prism 3100 capillary sequencer (Applied Biosystems, Foster City, CA, USA). Sequencing reactions were performed using the BigDye Terminator Cycle Sequencing Kit (Applied Biosystems, Foster City, CA, USA) using M13 forward primers (5'-GTAAAACGACGGCCAGT-3').

2.13. RACE amplification to obtain a full length sequence

The BD SMART™ RACE cDNA Amplification Kit was used to perform both 5' and 3' amplification of cDNA ends (RACE). Gene specific primers (GSP) were designed using the partial lily KDEL-cysteine protease sequence (GSPR: CAGCCCCTTTCTGTCTCCAATCAACA and GSPF: GCAGTCGAGGGCATAAACCAGATCAA) and the partial VPE sequence (GSPR: TACGGGAGTCTAGGTCTTACAACAG and GSPF: CATTCCAAGAACACCAGGTCCGCCG) The first strand cDNA synthesis was made using 1 µg of total RNA. The reaction was performed following the BD SMART™ RACE cDNA Amplification Kit User Manual (BD Biosciences Clontech). For preparation of 5' RACE-ready cDNA 1µg of RNA was mixed with 1µL of 12 µM 5'CDS primer and 1 µL of 12 µM

BD SMART II A Oligonucleotide. For 3'RACE-ready cDNA 1µL of 12 µM 3'CDS primer was combined with 1 µg of total RNA. Sterile H_2O was added to a final volume of 5 µL for each reaction. The tubes were incubated at 70°C for 2 min and on ice for a further 2 min before adding 2 µL of 5X First-Strand Buffer, 1 µL DTT (20 mM), 1 µL dNTP (10 mM) and 1 µL BD PowerScript Reverse Transcriptase. Then, the tubes were incubated at 42°C for 1.5 hr. Specific lily PCR primers were designed from the partial cysteine protease sequences and used for checking the first strand cDNA (LLCYPF: GCCAGGAGTTCCGCTCCA; LLCYPR: CGCCGTTGCATCCTTGGT and LlVPEF: CCTATCCTTACCTTTATGCCGAC and LlVPER: GGTTTTGGAGATGCTCGTAGC). In house purified Taq was used and the PCR reaction was cycled for 36 cycles of {95°C 1 min, 64°C 1 min, 72°C 1 min}. Amplification of cDNA ends was performed using 2.5 µL of first strand cDNA. For the RACE reaction 5 µL of UPM (10X) (Long: CTAATACGACTCACTATAGGGCAAGCAGTGGTATCAACGCAGAGT; short: CTAATACGACTCACTATAGGGC) and 1 µL of GSPR (10 µM) or 1 µL of GSPF (10 µM) were combined. After adding 41.5 µL of Master Mix (5 µL 10X BD Advantage 2 PCR Buffer, 1 µL dNTP Mix (10mM), 1 µL 50X BD Advantage 2 Polymerase Mix) the following thermal profile was used in a GeneAmp PCR system 2700 machine (Applied Biosystems): 5 cycles {94°C 30 sec, 72°C 3 min}, 5 cycles {94°C 30 sec, 70°C 30 sec, 72°C 3 min}, 25 cycles {94°C 30 sec, 68°C 30 sec, 72° 3 min}. PCR products were separated on a 1% agarose gel to check the presence and the size of cDNA. Purification of the bands, cloning, purification of plasmid and sequencing were as described in previous sections 2.9, 2.10, 2.11, 2.12.

2.14. Semi-quantitative RT-PCR

RNA extraction and cDNA synthesis were performed as described in sections 2.5 and 2.7. Forward and reverse primers were designed on the basis of the partial cDNA sequences obtained from amplification with degenerate primers and were analyzed through IDT SciTools OligoAnalyzer 3.1 (http://eu.idtdna.com) (LlCypF: GCCAGGAGTTCCGCTCCA LlCypR: CGCCGTTGCATCCTTGGT). Primers amplified a 303 bp nucleotide sequence.

PCR was carried out in a 25 µl volume containing 1 µL cDNA, 0.5 µL 10 mM dNTP, 2.5 µL PCR Buffer (100 mM Tris-HCl pH 8.8, 200 mM KCl, 15 mM $MgCl_2$), 1 µL each primer 10 µM, 0.125 µL in house purified Taq DNA polymerase. As a negative control, a PCR reaction containing a volume of water replacing cDNA was performed for each set of PCR reactions to ensure there was no contamination in any of the PCR reagents. For LlCyp gene the PCR

reaction was cycled in a GeneAmp PCR system 2700 machine (Applied Biosystems) as follows: initial denaturation at 95 ºC for 1 min; cycles of 95 ºC for 1 min, 64 ºC for 1 min and 72 ºC for 1 min; final extension at 72 ºC for 15 min.

To establish the optimal number of cycles, an equal amount of the cDNA from each sample was mixed and two dilution (1/2 and 1/4) were prepared with sterile distilled water. Graphs plotting cDNA concentration and band intensity were performed in order to find the exponential phase and therefore the optimum number of cycles for semi-quantitative RT-PCR. Limiting the cycle number ensures that the reaction remains in exponential phase, and thus differences in band intensity are proportional to differences in the number of transcripts of the initial mRNA population. For LlCyp primers in these experiments the optimum number of cycles was 36.

Normalization controls were performed using the PUV primers (PUV2: TTCCATGCTAATGTATTCAGAG; PUV4: ATGGTGGTGACGGGTGAC), which amplify a 488 bp fragment of 18S rRNA. PCR products obtained from the 18S target were used to normalise results of the other primer sets. Although the cDNA was synthesised using oligo dT and hence would be expected to only contain mRNA sequences, in fact sufficient rRNA is retro-transcribed to be used for normalisation purposes due to the highly AT rich composition of rRNA. This has been used successfully in a number of published studies including Wagstaff *et al.,* (2005), Price *et al,* (2008) and Orchard *et al.,* (2005). The optimal number of cycles was determined as described above and for LlCyp gene was 21 in these experiments. PCR was carried out in a 25 µl volume containing 1 µL cDNA, 0.5 µL 10 mM dNTP, 2.5 µL PCR Buffer (100 mM Tris-HCl pH 8.8, 200 mM KCl, 15 mM $MgCl_2$), 1 µL each primer 10 µM, 0.125 µL in house purified Taq DNA polymerase. The PCR reaction was cycled in a GeneAmp PCR system 2700 machine (Applied Biosystems) as follows: 95 ºC for 1 min; 21 cycles {95 ºC 1 min, 50 ºC 1 min, 72 ºC 1 min}; 72 ºC for 15 min.

The PCR products were analyzed on 1% agarose gels and band intensities were quantified in arbitrary units using the Gene genius bioimaging system and Genesnap software, both from Syngene (Synoptics Ltd., Cambridge, UK). Values were expressed as percentage of maximum giving a value of 100% to the highest intensity found in each reaction.

2.15. Quantitative RT-PCR

RNA extraction and cDNA synthesis were performed as described in sections 2.6 and 2.7.

For quantitative real-time PCR the SYBR Green method was used. The qRT-PCR reactions were performed with an ABI Prism 7000 sequence detection system (Applied Biosystems)

using the default ABI prism 7000 PCR program for PCR conditions. Relative quantitation of each individual gene expression was performed using the comparative threshold cycle method, as described in the ABI PRISM 7700 Sequence Detection System User Bulletin Number 2 (Applied Biosystems). PCR reactions were carried out in triplicate in a 15 µL volume containing 7.5 µL SYBR Green 2x PCR Master Mix (Applied Biosystems), 0.45 µL each primer, 50 ng cDNA and DEPC treated water up to 15 µL.

Primers were designed for LlCyp, LlVPE4 and LlVPE5 genes (LlCypF: CTACTGCTCGTCACACTTTCAC, LlCypR: GGATATGGTATGTTGGCTGCG; LlVPE4F: GTCATGGAATACGGGAGTCTAGG, LlVPE4R: GGTTTTGGAGATGCTCGTAGC). For LlVPEs, DNA sequences were aligned through BioEdit (v. 7.0.5.3) (Hall, 1999) in order to design forward and reverse primers able to discriminate between the different clones. Primers having a 40-60% G+C content were designed to give an amplicon of 80-150 bp and to have a Tm of 58-62°C. Primers were compared to the databases using BLAST (NCBI) to verify their specificity and a normal PCR was performed to check the amplification product before proceeding with real-time quantification. Normalization was performed using the PUV primers (PUV1: ATTCCAGCTCCATAGCGTATA, PUV2: TTCCATGCTAATGTATTCAGAG), which amplify a 226 bp fragment of 18S rRNA.

To test the primers for qRT-PCR a mix of all cDNA samples (dil. 0) was prepared. The mix was then diluted with DEPC treated water to obtain 1:10 (dil. 1), 1:50 (dil. 2), 1:100 (dil. 3), 1:1000 (dil. 4) dilutions. The qRT-PCR was done in triplicate for each primer combination plus one blank in which DEPC water was added instead of cDNA. In order to asses the PCR efficiency, a standard curve of the C(t) values against the amount of template was plotted. The efficiency of PCR was calculated on the base of the slope of the curve as follow: Efficiency = $10^{(-1/Slope)}-1$.

2.16. Cloning of the full length LlCyp

The open reading frame of LlCyp was cloned using BamHI and NotI restriction sites (Forward 5'-CCGGATCCGATGGAGAACCAATCTATAC-3', Reverse 5'-ATGCGGCCGCGAGTTCATCTTTTTCTGG-3'). For the PCR reaction 3 µL of cDNA from stage T4 was mixed with 0.5 µL 10 mM dNTP, 2.5 µL PCR buffer (Tris-HCl, KCl, $(NH_4)2SO_4$, 15 mM $MgCl_2$; pH 8.7), 1 µL each primer 100 µM, 0.125 µL Hot Start Taq (Qiagen). The PCR reaction was cycled in a GeneAmp PCR system 2700 machine (Applied Biosystems) as follows: 95 ºC for 15 min; 40 cycles {95 ºC 1 min, 64 ºC 1 min, 72 ºC 2

min}; 72 ºC for 15 min.The full gene was digested as described below and cloned into pET21b vector (Novagen) and into pGreen0029 vector using T4 ligase (Promega).

2.17. Restriction Digestion

The digestion of plasmids and PCR products with restriction enzymes was carried out as follows: 2 µg of plasmid or 30 µL of PCR reaction were mixed with 4 µL of appropriate buffer, 0.4 µL 100x BSA, 1µL of enzyme (Promega) and water up to 40 µL. The reaction was incubated at 37°C for 1.5 hour. For double digestions of vector reactions with the two enzymes were performed sequentially and after digestion with the the first enzyme 5 µL of the mix were run on a 1% agarose gel to check for full digestion. The reaction mix was purified using the QIAquick Spin Column (Qiagen) following the manufacturer's instructions and the second reaction was prepared by adding components as described above and the reciprocal enzyme for each of the pair of reactions. The mix was incubated for 1.5 hours at 37°C. Afterwards, the plasmids were dephosphorylated using the following mix: 5 µL CIAP Buffer, 0.5 µL CIAP enzyme (Promega), 40 µL digested vector and water up to 50 µL. The reaction was incubated for 30 min at 37°C and, after adding 0.5 µL of CIAP enzyme, for a further 30 min at 37°C. A QIAquick Spin Column (Qiagen) was used to purify the plasmid and to stop the reaction.

2.18. Protein extraction for Coomassie gel and western blotting

Before protein extraction an appropriate amount of lysis buffer (50 mM Tris-HCl pH 7.5, 75 mM NaCl 15 mM EGTA, 15 mM $MgCl_2$, 60 mM β-glycerophosphate) was prepared by adding 42 µL 25x PI (complete protease inhibitors (Roche) dissolved in 2 mL sterile d H2O and filter sterilized), 21 µL 50x PPI (50 mM NaF, 10 mM Na_3VO_4, 100 mM $Na_4P_2O_7$) and 1.05 µL 1M DTT per mL. Then 200 mg of plant tissue from each stage were ground in a mortar with liquid nitrogen and 200 µL of lysis buffer were added. The samples were transferred into 14 ml culture tubes and were sonicated four times for 30 sec at 10 µA. The homogenized material was transferred into Eppendorf tubes and centrifuged at 14000 rpm at 4°C for 30 min in a Beckman Coulter AllegraTM 21R centrifuge fitted with a F2402H rotor. The supernatant was collected and stored at -80°C until use.

2.19. Total proteolytic activity

Protein extraction was performed by grinding tepal tissues of each stage in a mortar with one volume of ice-cold extraction buffer (Tris-HCl 50 mM pH 7.4, EDTA 1 mM, DTT 1 mM,

Triton X-100 0.1% v/v). The samples were placed in 15 mL tubes and centrifuged for 10 min at 14000 rpm at 4°C. The supernatant was collected, transferred into clean Eppendorf tubes and, if not immediately used, stored at –80°C. For the proteolytic activity assay 500 µL of the reaction mixture were prepared using 225 µL of 50 mM acetate buffer or 50 mM Na-phosphate buffer, 250 µL 0.4% (w/v) azocasein, 5 µL 0.25 M βMe and 20 µL of extract. The reaction was incubated at 37°C overnight in a water bath. Afterwards it was stopped by adding 125 µL 50% (w/v) TCA. Reaction mixtures were centrifuged at 17000xg, for 15 min, at 4°C and the absorbance at 420 nm of the samples was measured with a spectrophotometer UV-1204 (Shimadzu Europe, Gmbh). With the purpose of determining the optimum pH for the proteolytic activity, the reactions were conduced at pH 3.5, 4, 4.5, 5, 5.5 (acetate buffer) and pH 6, 6.5, 7, 7.5 (Na-phosphate buffer).

2.20. *In vitro* caspase substrate cleavage assay

For caspase assays, samples were homogenised in one volume of ice-cold extraction buffer (50 mM HEPES-KOH pH 7.0, 10% w/v sucrose, 0.1% w/v CHAPS, 5 mM DTT, 1 mM EDTA) and immediately transferred to 15 mL centrifuge tubes and centrifuged at 17000xg, for 15 min, at 4°C. The supernatant was collected and transferred into clean Eppendorf tubes and stored at -80°C until used. Caspase-like activity was assayed using the following tetrapeptide colorimetric substrate dissolved in water or DMSO depending on the tetrapeptide: Ac-YVAD-pNA, Ac-DEVD-pNA, and Ac-VEID-pNA (Sigma). Proteolytic activity was measured in 500 µL reaction mixtures containing 50 µL of extract, 75 µM colorimetric substrate buffer. To determine the optimum pH for caspase-like activity 50 mM acetate buffer (pH 3.5, 4, 4.5, 5, 5.5) and 50 mM HEPES- KOH (6, 6.5, 7, 7.5) were used. The reaction was incubated for 5 hours at 32°C in a water bath, the tubes were centrifuged at 17000xg, at 4°C, for 15 min and then the absorbance at 405 nm was measured with a UV-1204 spectrophotometer (Shimadzu Europe, Gmbh) against a blank with buffer and substrate alone. To characterize the caspase –like activity several caspase and protease inhibitors were used. After their addition the mix was incubated at 30°C for 15 min, before adding the substrates. The following inhibitors were used: 5 µM E-64, 10 µM pepstatin, 1 mM PMSF, 100 µM leupeptin, 1 mM NEM, 100 µM Ac-YVAD-CHO, 100 µM Ac-DEVD-CHO, 100 µM Ac-VEID-CHO (Sigma)

2.21. *In vitro* VPE activity assay

For VPE assays, samples were homogenised in one volume of ice-cold extraction buffer (50 mM HEPES-KOH pH 7.0, 10% w/v sucrose, 0.1% w/v CHAPS, 5 mM DTT, 1 mM EDTA) and immediately transferred to 15 mL centrifuge tubes and centrifuged at 17000xg, for 15 min, at 4°C. The supernatant was collected and transferred into clean Eppendorf tubes and stored at -80°C until used. VPE activity was assayed using Ac-AAN-MCA fluorogenic substrate which is conjugated with α-(4-methyil-cumaril-7-amide) (MCA) (Biochem). Proteolytic activity was measured in 500 µL reaction mixtures containing 10 µg of extract, 10 µM fluorogenic substrate buffer and 0.2% β-mercaptoethanol. To determine the optimum pH for VPE activity 50 mM acetate buffer (pH 3.5, 4, 4.5, 5, 5.5) and 50 mM HEPES- KOH (6, 6.5, 7, 7.5) were used. The reaction was incubated for 5 hours at 32°C in a water bath. An increase in the fluorescence was measured at 465 nm with a UV-1204 spectrophotometer (Shimadzu Europe, Gmbh) against a blank containing the extract and in which the substrate was omitted.

2.22. Bradford assay

The concentration of protein extracts was determined using a Bradford assay (Bradford, 1976) and multi-well plate or 1.5 mL cuvettes. First, protein standards were prepared by mixing 40, 20, 10 and 5 µg of BSA with 20 µL of extraction buffer. Afterwards 5 µL of each standard and sample were added to separate wells of a multi-well plate. Then 250 µL of Bradford reagent (Sigma) were added to each well and after mixing gently the samples were incubated at room temperature between 10 and 30 min and the absorbance was read at 590 nm in a UV-1204 spectrophotometer (Shimadzu Europe GmbH).

Using cuvettes, a mix was prepared with 5 µL or 10 µL of extract, 800 µL of dH_2O and 200 µL of Bradford reagent (Sigma). As standard 20, 10, 5, and 2.5 µg of BSA were used. A standard curve was drawn and the concentration of the samples was determined using the plot.

2.23. TUNEL assay

Small pieces of tissue were cut from the upper part of the outer tepals at each stage, avoiding the central midrib. The pieces were immersed in a solution of paraformaldeyde 4% in phosphate buffer pH 7.4 under vacuum for 1 hour at room temperature. Then the fixation was allowed to proceed overnight in a refrigerated chamber at 4°C. Afterwards the material was dehydrated through immersion in 30%, 50%, 75% and 100% ethanol solutions for 3 hours

each at 4°C and in 100% ethanol overnight at 4°C. The tissue was treated with increasing concentrations of xylene with incubations of 3 hours. The final incubation in 100% xylene was for 3 hours and then overnight. Subsequently the samples were embedded in Paraplast Plus paraffin (Paraplast, Sherwood Medical Industries). The paraffin, in which plant material was placed, was changed three times during the day and then left overnight in an oven at 60°C. Sections of 10 µm were cut and stretched on poly-lysine coated slides. The slides were dewaxed in xylene and then rehydrated in decreasing concentrations of ethanol before the TUNEL assay.

The TUNEL assay was performed using an "In situ cell death detection kit" (Promega) according to the manufacturer's instructions. After washes with NaCl, PBS and fixation in paraformaldeyde the samples were treated with proteinase K (20 µg/mL) for 20 min to facilitate the entry of the TdT enzyme for the reaction. For the negative control the TdT enzyme was omitted from the reaction mixture. In the positive control permeabilized sections were treated with DNase I (10 U mL^{-1}) for 10 min before assay. Toluidine blue 0.05% (w/v) in $NaCO_3$ 1% pH 8.2 was used as a counterstain. Fluorescence was detected using a Leica DMLB microscope equipped with a filter set for fluorescein and a Leica DC 300F CCD camera.

2.24. Coomassie staining

For SDS-PAGE 20 µg of proteins for each stage were used. Coomassie staining was used to detect proteins on SDS-PAGE gels. The gels were immersed in Coomassie Brilliant Blue solution (2.5 g Coomassie Brilliant Blue R-250 (Sigma), 450 mL EtOH, 100 mL acetic acid, 450 mL dH_2O) for 1 hour and then deistained in destaining solution (450 mL EtOH, 100 mL acetic acid, 450 dH_2O) for 3 hours.

2.25. Western blot

The samples from each stage were loaded on a SDS-PAGE gel and run as described in section 2.4. For western blotting a piece of Hybond-P PVDF membrane (Amersham Pharmacia Biotech) was pre-wetted in 100% MeOH for 30 sec and rinsed in dH_2O for 5 min. Afterwards the membrane, the SDS gel, sponges and filter paper were incubated in blotting buffer (20% MeOH, 0.01% SDS, 14 g/L glycine, 3 g/L Tris base) for 15 min. Then, a sandwich of sponge, 3x filter paper, SDS gel, membrane and sponge was prepared and placed in the cassette of a Mini Trans Blot Western Blotting system (Bio-Rad). The cassette was placed in the gel tank together with an ice tablet. The gel tank was filled with blotting buffer,

placed on ice and on a magnetic stirrer. The gel was run 1 hour at 100 V and then the cassette was disassembled. The PVDF membrane was placed in 25 mL blocking solution (20 mM Tris-HCl pH 7.5, 150 mM NaCl, 0.05 Tween 20 and 5% dry milk powder) and incubated on a shaking platform for 1 hour. Afterwards the membrane was rinsed in basic buffer (20 mM Tris-HCl pH 7.5, 150 mM NaCl, 0.05 Tween 20), the primary antibody SlCyp was added (1:1000) in 25 ml blocking solution and incubated for 1 hour on shaker. The membrane was rinsed twice in wash buffer (20 mM Tris-HCl pH 7.5, 150 mM NaCl, 0.05% Tween 20 and 1% triton X-100), washed once for 20 min and again twice for 5 min. The secondary antibody α-rabbit IgG (1:2500) was added in 25 mL blocking solution, the membrane was incubated for 1 hour on a shaker and afterwards washed in wash buffer as previously described. The membrane was developed using the ECL Western Blotting detection reagent (Amersham Pharmacia Biotech). The PVDF membrane was placed on cling film and 0.125 mL/cm^2 ECL solution (Solution A: Solution B (40:1)) were added. After 1 min the detection reagent was removed and the membrane was wrapped in cling film and placed in a X-ray cassette (GRI Molecular Biology). A piece of HyperfilmTM ECL (Amersham Biosciences) was placed on top of the PVDF membrane and exposed for 2 min. The film was developed using a Curix 60 developer (Agfa).

2.26. Tissue preparation for microscopy

Pieces (2x2 mm) from the margin and the central region of the outer tepals at stage T0, T3 and T5 were prepared for electron and light microscopy. Tissue infiltration was carried out using LR White acrylic resin (LRW) (Agar Scientific Ltd., Stansted, UK) at 4°C or low temperature embedding resin (Lowicryl HM20 consisting of 2.98 g Crosslinker, 17.02 g Monomer, 0.10 g Initiator) (Agar Scientific Ltd., Stansted, UK).

For LRW infiltration, flower tissues were incubated for 1.5 hr at room temperature in a mixture of 3% (v/v) formaldehyde and 3% (v/v) glutaraldehyde in phosphate buffer pH 7.4. Samples were washed twice in phosphate buffer for 15 min and post-fixed in 2% (w/v) OsO_4 in phosphate buffer pH 7.4 for 1.5 hr at room temperature. After two washes of 10 min in distilled water, samples were dehydrated in 70% ethanol (1 hr), 90% ethanol (1 hr) and 100% ethanol overnight, at 4°C. After washing in 100% ethanol, samples were infiltrated in ethanol and LRW 1:3 (1 hr), 100% LRW for three times (1 hr each) and left over-night in 100% resin at 4°C. Samples were embedded in gelatine capsules and polymerised for 48 h at 4°C.

For the Lowicryl resin infiltration, a progressively lowering temperature (PLT) method was used and the procedure was as follows: petal pieces were washed in phosphate buffer and

infiltrated in a mixture of 2% paraformaldehyde, 1% glutaraldehyde and 0.5% OsO_4 in phosphate buffer (pH 7.4), for 1 hr at 4°C. Samples were washed twice (2x15 min) in a cryoprotectant solution (0.05M phosphate buffer pH 7.4, containing 25% sucrose and 10% glycerol) at 4°C and then immersed in 30% ethanol in the cryoprotectant for 30 min at 4°C. Afterwards, the tissues were transferred into an automated freeze substation chamber (Reichert AFS, Leica Co. Ltd) at -25°C and dehydrated in 50% ethanol (30 min), 70% ethanol (30 min) and three changes of 100% ethanol (each for 30 min). Samples were then infiltrated in the following graded series of Lowicryl HM20 concentrations: ethanol 1:1 (over-night), 2:1 (30 min), 3:1 (30 min) and pure Lowicryl HM20 (4x30 min). The resin infiltrated tissues were transferred to fresh resin under UV light for 24 hr at -25°C; the temperature was gradually increased up to 20°C, and the resin blocks were polymerised under UV light for a further 24 hr.

Thin sections (100 nm) were cut with a diamond knife on an ultracut microtome (Reichter E, Leica Co., Ltd., UK). For light microscopy examination, the thin sections were placed onto polylysine-coated slides. For transmission electron microscopy, the sections were collected on pioloform-coated copper or nickel grids (200 square mesh) and counterstained for 10 min in drops of 2% (w/v) uranyl acetate solution. After two washes in distilled water, the grids were placed in Reynold's lead citrate (1.33g $Pb(NO_3)_2$, 1.76 $Na_3(C_6H_5O_7)2H_2O$, distilled water up to 30 mL) for 5 min and then washed twice with distilled water before being examined in a Philips EM 208 transmission electron microscope (FEI Ltd., Eindhowen, The Netherlands) at 80 kV accelerating voltage.

2.27. Immunocytochemistry

The whole procedure was carried out on 10 µL drops on Parafilm. During transfer, excess liquid was removed with filter paper. Thin sections on nickel grids were incubated for 15 min in freshly prepared 5% (w/v) sodium periodate to remove osmium and then washed through five changes of distilled water. Grids were incubated for 5 min in 0.1 N HCl and washed again three times in distilled water. Blocking was performed in drops containing 0.5% (w/v) BSA, 0.05% (v/v) Tween 20 and 0.05% (v/v) glycine in PBS (10 mM phosphate, 0.15 M NaCl). Grids were then transferred to drops of affinity-purified rabbit-anti SlCysEP IgG (diluted 1:50 in blocking solution; Senatore *et al.*, 2009), and incubated overnight at 4°C. After washing through three changes in blocking solution, the grids were incubated for 2 h at room temperature with secondary antibody, goat anti-rabbit IgG conjugated to 10 nm gold (Biocell Co. Ltd. Cardiff, UK), diluted 1:100 in blocking solution. The grids were washed in

PBS 3 x 1 min and fixed for 3 min in 2% (v/v) glutaraldehyde in PBS. Grids were then rinsed in distilled water, stained with 2% (w/v) uranyl acetate (10 min at room temperature) and Reynold's lead citrate (5 min at room temperature; Reynolds, 1963) before being examined in a Philips EM 208 electron microscope at 80 KV accelerating voltage. Control grids were treated identically using pre-immune rabbit antiserum instead of primary antibody.

2.28. Preparation of the YFP construct

In order to discover the subcellular localization of KDEL-tailed LlCyp protein, the gene was fused with a yellow fluorescent protein (YFP). For the SP-LlCyp-YFP construct, the full gene was amplified using BamHI and NotI restriction sites as described in section 2.17.and inserted in the pGreen based vector 35S-YFP-nosT. Digestion and ligation reactions were carried out as described in section 2.8 and 2.10.

2.29. Protoplast preparation and transient expression

For sterile cultures, seeds were treated with a solution of sodium hypochlorite 10% (v/v) for 5 min, ethanol mix (Ethanol 70%, distilled water 10%, and sodium hypochlorite 20%, v/v) for 5 min. After thorough washing with SDW (3 times for 5 min) the seeds were sown onto Petri dishes containing M&S medium (4.708 g L-1 of M&S (Duchefa Biochemie) 30 g L-1 of sucrose and 1% agar, pH 5.7). The plated seeds were left at 4ºC for 48 h to ensure uniform germination, and then moved to the growth chamber at 21ºC, and grown under 16 h light and 8 h dark for three weeks. Arabidopsis seedlings were transferred to Petri dishes with 15-20 mL of enzyme solution (0.5% cellulose Yacult, Japan), 0.2% macerozyme (Yacult, Japan) in K3 medium with 0.4 M sucrose at pH 5.6-5.8 (Stock solutions: 10xB5 medium including vitamins, 200x MES (0.1g/ml), 500x myo-inositol (0.05g/ml), 100x NH_4NO_3 (25 mg/ml), 100x $CaCl_2{\cdot}2H_2O$ (75 mg/ml), 100x D-xylose (25mg/ml)) and cut with a scalpel. Plates were incubated overnight in the dark. The enzyme solution was removed with a sterile Pasteur pipette, 10 mL K3 medium were added and the plates were gently swirled to release the protoplasts. Protoplasts were filtered through a 30 µM nylon filter and transferred into sterile round bottom tubes. After 1 hour protoplasts floated to the top of the solution. Protoplasts were transferred with a sterile Pasteur pipette into new tubes and 5 mL of K3 medium were added. Protoplasts were allowed to float again and another wash with K3 medium was made. The bottom layer was removed and 2 mL of protoplast suspension medium (0.4 M mannitol, 20 mM $CaCl_2*2H_2O$, 5 mM MES, pH 5.7) were added. 250 µL of suspended protoplasts were mixed with 10-20 µg of plasmid DNA and an equal volume of PEG solution (40% PEG

4000 (FLUKA), 0.4 M mannitol, 100 mM $Ca(NO_3)_2$, pH 7) was added. The spRFP-AFVY construct was used as vacuolar marker. After 30 min at room temperature 2 mL of K3 medium were used to dilute the PEG solution and the tubes were allowed to stand for 1-2 hours. The solution under the protoplast layer was aspired, 2 mL of K3 medium were added and the solution was incubated overnight at RT in the dark. Transient expression was studied by confocal laser scanning microscopy using a Leica TCS SP2 AOBS spectral confocal microscope (Leica Microsystems GmbH, Wetzlar, Germany). YFP was excited at 514 nm and detected in the 525- to 583-nm range. RFP was excited at 543 nm and detected in the 553- to 638-nm range. Chlorophyll autofluorescence was detected in the 660- to 700-nm range.

2.30. Agroinfiltration

Leaves from 4–6-week-old *Nicotiana tabacum plants* were used for agroinfiltration, as described previously (Batoko *et al.*, 2000). Each expression vector was introduced into *A. tumefaciens* strain GV3101. A single colony from the transformants was used to inoculate 2 mL of YEB medium (per liter: 5 g of beef extract, 1 g of yeast extract, 5 g of sucrose, and 0.5 g of $MgSO_4 \cdot 7H_2O$). The bacterial culture was incubated at 28 to 30°C with agitation until reaching the stationary growth phase. One mL of culture was transferred into an Eppendorf tube, and the bacteria were pelleted by centrifugation at 2200*g* for 5 min in a microcentrifuge at room temperature. The pellet was washed twice with 1 mL of the infiltration buffer (50 mM Mes, pH 5.6, 2 mM Na_3PO_4, 0.5% glucose [w/v], and 100 mM acetosyringone [Aldrich]) and then resuspended in 1 mL of the same buffer. The bacterial suspension was diluted with infiltration buffer to adjust the inoculums concentration to the stated final OD_{600} value. The inoculum was delivered to the lamina tissues of tobacco leaves by gentle pressure infiltration through the stomata of the lower epidermis, by using a 1-mL syringe without a needle. For experiments requiring co-infection of more than one construct, bacterial strains containing the constructs were mixed before performing the leaf infection, with the inoculum of each construct adjusted to the required final OD_{600}. The infected area of the leaf was delimited and labelled with an indelible pen, and the plant was incubated under normal growing conditions for 2–3 days at 25°C in daylight before observation. Small sections of infiltrated leaves were placed on a microscope slide using double-sided tape and visualized without a coverslip with a 63× water immersion objective attached to a Leica SP2 AOBS confocal laser scanning microscope. YFP was excited at 514 nm and detected in the 525- to 583-nm range. RFP was excited at 543 nm and detected in the 553- to 638-nm range.

2.31. Heterologous expression

For heterologous expression of LlCyp gene 10 mL of LB medium were inoculated with *E. coli* BL21 containing the expression vector pET21b and incubated overnight in an orbital shaker at 200 rpm.

The overnight culture was used to inoculate 100 mL of fresh LB medium to an OD_{600} of 0.05-0.1 (~1:20 dilution of the overnight culture). The culture was incubated at 37°C 200 rpm until an OD_{600} of 0.4 had been reached. Afterwards, the expression was induced adding IPTG (Sigma) to a final concentration of 0.5 mM and incubating overnight at 22°C. After collecting the cells by centrifugation at 6000xg 10 min at 4°C, the supernatant was discarded and the pellet resuspended in 2 mL lysis buffer. Lysozyme was added to a final concentration of 1 mg/ml and the solution was incubated on ice for 1 hour. After sonication for three times, 30 s at 10 mÅ, samples were transferred into Eppendorf tubes. The tubes were centrifuged for 30 min, at 13000 rpm, 4°C and the supernatant was transferred into fresh Eppendorf tubes. The supernatant was checked by SDS gel electrophoresis and with western blotting using the antibody raised against tomato SlCyp.

2.32. Extraction and purification of free indolacetic acid

For free indolacetic acid (IAA) quantification, approximately 2 g of floral tissue were used for each stage. Samples were homogenised with a mortar and pestle in cold 70% (v/v) acetone (1:5 w/v). The homogenate was supplemented with 50 ng of $[^{13}C]_6$IAA (Olchemim Ltd) as an internal standard, then stirred for 4 h at 4°C, before centrifugation at 2000 g for 15 min. The supernatant was recovered and stored at 4°C while the pellet was re-extracted twice (4 hr each extraction) and then left overnight stirring at 4°C. The supernatant containing solvent was reduced to the aqueous phase (approximately to a volume of 10 mL) under vacuum at 35°C, adjusted to pH 2.8 with 0.1 N HCl and partitioned 5 times against equal volumes of ethyl ether. The pooled ethyl ether extracts were kept at –20°C overnight, to freeze and separate traces of water. Ethyl ether was then evaporated, the dried samples were dissolved in a small volume of 10% (v/v) aqueous acetonitrile containing 0.1% (v/v) acetic acid and purified by HPLC.

2.33. Extraction and purification of gibberellins

For gibberellin (GA) quantification, 3 g of floral tissue were used for each stage. Samples were homogenised with a mortar and pestle in cold 80% (v/v) methanol (1:5 w/v). The homogenate was supplemented with 50 ng of deuterated GA_9, GA_4, GA_{34}, GA_7, GA_{51} and

100 ng of deuterated GA_{19}, GA_{20}, GA_1, GA_8, GA_5, GA_3, GA_{29} (Olchemim Ltd) as internal standards, then stirred for 4 h at 4°C, before centrifugation at 2000 g for 15 min. The supernatant was recovered and stored at 4°C while the pellet was re-extracted twice (4 hr each extraction) and then left overnight stirring at 4°C. The supernatant containing solvent was reduced to the aqueous phase (approximately to a volume of 10 mL) under vacuum at 35°C, adjusted to pH 2.8 with 0.1 N HCl and partitioned 5 times against equal volumes of ethyl acetate. The pooled ethyl acetate extracts were kept at –20°C overnight, to freeze and separate traces of water. Ethyl acetate was then evaporated, the dried samples were dissolved in a small volume of 10% (v/v) aqueous acetonitrile containing 0.1% (v/v) acetic acid and purified by HPLC.

2.34. Extraction and purification of abscisic acid

For abscisic acid (ABA) quantification, approximately 1.5 g of floral tissue were used for each stage Samples were homogenized in cold 80% (v/v) methanol. The homogenate was supplemented with a suitable amount of $[^2H]_6$ABA (Olchemim Ltd) as internal standard, then the extraction followed the same procedure described for GAs. After partitioning, the dried samples were resuspended in a small volume of 10% (v/v) aqueous acetonitrile containing 0.05% (v/v) acetic acid and purified by HPLC.

2.35. HPLC

Samples for GAs and IAA were purified by reverse phase HPLC using a Kontron PUMP 422 (Kontron, Germany).

For the IAA, the detector was operated at 254 nm wavelength. A C18 Hypersil column (Thermo) 150 x 4.6 mm i.d. particle size 5 µm, eluted at a flow rate of 1 mL min^{-1} was used. Samples were applied to the column and the fraction containing IAA was collected while the column was being eluted with a linear gradient of acetonitrile in water and 0.1% acetic acid, from 10% to 30% for 15 min and then from 30% to 100% in 40 min. The fraction was dried under vacuum, dissolved with 30% (v/v) aqueous methanol containing 0.5% (v/v) acetic acid and purified by HPLC equipped with a Nucleosil $N(CH_3)_2$ column (Macherey-Nagel) and eluted with a flow rate of 1 mL min^{-1}. Samples were applied to the column and the fraction containing IAA was collected while the column was being eluted continuously with 30% (v/v) methanol in water containing 0.5% (v/v) acetic acid.

The fractions containing IAA were dried, eluted with 250 µL of 100% acetone and transferred into capillary tubes and dried under vacuum. After adding 100 µL of 100% diazomethane the capillary tubes were dried to remove water residues and silylated with bis(trimethylsilyl)trifluoroacetamide containing 1% trimethylchlorosilane (Sigma) for 1 hr at 70°C.

For the GAs, the detector was operated at 216 nm wavelength. A C18 Hypersil column (Thermo) 150 x 4.6 mm i.d. particle size 5 µm, eluted at a flow rate of 1 mL min^{-1} was used. Samples were applied to the column and six fractions containing GAs were collected while the column was being eluted with a linear gradient of acetonitrile in water and 0.1% acetic acid, from 10% to 30% for 15 min and then from 30% to 100% in 40 min. The fractions were dried under vacuum, dissolved with 30% (v/v) aqueous methanol containing 0.5% (v/v) acetic acid and purified by HPLC equipped with a Nucleosil $N(CH_3)_2$ column (Macherey-Nagel) and eluted with a flow rate of 1 mL min^{-1}. Samples were applied to the column and the fractions containing GAs were collected while the column was being eluted continuously with 30% (v/v) methanol in water containing 0.5% (v/v) acetic acid.
The fractions were dried, eluted with 250 µL of 100% methanol, transferred into capillary tubes and dried under vacuum. After adding 100 µL of 100% diazomethane the capillary tubes were dried to remove water residues and silylated with bis(trimethylsilyl)trifluoroacetamide containing 1% trimethylchlorosilane (Sigma) for 1 hr at 70°C.

For ABA, the detector was operated at 254 nm wavelength. A C18 Hypersil column (Thermo) 150 x 4.5 mm i.d. particle size 5 µm, eluted at a flow rate of 1 mL min-1 was used. Samples were applied to the column and elution was with a linear gradient of acetonitrile in water supplied with 0.05% acetic acid, from 10% to 30% in 15 min and then from 30 to 100 in 10 min. The fraction corresponding to the elution volume of ABA standard was dried under vacuum, redissolved in a suitable volume of diethyl ether, dried under vacuum and methylated by homemade ethereal diazomethane.

2.36. GC-MS

Gas chromatography-mass spectrometry analysis was performed on a Saturn 2200 quadrupole ion trap mass spectrometer coupled to a CP-3800 gas chromatograph (Varian,

Palo Alto, CA) equipped with a MEGA 1 capillary column (MEGA, Legnano, Italy) 25 m x 0.25 mm ID x 0.25 mm film thickness, coated with 100% dimethylpolysiloxane. The injection was splitless with 2 min purge off, at 250°C. The temperature of the transfer line between the gas chromatograph and the mass spectrometer was set at 250°C.

For IAA analysis, oven temperature was 120°C for 2 min, followed by a gradient from 120°C to 190°C at 35°C min^{-1}, then from 190°C to 210°C at 6°C min^{-1} and a final ramp from 210°C to 300°C at 35°C min^{-1} with a final hold of 10 min. Full scan mass spectra were obtained in EI+ mode with an emission current of 30 μA, an axial modulation of 4 V and the electron multiplier set at –1500 V. Data acquisition was from 70 to 350 Da at a speed of 1.4 scan s^{-1}. The following ions were monitored for IAA analysis: m\z 202 and 319 for IAA, and 208 and 325 for the 13C-labelled internal standard. Quantification of IAA was carried out by reference to a calibration plot obtained from the GC-MS analysis of a series of mixtures of the standard hormone with its labelled form.

For analysis of GAs, the oven temperature was maintained at 80°C for 2 min and increased to 300°C at a rate of 20°C min^{-1}. Injector and transfer line were set at 250°C and the ion source temperature at 200°C. Full scan mass spectra were obtained in EI+ mode with an emission current of 10 μA and an axial modulation of 4 V. Data acquisition was from 150 to 600 Da at a speed of 1.4 scan s^{-1}. The different gibberellins were identified by comparison of full mass spectra with those of authentic compounds. Quantification was carried out by reference to standard plots of concentration ratios versus ion ratios, obtained by analysing known mixtures of unlabeled and labelled GAs.

Data for each sample are the mean of three replicates ± SD; the value of each replicate was calculated by averaging the values of the corresponding three subsamples.

For ABA analysis, oven temperature was 120°C for 2 min, followed by a gradient from 120°C to 190°C at 35°C min^{-1}, then from 190°C to 210°C at 6°C min^{-1} and a final ramp from 210°C to 300°C at 35°C min^{-1} with a final hold of 10 min. Full scan mass spectra were obtained in EI+ mode with an emission current of 30 μA, an axial modulation of 4 V and the electron multiplier set at –1500 V. Data acquisition was from 70 to 350 Da at a speed of 1.4 scan s^{-1}. The following ions were monitored for ABA analysis: m\z 190 and 162 for IAA, and 194 and 166 for ^{13}C-labelled internal standard. Quantification of ABA was carried out by reference to a calibration plot obtained from the GC-MS analysis of a series of mixtures of the standard hormone with its labelled form.

2.37. Statistical analysis

Data were analyzed with GraphPad Prism 5, using ANOVA and "Newman-Keuls Multiple Comparison Test".

3. RESULTS

3.1 Progression of flower opening and senescence in lily

To establish a useful system for holding lily flowers, vase life was evaluated both in isolated flowers cut above the last leaf and flowers with a stem of 80 cm. No differences were found in flower longevity, and flowers without leaves were used for the experiments.

An easily identifiable stage in which flower tips begin to separate and anthers begin dehiscence was chosen as reference (Fig1A and B). Each flower takes 10 d to complete its development from opening bud to complete tepal senescence.

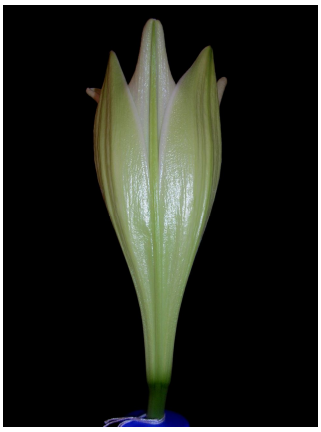

A

B

Fig.1. Lily flowers at stage T0. Tepals begin to separate (A) and anthers begin to dehiscence (B).

Six stages were identified based on number of days after the reference stage: 2 days (T2), 3 days (T3), 4 days (T4), 5 days (T5), 7 days (T7), 10 days (T10) after the reference stage. An additional stage corresponding to the harvest time was designed T-2 (Fig. 2). At stage T4 the increase in tepal translucence was the first visible sign of senescence, which became clearly evident at stage T5.

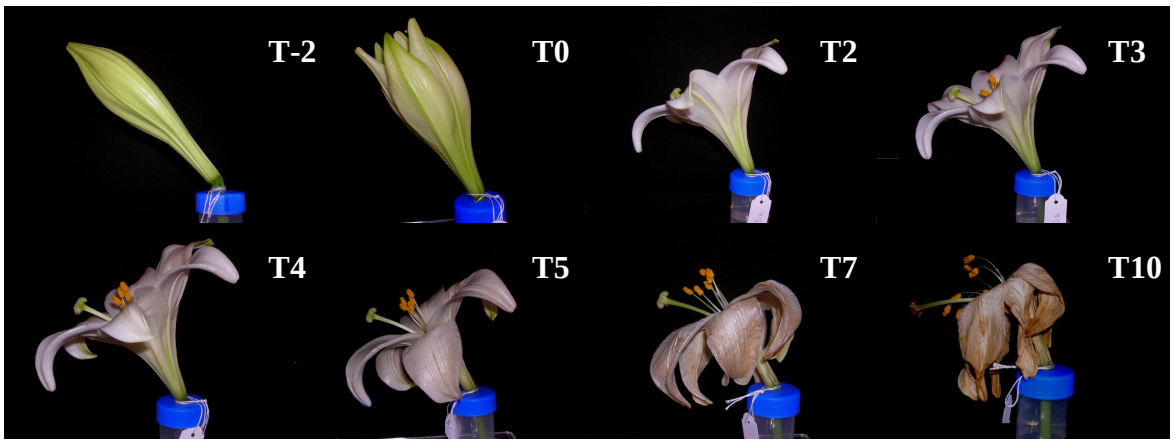

Fig. 2. Lily flower stages, from close bud to complete senescence

Since all floral organs, including tepals, are derived from leaves we might expect commonality in their senescence mechanism (Price *et al.*, 2008). Few of our analysis were carried out also using leaf tissues undergoing senescence. We identified three stages based on leaf colour: green leaves (G), light green leaves with a visible decrease in chlorophyll content (YG) and completely yellow leaves (Y).

In order to increase vase life and modify the progression of flower senescence, flowers were treated with different compounds at different concentrations (Tab.1). Suitable molecules were selected on the basis of their role in mediating programmed cell death and senescence in plant systems.

Compound	**Concentration**
α, α – Trehalose	30-300 mM
Zinc chloride ($ZnCl_2$)	1-5 mM
Lanthanum(III) chloride hydrate ($LaCl_3$ x H_2O)	1-5 mM
E-64	25 µM
3-Amino-1,2,4-triazole (3-AT)	2 nM
Calcium chloride ($CaCl_2$)	1-5 mM
L-NAME	300 µM
Sucrose	30-300 mM

Tab.1. Chemicals assayed to delay lily flower senescence. All chemicals were dissolved in water and applied in the vase solution.

Flower vase life expressed as a percentage of the control (distilled water) was significantly increased by addition of trehalose and sucrose, but in the case af trehalose and sucrose only at 300 mM and not at 30 mM. The increase in flower longevity was about 12% for both trehalose and sucrose treated flowers. Lanthanum chloride and 5 mM zinc chloride reduced flower longevity drastically while all other treatments had no effect or slightly reduced vase life (Fig. 3).

To understand the role of flower organs during lily flower senescence, stamen and ovaries were selectively removed from flowers at stage T0. A hole was made at the base of the tepals to remove the ovary and vase life was measured against a control processed in the same way (Fig.4). The treatments had no effect on flower longevity (Fig. 5).

Fresh and dry weight for each flower developmental stage were determined for outer and inner tepals held in water (control) or sucrose solution. Tepal fresh weight of control flowers increased until stage T2 and subsequently decreased sharply, reaching the minimum value at

complete tepal senescence (Fig. 6). In outer tepals, the loss of weight was slightly faster then in inner tepals suggesting a precocious progression of senescence in the outer whorl. This was confirmed by visual signs of senescence appearing before in outer tepals (Fig. 7).

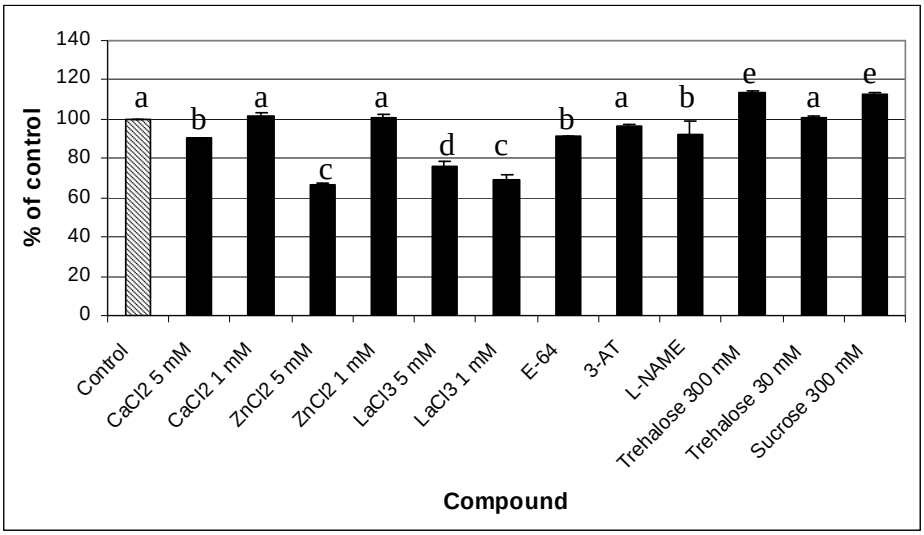

Figure 3. Effect of chemicals on the time course of tepal senescence. Error bars represent ±SD (n=3). Means with different letters are significantly different at $P<0.05$.

Figure 4. Ovary was removed throughout a hole at the base of outer tepals.

Figure 5. Control flowers (A), flowers without ovary and stamen (B) and flowers without stamen (C).

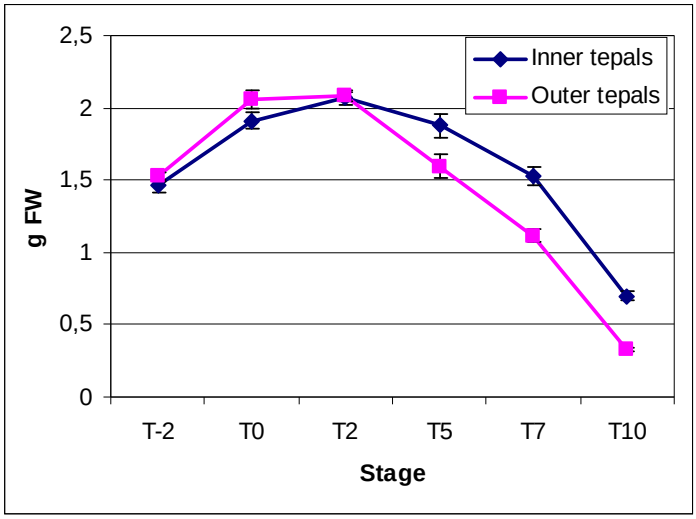

Figure 6. Fresh weight (FW) of lily flower during development and senescence. Error bars represent ± SE (n=6).

Figure 7. Control flower at stage T5. Senescence is clearly evident in outer tepals showing browning and wilting. Inner tepals look translucent but without browning and reduced wilting.

No differences in dry weight were observed between inner and outer tepals both in control and treated flowers. A decrease in dry weight was measured after stage T2. Dry weight was consistently higher in the tepals of flowers held in the sucrose solution compared with control flowers (Fig. 8A and B). The differences were statistically significant, unless stage T-2 and T4 ($P<0.05$).

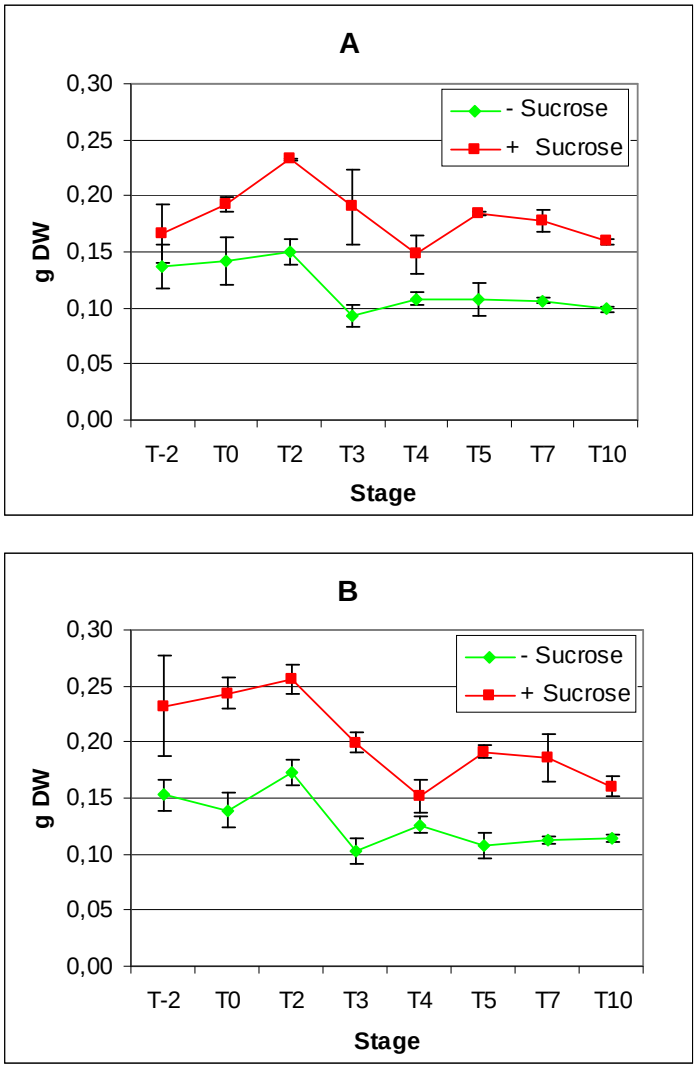

Figure 8. Dry weight (DW) of inner (A) and outer (B) tepals from control and sucrose treated flowers. Error bars represent ± SE (n=3).

In control flowers, the dry weight-fresh weight ratio did not change until stage T5 remaining similar in inner and outer tepals (Fig. 9A). The ratio sharply increased in outer tepals after stage T7 indicating a dramatic decrease in water content. In inner tepals the increase was less evident confirming that senescence starts earlier or is faster in outer tepals. In sucrose treated flowers, dry weight-fresh weight ratio was constant until stage T5 (Fig 9B). The increase in the ratio starting from stage T7 was less steep than in control flowers suggesting a lower rate of water loss from the tissues.

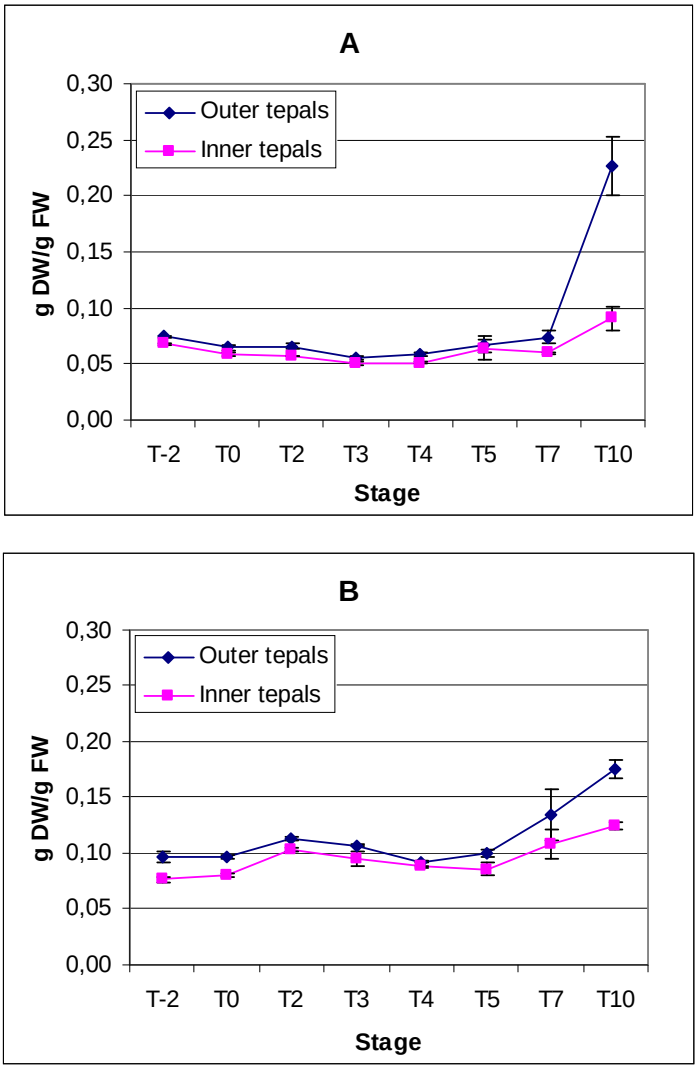

Figure 9. Dry weight-fresh weight ratio in control (A) and sucrose treated (B) flowers. Error bars represent ± SE (n=3).

Dry weight-fresh weight ratio was significantly ($P<0.05$) higher in flowers held in sucrose reflecting the higher content in dry matter (Fig 10A and B). In outer tepals, the increase in ratio after stage T5 was less sharp in sucrose treated flowers that showed a delay of flower senescence. In inner tepals there were no differences in the pattern of dry weight-fresh weight ratio (Fig. 10B).

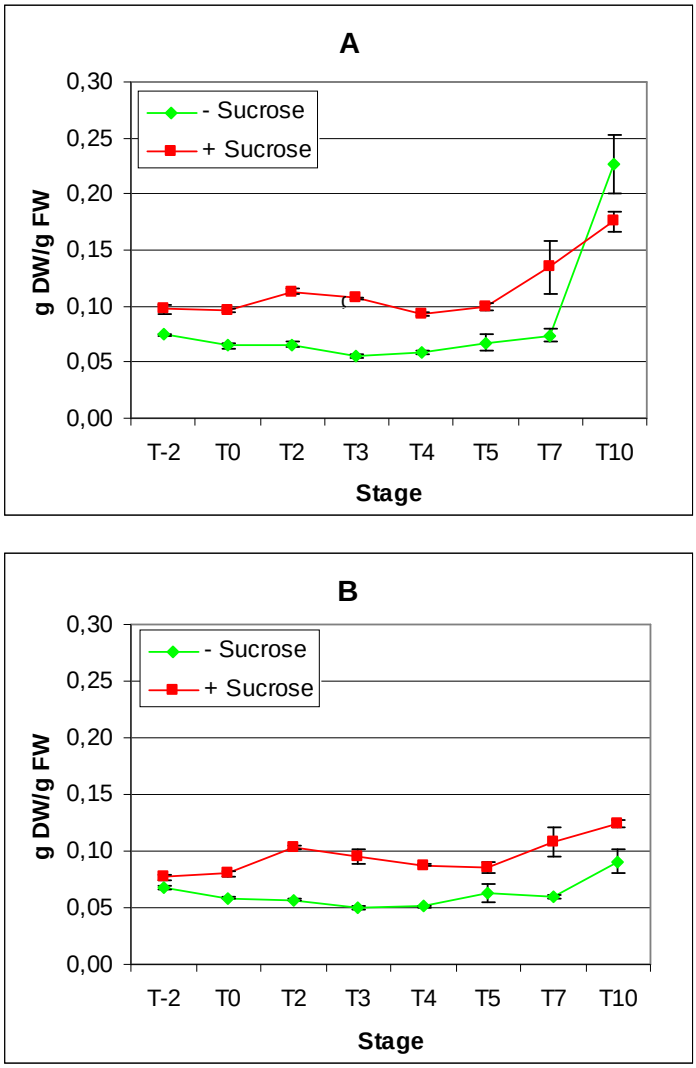

Figure 10. Dry weight/fresh weight ratio in outer (A) and inner (B) tepals. Error bars represent ± SE (n=3).

To better define the timing of lily flower senescence, we measured the release of electolites from the tepal surface. The increase of electrolyte leakage from tissues is the result of the loss of membrane permeability due to changes in the composition of fatty acids and proteins, and may be used to monitor the progression of senescence (Leverentz *et al.*, 2002).

Discs cut from outer tepals 48 hr before flower opening (stage T-2) and floated on distilled water showed a slow rate of ion leakage until day 4 (corresponding at stage T2) (Fig. 11). After that stage, the leakage rate increased reaching a maximum of 38 µS by 10 d (stage T7). In completely senescent flowers the ion leakage decreased. A similar pattern of ion leakage was observed in inner tepals (Fig 11). In this case, the ion efflux was constant until day 5 (stage T3) and increased steeply from day 6 reaching a maximum of 56 µS by 10 d. In the latest stages of senescence the leakage rate decreased. In spite of their similarity from a morphological point of view the two tepal whorls of the lily flower show a different

behaviour in terms of progression of senescence. For our study we decided to carry on experiments using only outer tepals because they are the first to undergo senescence.

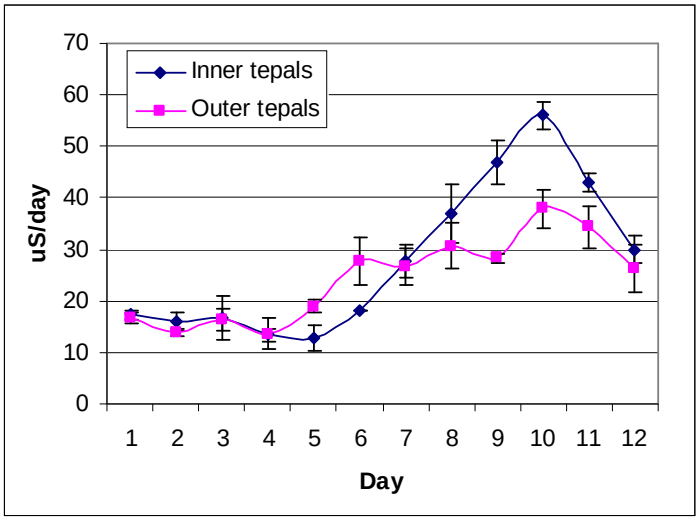

Figure 11. Ion leakage from inner and outer tepals of flowers held in water. The leakage rate is expressed as µS per day. Error bars represent ± SE (n=3).

3.2. Endogenous hormone quantification

For hormonal analysis flowers were sampled at stage T-2, T0, T2, T5, T7 and T10. Extracts from lily tepals were first purified through HPLC and then analyzed by GC/MS. Free indolacetic acid, abscisic acid and gibberellins were determined with the aim of understanding the role of hormones other than ethylene in lily flower senescence.

The pattern of free indolacetic acid content was not significantly different when it was expressed per fresh weight (data not shown), dry weight or per tepal (Fig. 12). IAA decreased soon after flower opening and increased steeply in flowers in advanced stage of senescence reaching the maximum value at stage T10 in completely wilted tepals.

Abscisic acid level throughout the senescence process showed differences when expressed per fresh weight, dry weight or per tepal (Fig. 13). When expressed per fresh weight ABA was shown to increase significantly ($P<0.05$) during senescence (T7, T10) reaching the maximum value at stage T10 (Fig. 13A). Because of the steep decrease in tepal fresh weight during senescence ABA content was also expressed per dry weight and per tepal. When expressed per dry weight, ABA content significantly ($P<0.05$) increased during senescence (Fig. 13B), even though there was no difference in ABA level between senescing stages (T5,T7,T10). The differences in endogenous ABA level during flower development end senescence were less evident when ABA content was expressed per petal (Fig. 13C). An increase was only measured at stage T7 and stage T10 but it was not statistically significant.

During flower opening and in early senescing stages there were no differences in ABA content.

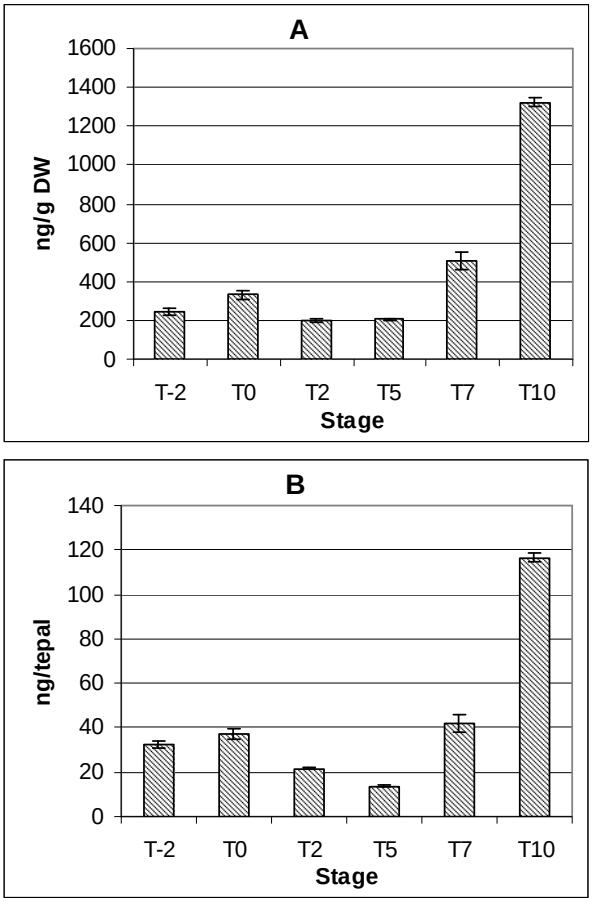

Figure 12. Endogenous free IAA in outer lily tepals during flower development and senescence. IAA is reported as ng/g DW (A) or ng per tepal (B). Error bars represent ±SE (n=3).

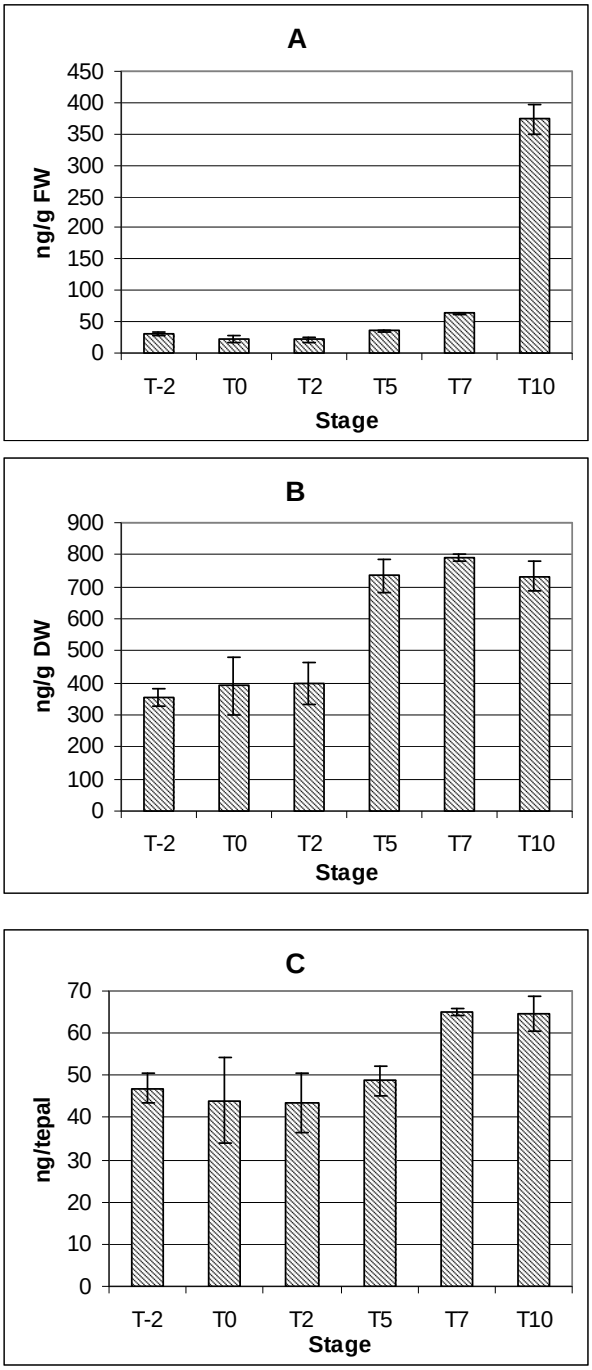

Figure 13. Endogenous ABA in outer lily tepals during flower development and senescence. ABA is reported as ng/g FW(A), ng/g DW(B) and ng/tepal (C). Error bars represent ±SE (n=3).

After fractionation of extracts by reverse phase HPLC, seven 13-hydroxylated GAs and five non-13-hydroxylated GAs were identified (Table 2), based on a comparison of full scan mass spectra and KRIs with those obtained for standard GAs.

The amount of endogenous GAs varied from 14.24 ng/g DW for GA_1 in senescing flower to 493,16 ng/g DW for GA_7 at stage T0 and flowers harvested at different stage showed a considerable variation in GA content (Fig. 14 and Fig. 15). The prevalent biosynthetic

pathway in lily seemed to be the non-13-hydroxylated and the major active molecule appeared to be GA_7 (Fig. 15). The amount of bioactive GA_4, GA_7, GA_1 and GA_3 decreased after flower opening and during senescence. Also GA_{19}, GA_{20} and GA_9 decreased after flower opening indicating a reduction of gibberellin biosynthesis. The same results were obtained by expressing GAs content per fresh weight or per petal (data not shown).

13-OH pathway	**Non-13-OH pathway**
GA_{19}	GA_9
GA_{20}	GA_4
GA_1	GA_{34}
GA_8	GA_7
GA_5	GA_{51}
GA_3	
GA_{29}	

Tab. 2. 13-hydroxylated GAs and non-13-hydroxylated GAs identified in lily tepals.

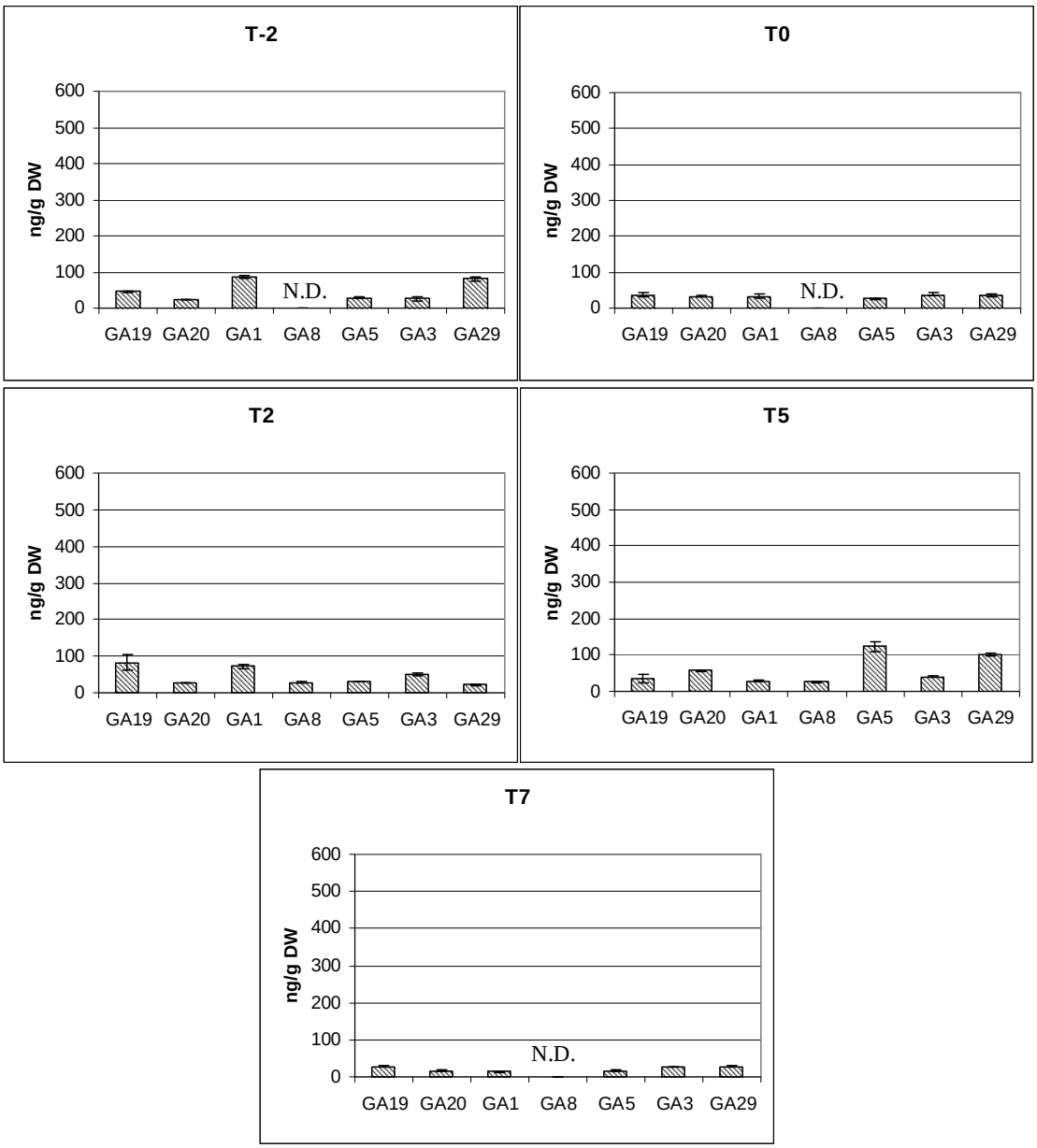

Figure 14. Endogenous levels (ng/g DW) of 13-hydroxylated GAs in outer lily tepals during flower development and senescence. N.D., undetectable. Error bars represent ±SE (n=3).

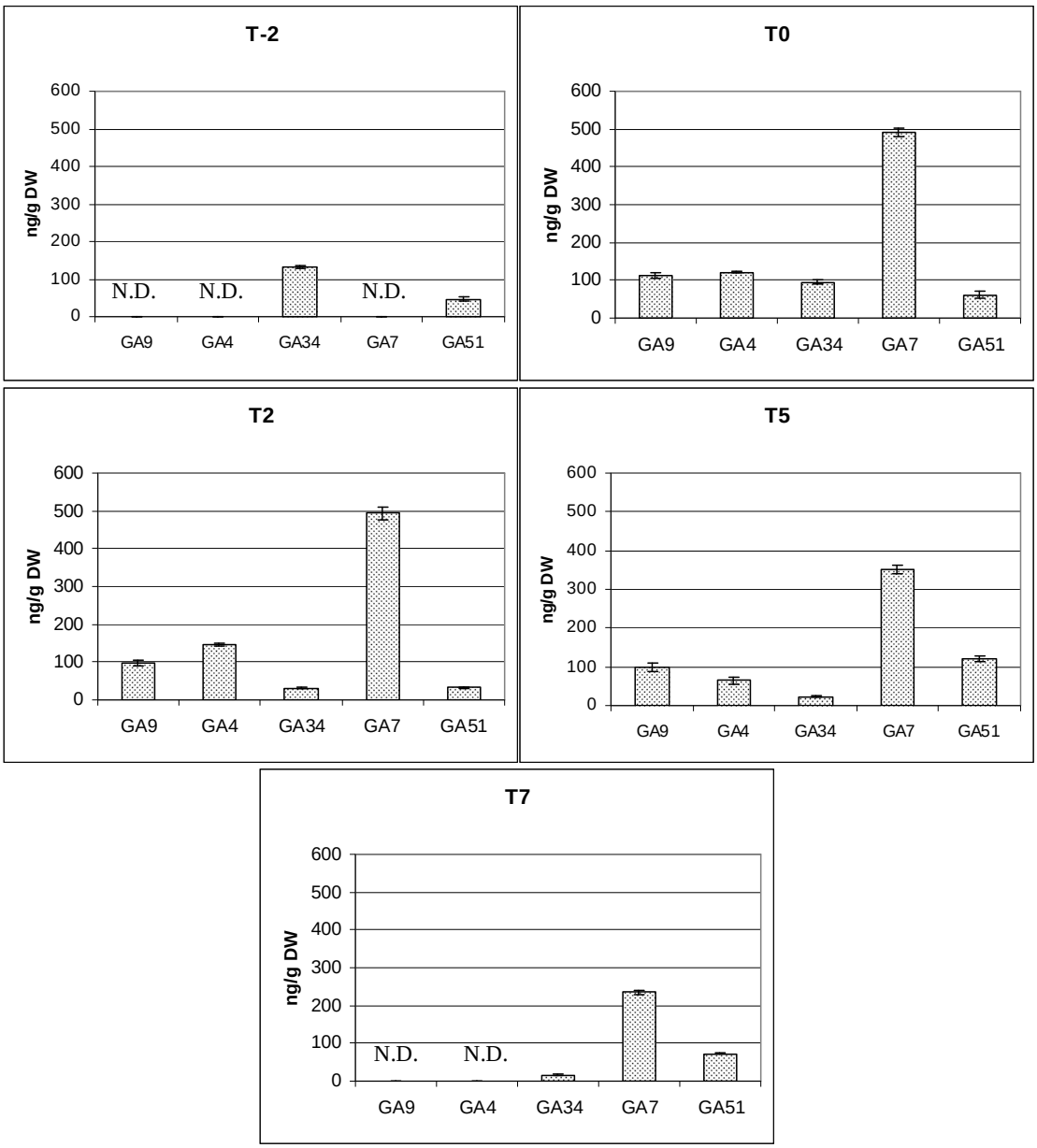

Figure 15. Endogenous levels (ng/g DW) of non-13-hydroxylated GAs in outer lily tepals during flower development and senescence. N.D., undetectable. Error bars represent ±SE (n=3).

3.3. Flower structure

Sections of toluidine blue-stained lily tepals are shown in Fig. 16B (tepal margin) and Fig. 16C (inner tissue), along with photographs of the whole flower at corresponding developmental stages (Fig. 16A). Flowers at the early opening stage (T0) had well defined upper and lower epidermis and a mesophyll rich in free spaces both in the margin and inner tissues. In the margin, the mesophyll layer became progressively disordered as the flower reached full bloom (T3) and started to senesce. Upper epidermis remained intact through flower opening and senescence while lower epidermis lost its organization and appeared

already completely degraded at full bloom. In the inner region of the tepal, mesophyll cells lost their organization after flower opening. At stage T5, coinciding with visible signs of senescence, mesophyll structure completely collapsed with intact vascular tissues existing within a compressed strip of parenchyma cells, while both upper and lower epidermis appeared still intact.

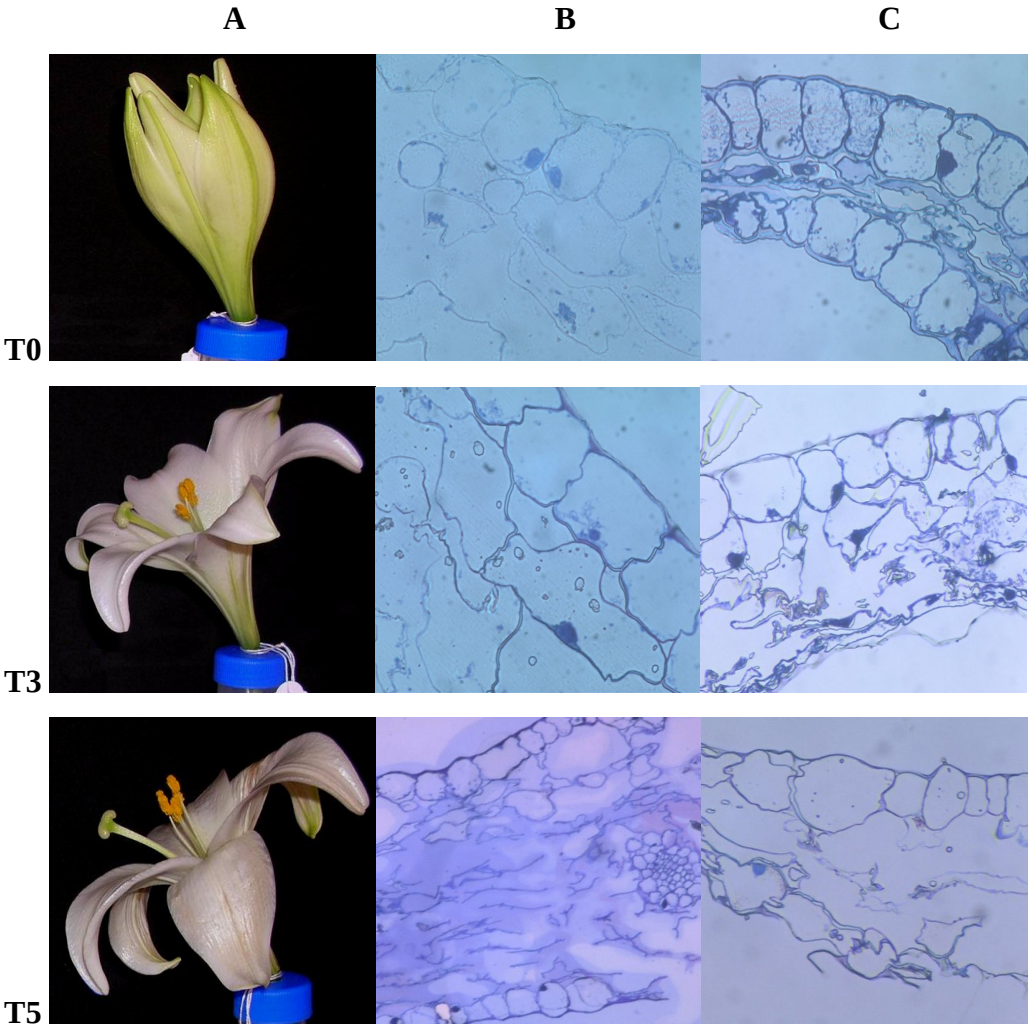

Figure 16. Cross-sections of lily tepals at flower opening (T0), full bloom (T3) and senescence (T5). Pictures of whole flowers at corresponding developmental stage (A). Sections from tissues close to the central midrib (B) and from tepal margins (C) were analyzed.

Ultrastructural analysis of tepals at the early stage of flower opening (T0) showed that the epidermal and mesophyll cells were essentially free of cytoplasmic or vacuolar abnormalities. Epidermal cells contained a large vacuole with an electron dense peripheral cytoplasm housing numerous mitochondria (Fig. 17A). Both the adaxial and abaxial petal surfaces had a thick cellulose cell wall, which is maintained until senescing stages. Mesophyll cells are

round in shape delimiting wide free spaces, had a large vacuole and were rich in amyloplasts and mitochondria within an electron dense cytoplasm (Fig. 17B and 17C).

At full bloom (T3) an increasing disorganization of cytoplasm was evident both in epidermal and mesophyll cells (Fig. 17D, 17E and 17F). It was accompanied by the accumulation of a variety of differing vesicles in the cytoplasm. Lost of tonoplast permeability or vacuole rupture was associated with a dilution of the cytoplasm and a consequent decrease in electron density, even if the complete set of organelles having a normal structure, mitochondria, rough ER, Golgi producing vesicles, plastids, and nuclei could still be observed. In mesophyll cells approaching autolysis the dilution of the cytoplasm was often accompanied by the shrinkage of the protoplast with a consequent detachment of the plasmalemma from the cell wall (Fig. 17F). Moreover, autophagic activity of the vacuole could be hypothesized due to the presence of cytoplasmic material and decaying organelles in the digestive compartment. In cells in advanced stage of degradation, the tonoplast completely lost its integrity and the vacuole was no longer distinguishable from the cytoplasm (Fig. 17F and 17G).

Autolysis of epidermal cells proceeded at stage T5 in which most of them are still intact, although their contents appeared to be greatly reduced and membrane shrinkage was observed (Fig. 17G). By stage T5 most mesophyll cells lacked any cytoplasm and there was little evidence of the previous mesophyll cell layer other than a series of collapsed cell walls (Fig. 17H and 17I). In contrast, vascular tissues had normal appearance, with only few cells showing vesicles and electron dense structures within the vacuole (Fig. 17I and 17L).

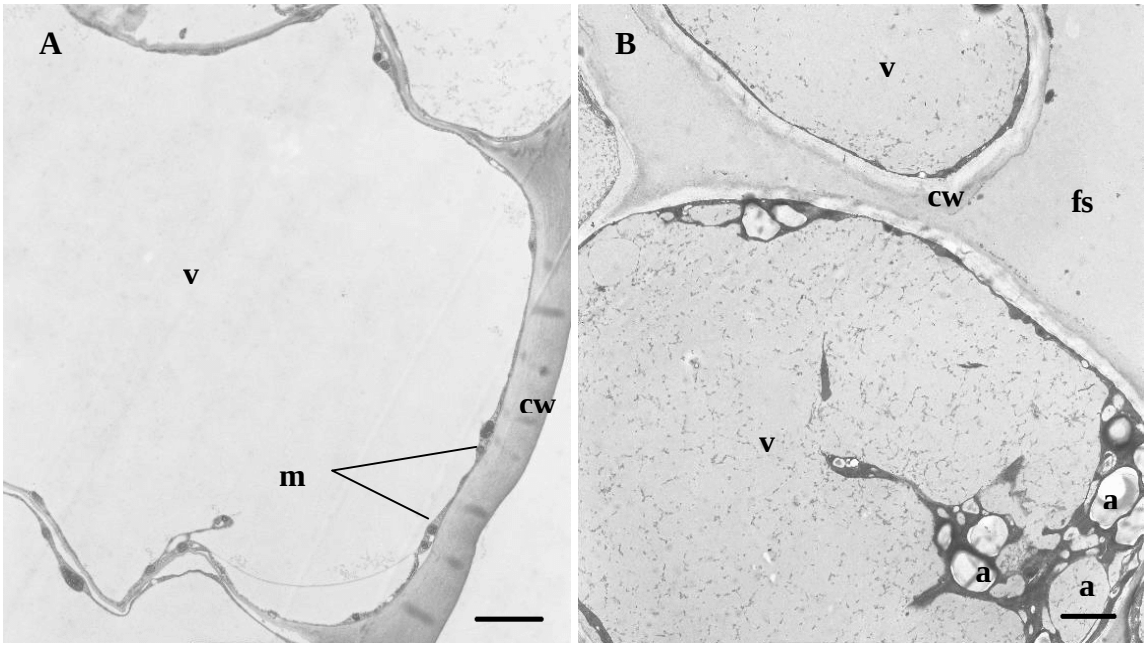

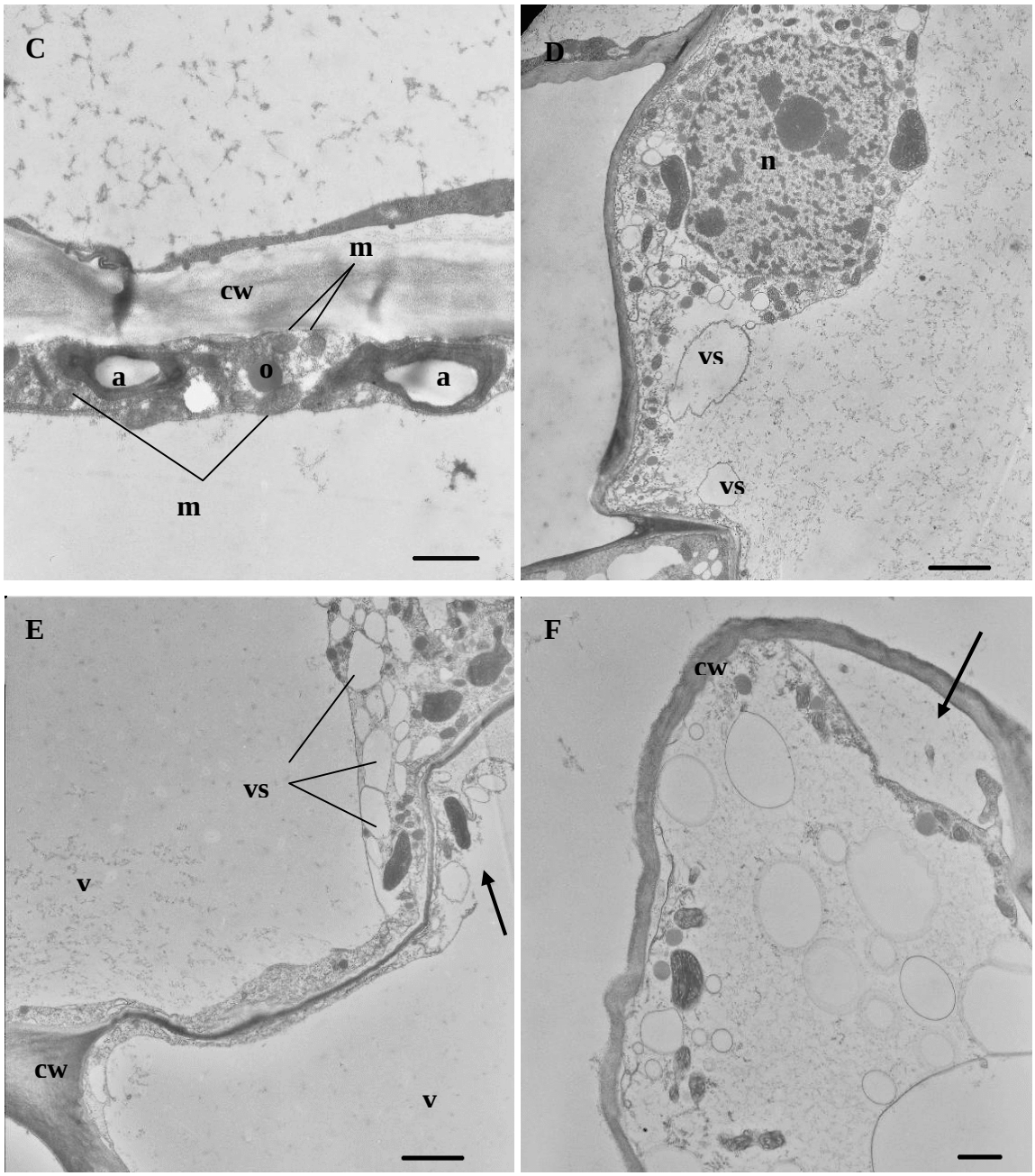
C
m
cw
a
o
a
m
D
n
vs
vs
E
vs
v
cw
v
F
cw

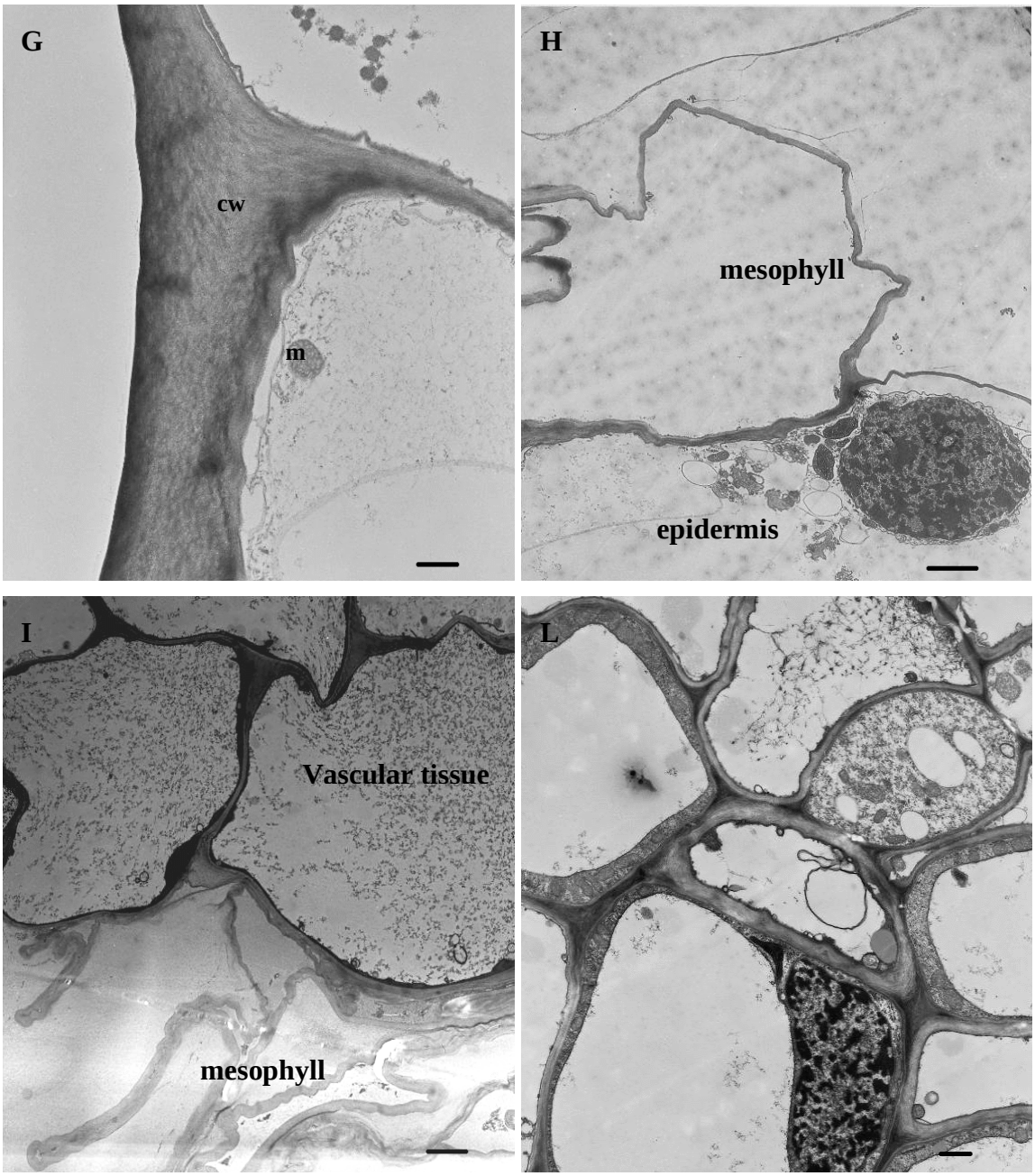

Figure 17. Transmission electron micrographs of epidermal and mesophyll cells of lily tepal. (A) Stage T0. Epidermal cell showing no abnormalities. Magnification 3.2 K, scale bar, 3 µm; (B) Stage T0. Round shaped mesophyll cells rich in amyloplasts and without signs of autolysis. Magnification 2.5 K, scale bar, 3 µm; (C) A particular of mesophyll cells at stage T0. Magnification 10 K, scale bar, 1 µm; (D and E) Epidermal cells at stage T3 showing a diffuse cytoplasm vesiculation and vacuole rupture (arrow). Magnification 3.2 K, scale bar, 3 µm; (F) Stage T3. Mesophyll cell undergoing autolysis and protoplast shrinkage (arrow). Magnification 6.3 K, scale bar, 1 µm. (G) Epidermal cells at stage T5. Magnification 6.3 K, scale bar, 1 µm. (H) Collapsed mesophyll cell and epidermal cell undergoing autolysis. Magnification 2.5 K, scale bar, 3 µm. (I and L) Stage T5. Micrographs showing intact vascular tissues and a completely collapsed mesophyll layer. Magnification respectively 2 and 5 K, scale bar, 3 and 1oo µm. Nuclei (n), vacuole (v), cell wall (cw), plastids (p), mitochondria (m), amyloplasts (a), free spaces (fs), vesicles (vs) and oleosomes (o).

3.4. Protein content and protease activity

To monitor the level of soluble proteins a crude extract in aqueous buffer was used. Protein level of control and sucrose treated flowers showed a similar pattern, although protein content was constantly higher in the control throughout flower development and senescence (Fig. 18). A marked decrease in protein level was observed before flower opening and after stage T3. In advanced senescing flowers the protein level reached the minimum value. When protein content was expressed per petal or dry weight a similar trend occurred without remarkable differences.

The decrease in protein level in tepals was accompanied by a decrease in high molecular weight molecules as shown in the SDS-PAGE gel (Fig. 20).

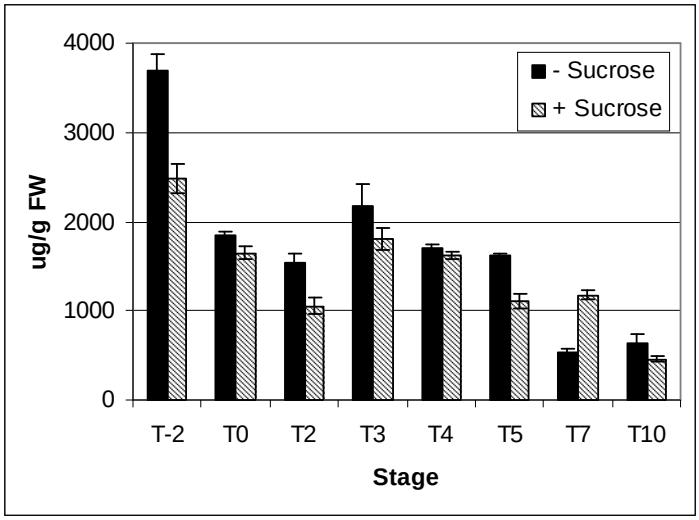

Figure 18. Soluble protein content in outer tepals of lily flower held in water or sucrose solution. Error bars represent ± SE (n=3).

In leaves, protein content decreased during senescence (Fig. 19). In light green leaves and yellow leaves protein content was significantly lower than in green leaves, suggesting a bulk degradation of protein throughout the senescence process together with substantial chlorophyll breakdown.

The decrease in protein content may be due to an increase in proteinase activity during senescence. Changes in proteinase activity were investigated using azocasein as substrate. A profile of quantitative activity was obtained using several pH values and analyzing all developmental and senescence stages of flowers (Fig. 21). At stage T-2 and T0 a very low detectable activity was measured. At stage T0 the greatest activity was measured at pH 4.5, and the same activity increased at stage T2. From stage T3 there was an increase in

proteinase activity with an optimum at pH 5.5. From this point onwards, the activity profile did not change and the activity increased until stage T6 slightly decreasing at stage T7.

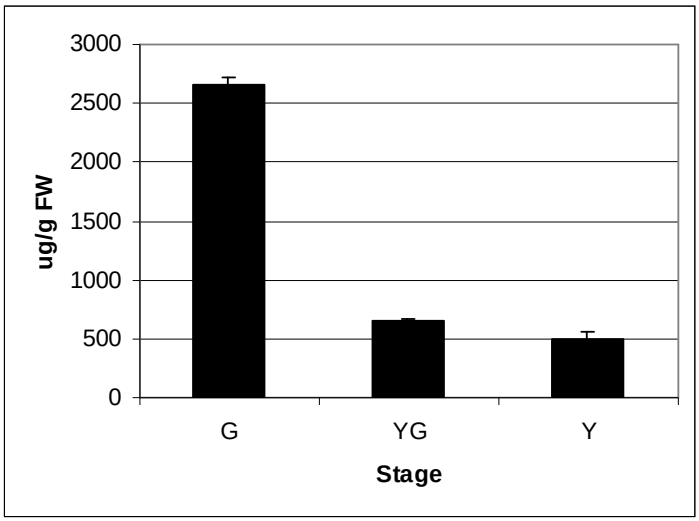

Figure 19. Protein content in green leaves (G), light green leaves (YG) and yellow leaves (Y) of lily held in water. Error bars represent ± SE (n=3).

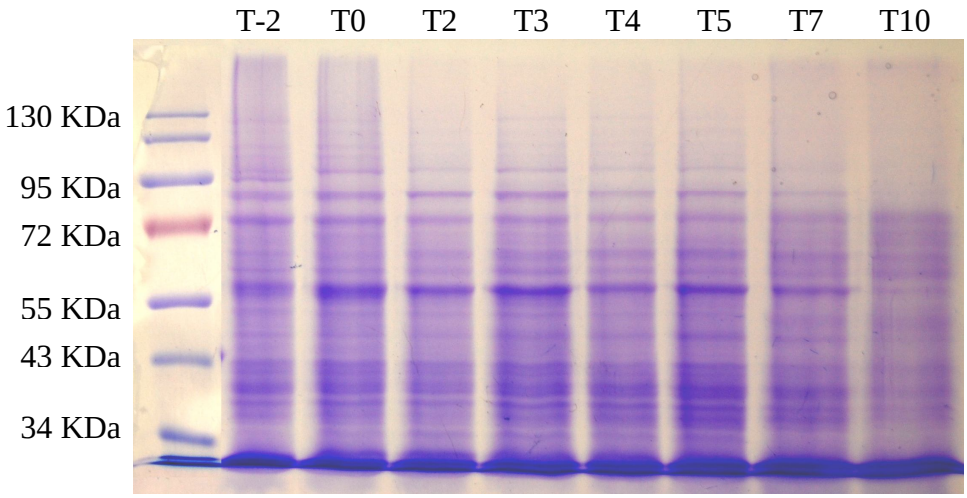

Figure 20. SDS-PAGE gel of protein extracts from lily outer tepals. 20 µg of proteins were run for each line.

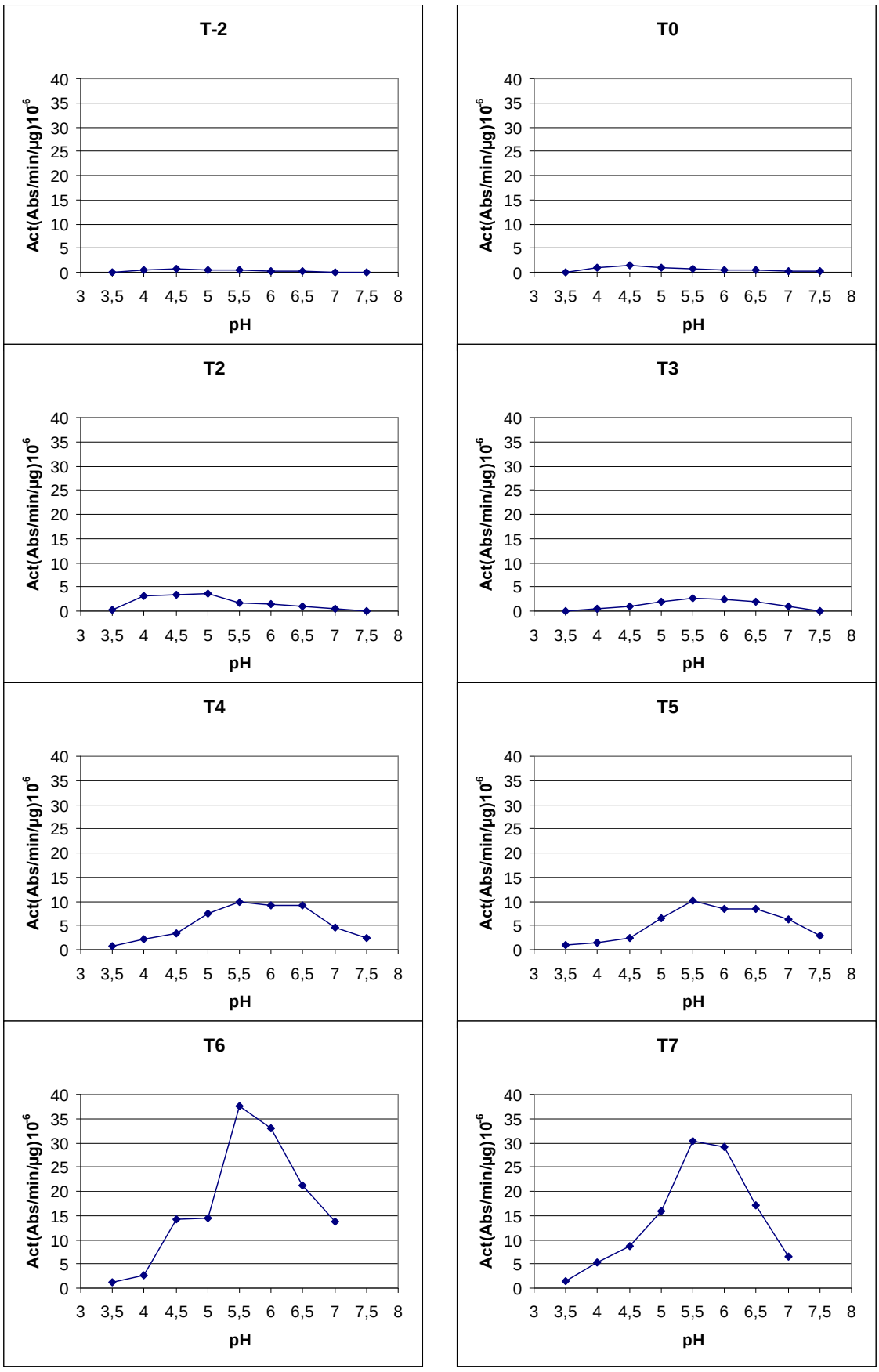

Figure 21. Proteinase activity profiling of extracts from lily tepals. The activity is expressed as increase in absorbance (Abs) at 420 nm per minute and µg of proteins.

New extractions from another biological replicate, held in water (control) or in sucrose solution, were made and used for activity profiling over time in tepals (Fig. 22A) at pH 5.5. In extracts from control flowers proteinase activity increased reaching a maximum by stage T7 and then decreasing during late senescence. In flowers held in sucrose solution, proteinase activity increased constantly and reached a maximum by stage T10. At stage T5, T7 and T10 proteinase activity was significantly lower ($P<0.05$) in sucrose treated flowers, indicating a possible delay in senescence. In leaves the highest activity was measured in senescing leaves (YG) being double that of green leaves. Protease activity decreased in completely senescent leaves (Y) (Fig. 22B).

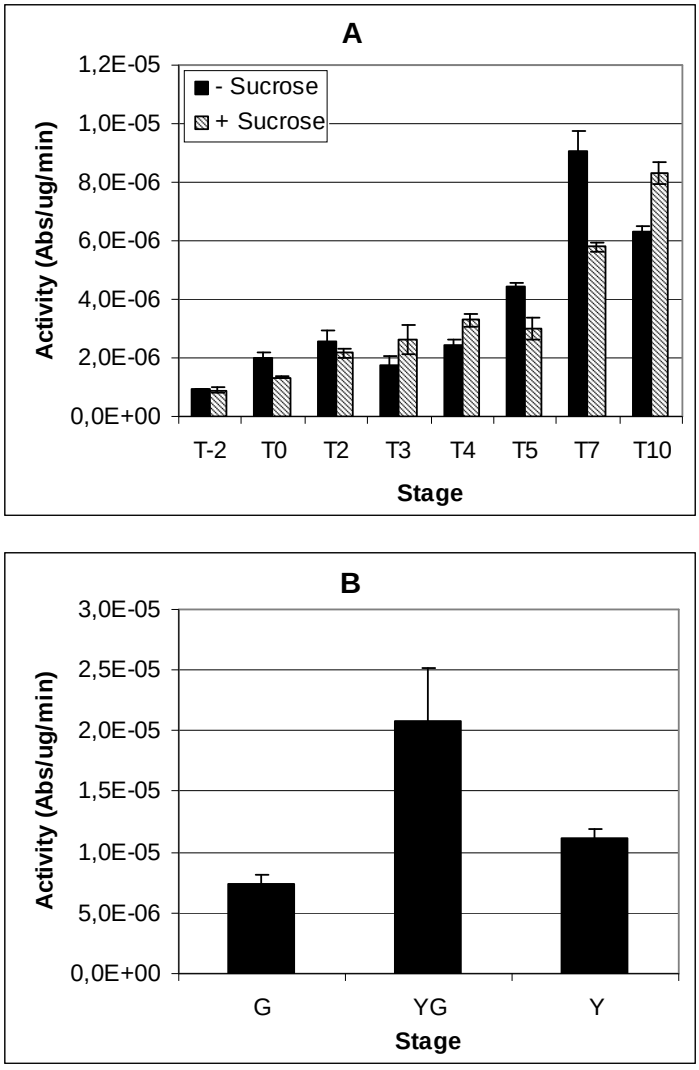

Figure 22. Changes in proteinase activity over time using azocasein as substrate in tepals (A) and leaves (B). Green leaves (G), light green leaves (YG) and yellow leaves (Y). The activity was measured at pH 5.5. Error bars represent ± SE (n=3).

Assays for specific proteases were carried out using specific substrates with the aim of identifying specific classes of proteases involved in flower senescence.

In order to identify caspase-like activities we used synthetic, colorimetric, four amino acid substrates for three distinct members of animal caspase protease family. The substrates tested were Ac-YVAD-pNA (for caspase-1), Ac-DEVD-pNA (for caspase-3) and Ac-VEID-pNA (for caspase-6). All three substrates were cleaved by cell-free extracts obtained from lily tepals and sampled at different stages. The assays were carried out at pH 5 or 5.5, based on previous analysis done with pH ranging from 3.5 to 8 (Fig. 23A). YVADase (caspase-1) specific activity was strongly induced during senescence, being 5 fold higher in senescing flowers and reaching a maximum at stage T7. DEVDase (caspase-3) and VEIDase (caspase-6) activities had a similar pattern and were two fold higher in flowers at stage T7 compared to stage T2 (Fig. 23).

The profile of caspase-like activities was modified by sucrose feeding. YVADase (caspase-1) and DEVDase (caspase-3) activitiy reached a peak two days earlier than in control flowers. Between T2 and T5 the activity was significantly ($P<0.05$) higher in sucrose treated flowers. Similarly, VEIDase (caspase-6) activity was greater in flowers held in sucrose following the same pattern of control flowers and reaching a peak by stage T7 which was even higher (by approximately 1.5-fold) compared to the control flower ($P<0.05$) (Fig. 23).

Caspase-like activity was measured in leaves held in water during senescence (Fig. 24). Caspase-like 1 and caspase-like 6 activity increased gradually during senescence and in yellow leaves a 10-fold increase in activity was measured. For caspase-like 3 activity the pattern was slightly different with the lowest value measured in light green leaves. In yellow leaves a 2-fold increase was measured compared to green leaves.

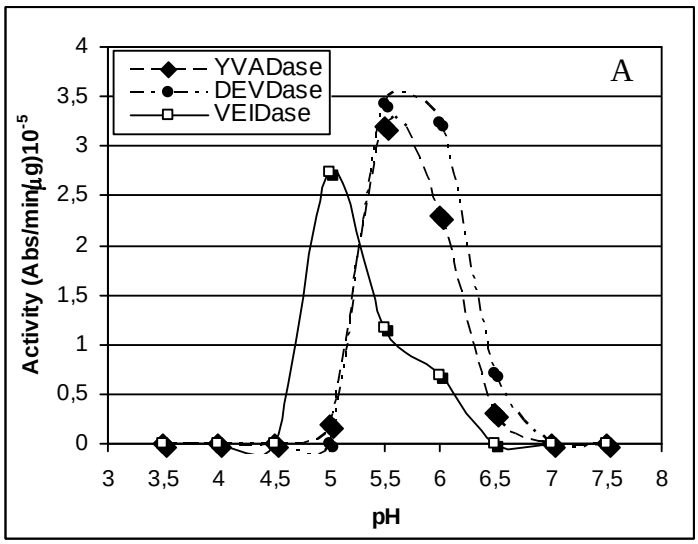

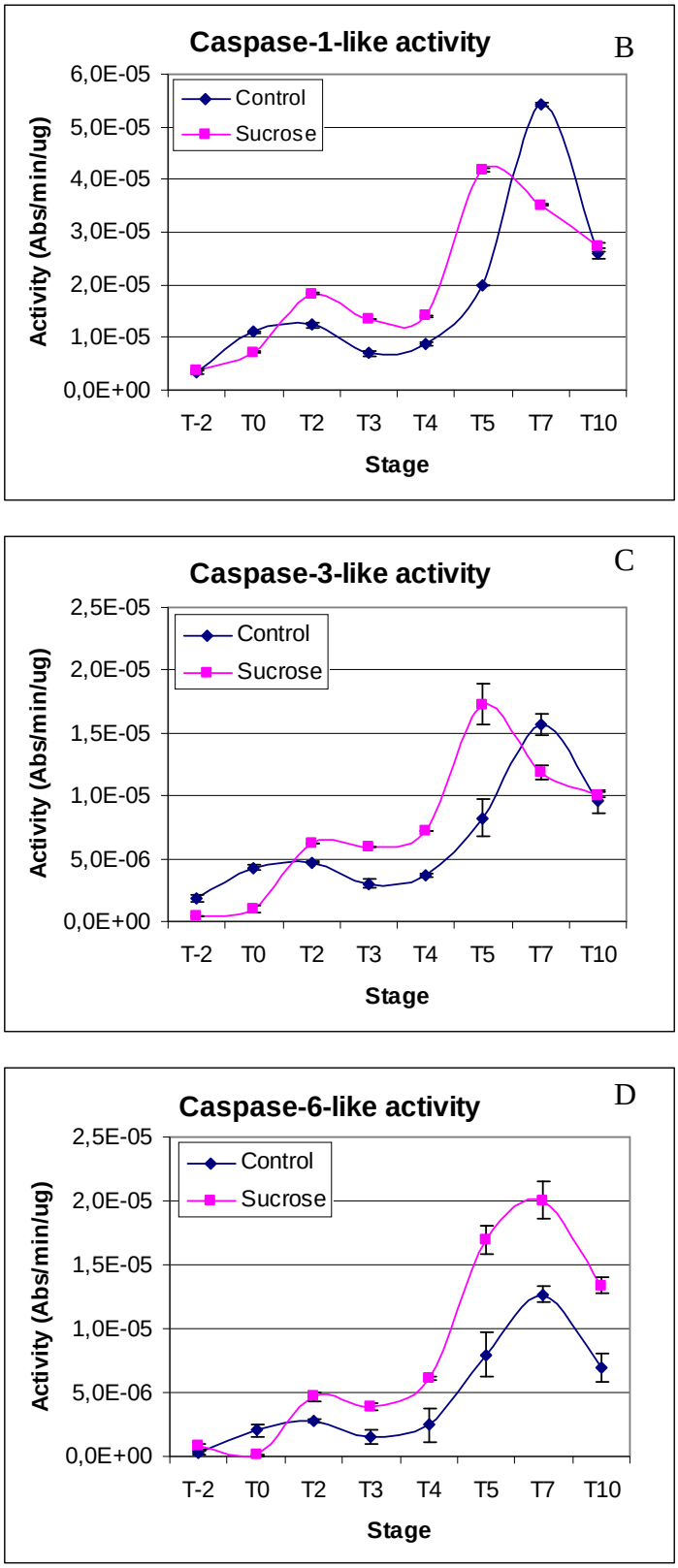

Figure 23. (A) pH profile for *in vitro* cleavage of mammalian caspase substrates by lily tepals crude extracts from stage T7. (B,C,D) *In vitro* cleavage of tetrapeptide substrates specific for the three different caspases. Crude extracts are from flowers held in water (control) or sucrose solution were used. Error bars represent ± SE (n=3).

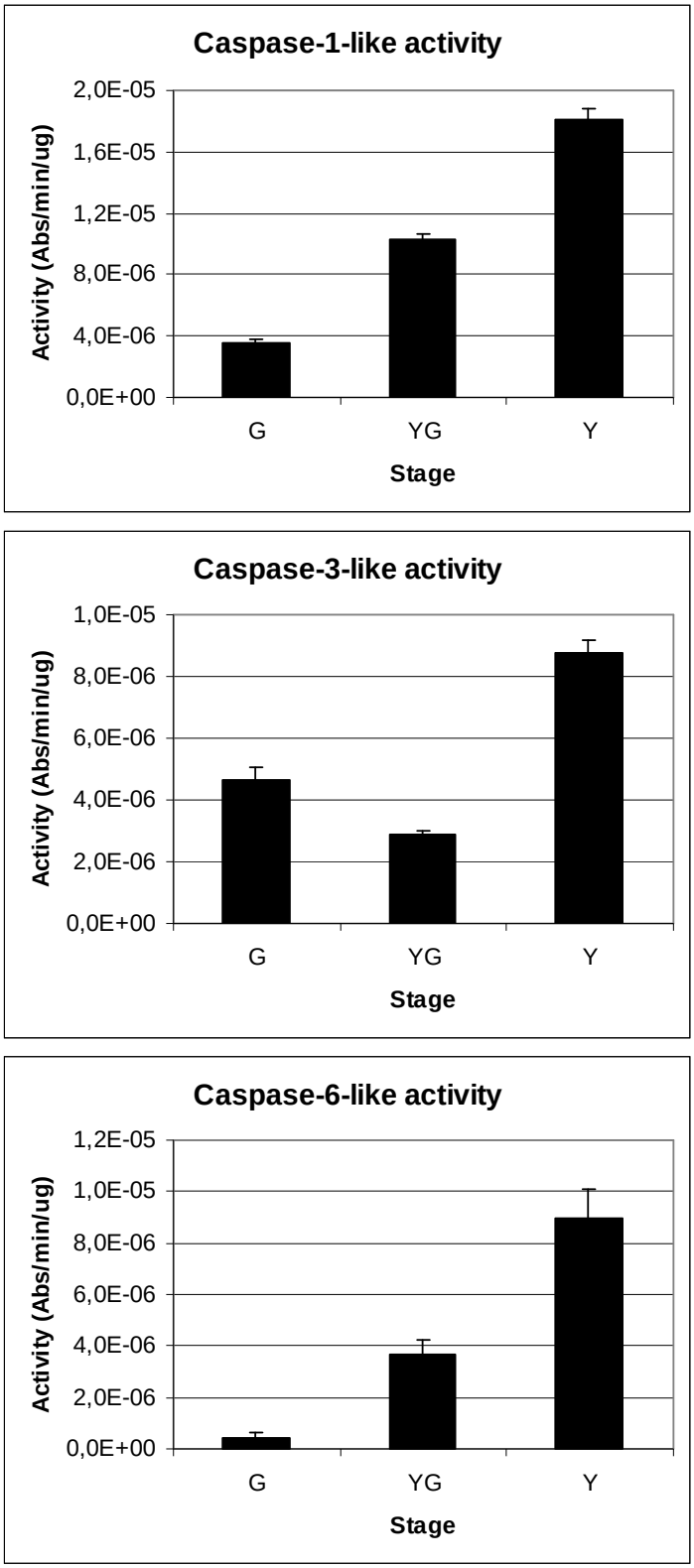

Figure 24. *In vitro* cleavage of tetrapeptide substrates specific for three different mammalian caspases. Crude extracts from green leaves (G), light green leaves (YG) and yellow leaves (Y) held in water were used. Error bars represent ± SE (n=3).

To test whether the cleavage of the three substrates during cell death was executed by specific caspase-like activities or actually by other generic proteases, we performed the

caspase assays in the presence of different inhibitors. Using extracts from control flowers we carried out preliminary experiments measuring DEVDase (caspase-3) activity in the presence of specific caspase inhibitors Ac-YVAD-CHO (for caspase-1), Ac-DEVD-CHO (for caspase-3), Ac-VEID-CHO (for caspase-6) and inhibitors of other classes of proteases (Fig. 25). The cysteine protease inhibitor E-64, the aspartic acid protease inhibitor pepstatin, the serine and cysteine protease inhibitor leupeptin and the cysteine protease inhibitor NEM had a limited effect in inhibiting the cleavage of the DEVD substrate. In contrast, when the specific inhibitors Ac-YVAD-CHO (for caspase-1), Ac-DEVD-CHO (for caspase-3), Ac-VEID-CHO (for caspase- 6) and the serine protease inhibitor PMSF were included in the assays, by about 70-80%. of the proteolytic activity was suppressed.

A second set of experiments was carried out for YVADase (caspase-1), DEVDase (caspase-3) and VEIDase (caspase-6) activity using only specific caspase inhibitors and the extracts from both control and sucrose treated flowers (Fig. 26). Ac-DEVD-CHO strongly reduced DEVDase (caspase-3) activity by up to 80%, confirming the result obtained with the preliminary experiment. Ac-YVAD-CHO and Ac-VEID-CHO were less effective and reduced the caspase-like activity by about 40-50% compared to the control. The effect of specific caspase inhibitors was similar in extracts from both control and sucrose treated flowers, suggesting the existence of a true caspase-like activity in tepals.

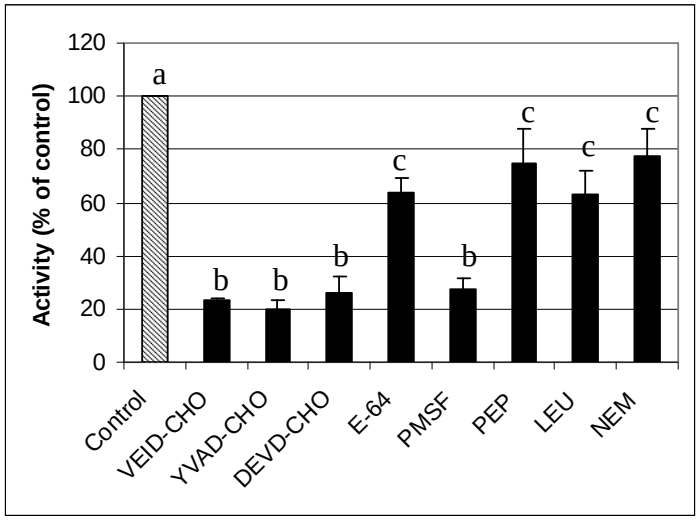

Figure 25. Effects of different protease inhibitors on DEVDase activitiy. The following inhibitors were used: 20 µM E-64, 20 µM pepstatin (PEP), 1 mM PMSF, 20 µM Leupeptin (LEU), 1 mM NEM and 100 mM Ac-YVAD-CHO or Ac-DEVD-CHO or Ac-VEID-CHO. Means with different letters are significantly different at $P<0.05$. Error bars represent ±SE (n=3).

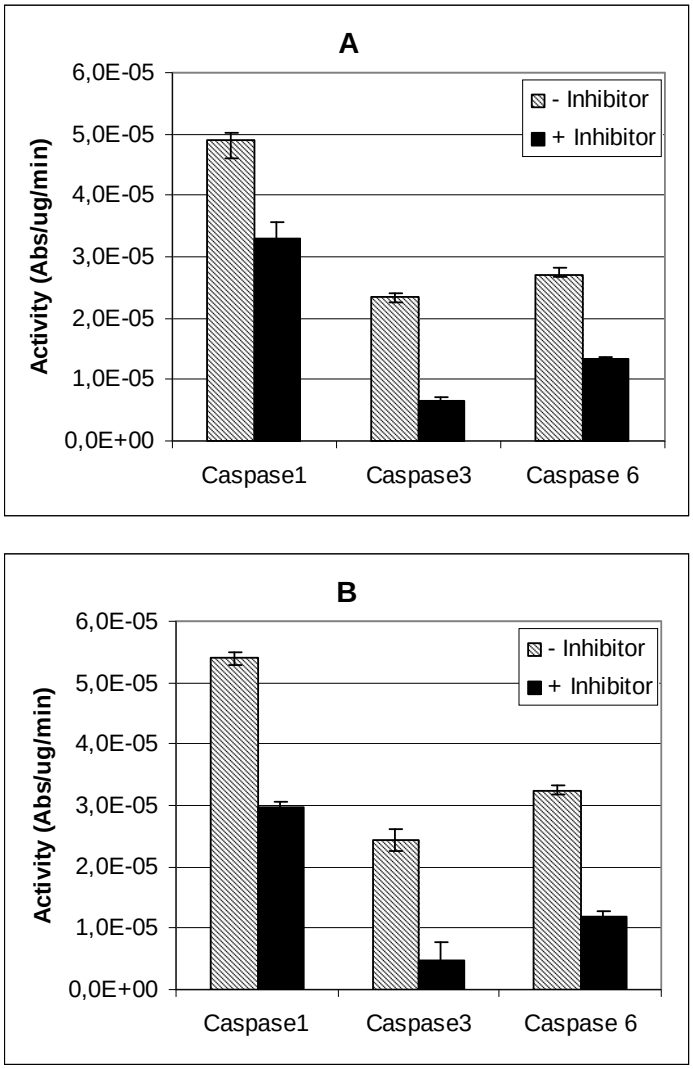

Figure 26. Effects of different caspase specific inhibitors on YVADase (Caspase1), DEVDase (Caspase3) and VEIDase (Caspase6) activities. Both extract from control (A) and sucrose treated flower (B) were used. Error bars represent ± SE (n=3).

VPEs are reported to be key regulators in the hypersensitive response, seed development, seed storage protein processing and leaf senescence (Yamada *et al.*, 2005). To test the possible involvement of VPEs during flower senescence we used a specific synthetic, fluorimetric, three amino acid substrate (Ac-AAN-MCA). The assay was carried out at pH 5 based on the optimum acidic pH typical of this class of proteases. Crude extracts from lily tepals and leaves were able to cleave the VPE specific substrate (Fig. 27 and Fig. 28). The assay was carry out using extracts from both control flowers and from flowers held in sucrose solution. In control flowers, VPE activity increased during flower opening decreasing soon after. A smaller, but statistically significant ($P<0.05$), peak was detected at stage T7 in which flowers are in an advanced stage of senescence. The treatment with sucrose induced a strong

increase in VPE activity, being 3 to 8 fold higher than in the control until stage T5. During late senescence there were no differences in activity between the control and treated flowers. In leaves there was a constant increase of VPE activity over the senescence process with the highest value in completely senescent leaves (Fig. 28).

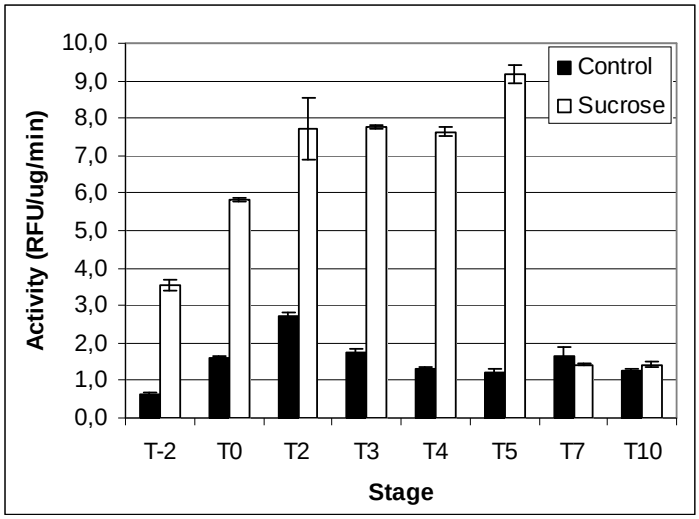

Figure 27. *In vitro* cleavage of a tripeptide substrate specific for vacuolar processing enzymes (VPE). Crude extracts were prepared from flowers held in water (control) or sucrose solution. Error bars represent ± SE (n=3).

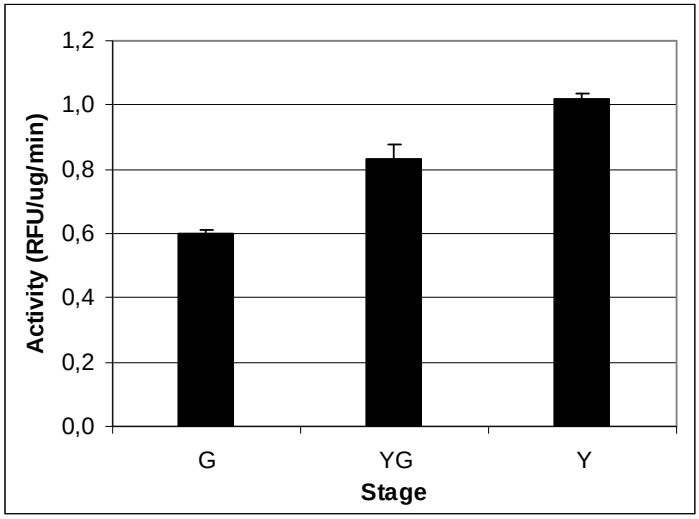

Figure 28. *In vitro* cleavage of a tripeptide substrate specific for vacuolar processing enzymes (VPE). Crude extracts were prepared from leaves. Error bars represent ± SE (n=3).

3.5. DNA content and degradation

DNA from each stage was run on 2% agarose gels to verify DNA degradation and laddering. Agarose gel analyses showed the almost complete absence of DNA degradation by the time of full flower opening (Fig. 29; T2). Extensive DNA degradation was seen from stage T3

until late senescence in which only small DNA fragments are visible. Only a smear was detected without any sign of inter-nucleosomal fragmentation. Total DNA, as determined by spectrophotometry, revealed an increase by stage T2 and subsequently a gradual decrease by stage T10, in accordance with the gel assay (Fig. 30).

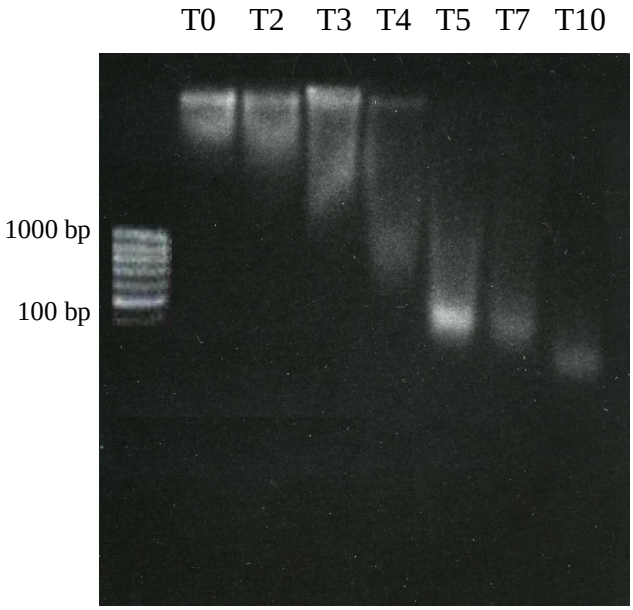

Figure 29. Agarose gel analysis of total DNA isolated from tepals of lily.

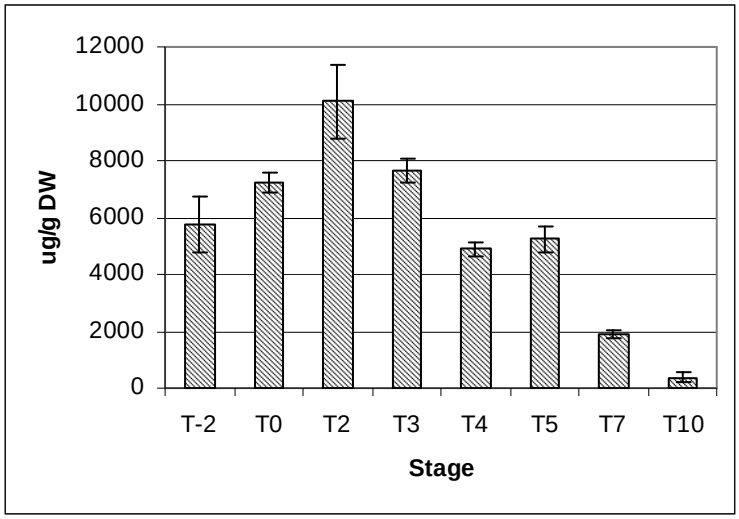

Figure 30. DNA content (µg/g DW) in tepals of lily. Error bars represent ± SE (n=3).

To investigate degradation of genomic DNA during tepal senescence in lily flowers at cellular level, the *in situ* detection of DNA breakdown was performed in whole tepals using TUNEL assay. This method preferentially labels double strand breaks that result from the

activity of endonucleases during programmed cell death. DAPI was used to counterstain the whole set of nuclei within the tepal sections. As a positive control, sections treated with a commercial endonuclease were used (Fig. 31). In close bud (Stage T-2) and just opening flowers (Stage T0) nuclei showing TUNEL staining were not detected. At full bloom (Stage T2) TUNEL positive nuclei were rarely observed. TUNEL positive nuclei that were observed in the vicinity of xylem vessels may be due to the presence of differentiating tracheary elements. In fully open flowers which did not show visible signs of tepal senescence (Stage T3 and T4), TUNEL positive nuclei were consistently observed reaching 50% of total nuclei. In senescing flowers (from stage T5), TUNEL staining became more frequent and from stage T6 more than 90% of nuclei were TUNEL positive.

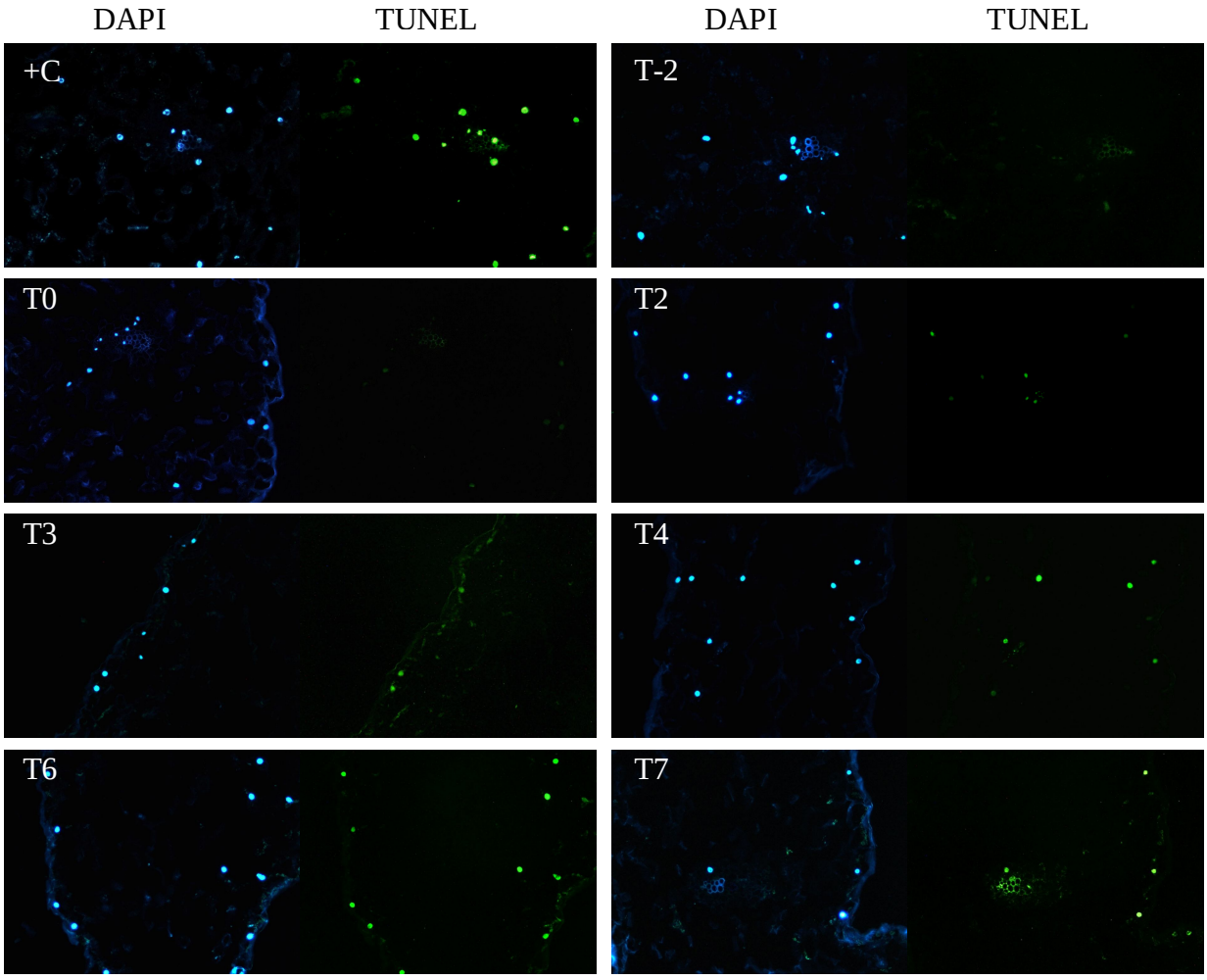

Fig. 31. DNA degradation in nuclei from lily flower tetals visualised using the TUNEL method. DAPI stain (blue) shows the nuclei present in the sections. TUNEL (green) shows only positive nuclei in which double strand breaks occurred.

3.6. Cloning and expression of a KDEL cysteine protease gene

Degenerate primers were used to isolate a partial cysteine protease cDNA from lily tepal tissues at stage T7, according to Wagstaff *et al*. (2002). A BLAST search of the National Center for Biotechnology Information database was conducted using the 340 bp fragment (http://www.ncbi.nlm.nih.gov/), revealing a high similarity with papain-like peptidades present in the database (Fig. 32). The alignment of the putative protein sequence deduced from the partial cDNA showed 68-76% homology with the same region of PRT5 (*Sandersonia aurantica*), ALSCYP1 (*Alstroemeria*), SEN 102 and SEN11 (*Hemerocallis*), CYS 2 (*Iris*) and CP7 (*Petunia*).

Sequences producing significant alignments:	Score (Bits)	E Value
qb|AAD28477.1|AF133839_1 papain-like cysteine protease [Sande...	130	5e-29
qb|AAK63125.1| putative cysteine protease [Alstroemeria hybri...	126	7e-28
sp|P43156.1|CYSP_HEMSP RecName: Full=Thiol protease SEN102; F...	123	8e-27
ref|XP_002511277.1| cysteine protease, putative [Ricinus comm...	123	8e-27
ref|XP_002278323.1| PREDICTED: hypothetical protein [Vitis vi...	122	1e-26
emb|CAA40073.1| endopeptidase (EP-C1) [Phaseolus vulgaris]	122	1e-26
sp|P25803.2|CYSEP_PHAVU RecName: Full=Vignain; AltName: Full=...	122	1e-26
emb|CBI14901.1| unnamed protein product [Vitis vinifera]	120	5e-26
dbj|BAC77521.1| cysteine proteinase [Glycine max] >dbj|BAC775...	119	1e-25
qb|AAB37233.1| cysteine proteinase [Phalaenopsis sp. SM9108]	118	2e-25
sp|P12412.1|CYSEP_VIGMU RecName: Full=Vignain; AltName: Full=...	118	2e-25
prf||1910332A Cys endopeptidase	118	2e-25
ref|XP_002321654.1| predicted protein [Populus trichocarpa] >...	118	2e-25
qb|AAA92063.1| cysteinyl endopeptidase [Vigna radiata]	118	2e-25
emb|CAA84378.1| cysteine proteinase [Vicia sativa]	118	2e-25
qb|ACU18368.1| unknown [Glycine max]	117	3e-25
dbj|BAC77523.1| cysteine proteinase [Glycine max] >dbj|BAC775...	117	3e-25
qb|ACU23531.1| unknown [Glycine max]	117	4e-25
qb|ABV22590.1| KDEL-tailed cysteine endopeptidase [Solanum ly...	117	4e-25
qb|AAP32192.1| cysteine protease 14 [Trifolium repens]	116	9e-25
qb|AAC35211.1| cysteine proteinase [Hemerocallis hybrid culti...	116	9e-25

Figure 32. BLAST database search using the 340 bp fragment (Altschul *et al.*, 1997). The first 21 sequences producing significant alignments are shown.

The predicted aminoacid sequence of LlCyp was shown to begin 87 amino acids from the N-terminus of PRT5 protease of *Sandersonia aurantica* and it did not extend to the C-terminal region supposed to possess a tetra-peptide ER retention signal (Fig. 33). However, LlCyp contained some elements characteristic of papain-like proteases such as the Cys forming the catalytic dyad and a Gln preceding the Cys involved in the formation of the 'oxyanion hole' (Fig. 33).

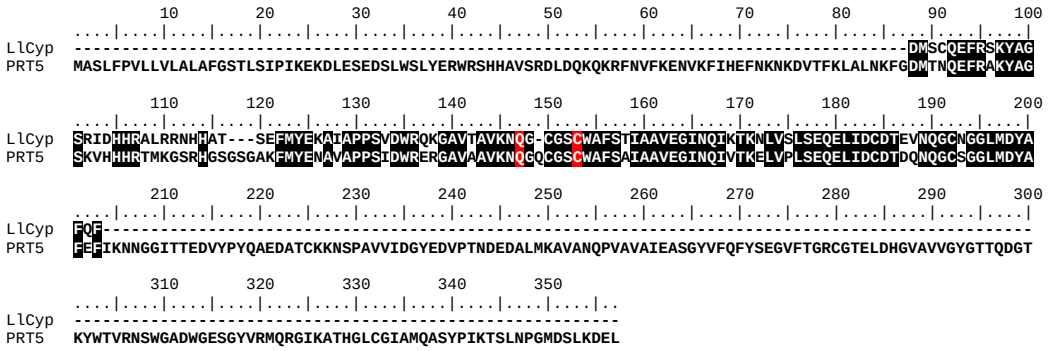

Figure 33. Alignment of LlCyp cloned from lily tepal with PRT5 from *Sandersonia aurantica*. Alignment was conduced using clustal analysis in BioEdit. Aminoacids matching the consensus are shaded. In red are the catalytic Cys and the Gln active site residues.

To obtain the full length open reading frame of LlCyp Rapid Amplification of cDNA Ends (RACE) was performed using GSPF and GSPR primers and the full gene was cloned as described in materials and methods. Two clones were selected that differed in nucleotide and aminoacid sequences (Fig. 34 and 35). The differences in nucleotide sequence did not always reflect a change at the aminoacid level and the two clones differed in only four aminoacids. In both clones several amino acids characteristic of papain-like peptidases were conserved and a KDEL ER-retention signal was present at the C-terminus of the consensus sequence. The catalytic residues of papain-type peptidases cysteine-154 and histidine-289 were conserved; other residues important for catalysis included glutamine-148, which helps form the “oxyanion hole”, and asparagine-310, which orientates the imidazolium ring of histidine-289. The so-called “ERFNIN motif” which is characteristic of pro-peptides related to papain, was also present (Rawlings and Barrett 1994).

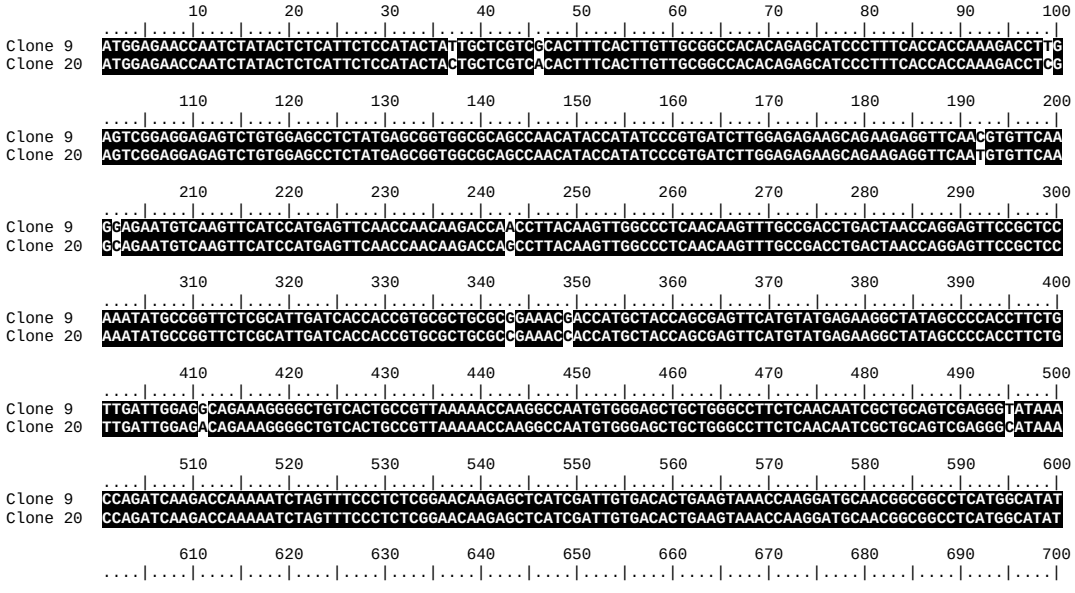

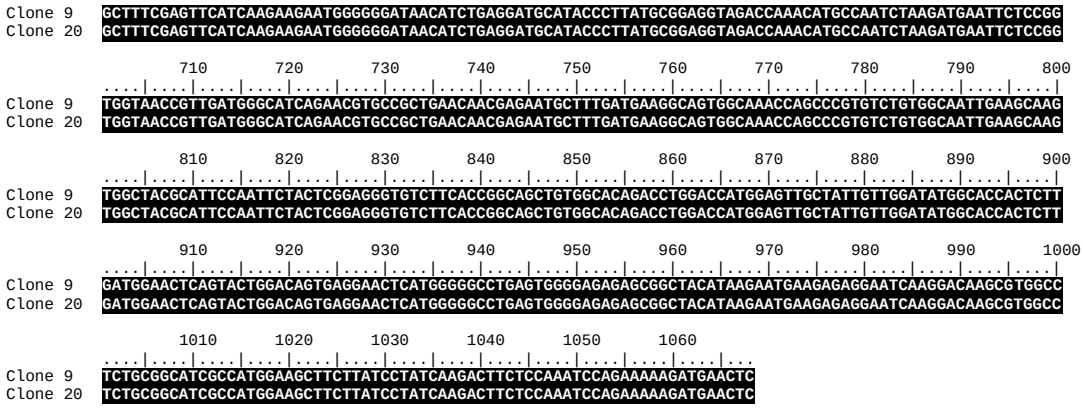

Figure 34. Alignment of LlCyp clones from lily tepal using clustal analysis in BioEdit. Matching nucleotides are shaded.

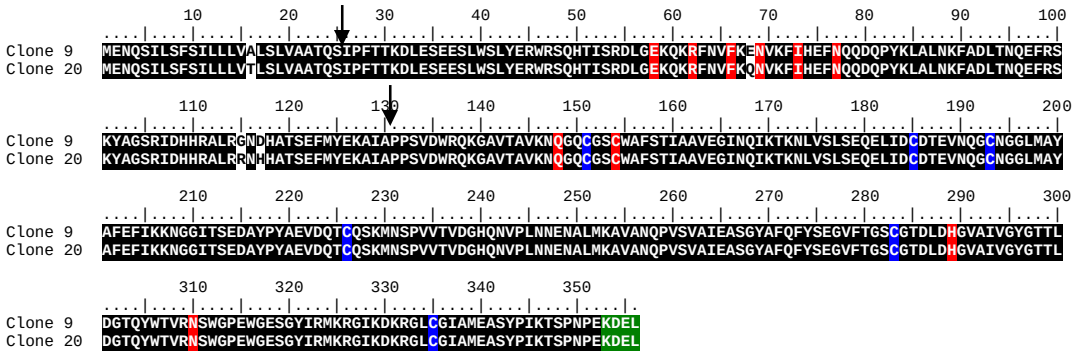

Figure 35. Alignment of LlCyp clones from lily tepal using clustal analysis in BioEdit. Matching aminoacids are shaded. The "ERFNIN motif" within the pro-sequence and amino acids belonging to the catalytic pocket (Cys-154 and His 289) or otherwise important for catalysis (Gln-148 and Asn-310) are in red. Cysteine residues involved in disulfide bridges are in blue and the C-terminal KDEL is in green. The arrows represent the predicted cleavage sites.

The full length LlCyp showed homology with papain-like peptidases found in other species (Fig. 36). *Lilium* gene clusters with other similar genes from mocotyledonous plants reflecting taxonomic relationships.

Peptidases of the papain family are synthesised with signal peptides (pre-sequences) and a pro-peptide intercalated between the signal peptide and the N-terminus of the mature enzyme (Rawlings and Barrett 1994). Using SignalP and TargetP the cleavage site of the signal peptide and the protein subcellular localization were predicted (Emanuelsson *et al.*, 2000; Bendtsen *et al.*, 2004) (Fig. 37). LlCyp protease possesses a 25 amino acids signal peptide and is not predicted to localise to chloroplasts or mitochondria but is probably secreted. The cleavage site of the pro-peptide was predicted between Ile-129 and Ala-130 by aligning LlCyp with other KDEL-tailed proteases found in the database in which the cleavage site is known.

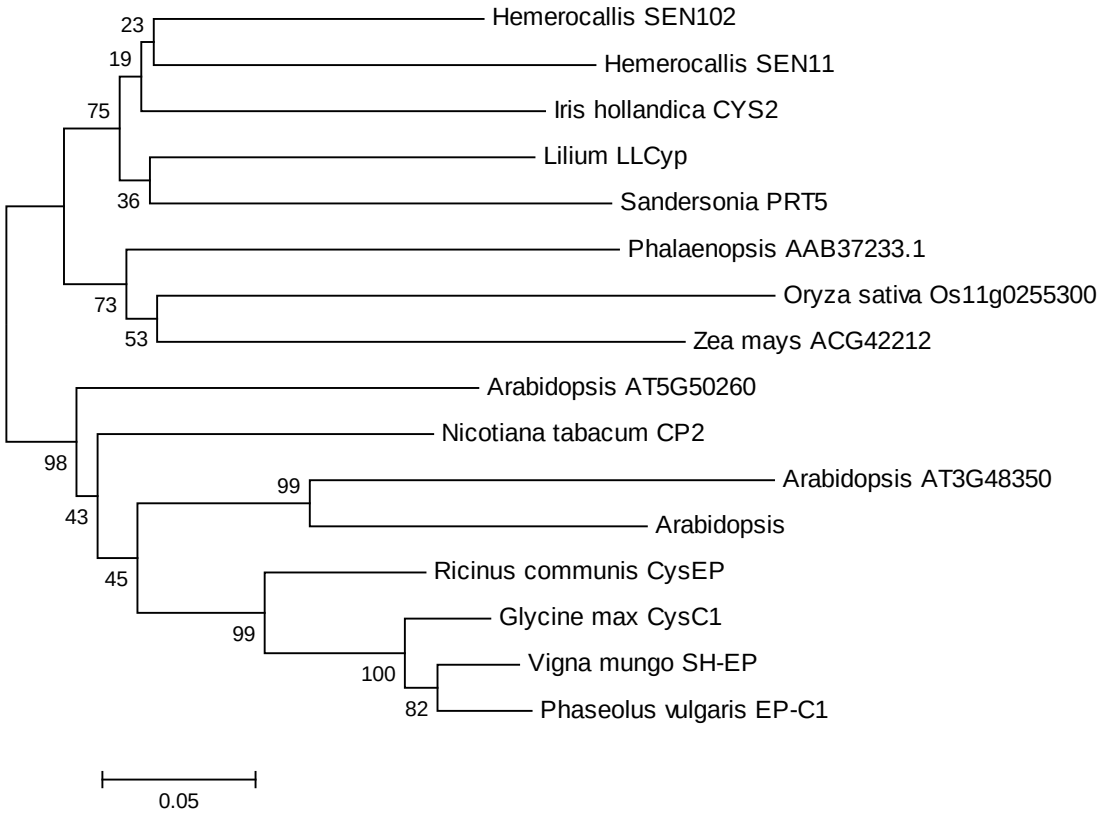

Figure 36. A phylogenetic tree of cysteine peptidase belonging to the papain-like family. The phylogenetic tree was constructed by the neighbor-joining method without gap regions which were generated for maximun matching. Numbers along each branch are bootstrap values.

Semi-quantitative RT-PCR was used to analyse the expression pattern of LlCyp during lily flower senescence. Degenerate tubulin primers which span an intron were used for checking for the presence of genomic DNA contamination of cDNA (Fig. 38). Only a 230 bp band was amplified indicating the absence of any contaminating genomic DNA. A strong up-regulation of LlCyp gene was found at flower opening (T0) and during the first stages of flower senescence (Fig. 39). Expression was low at stage T2 (early full bloom) and then increased by stage T5 in coincidence with senescence activation. In fully senescing flowers (T7 and T10) LlCyp expression decreased, returning to the lower level.

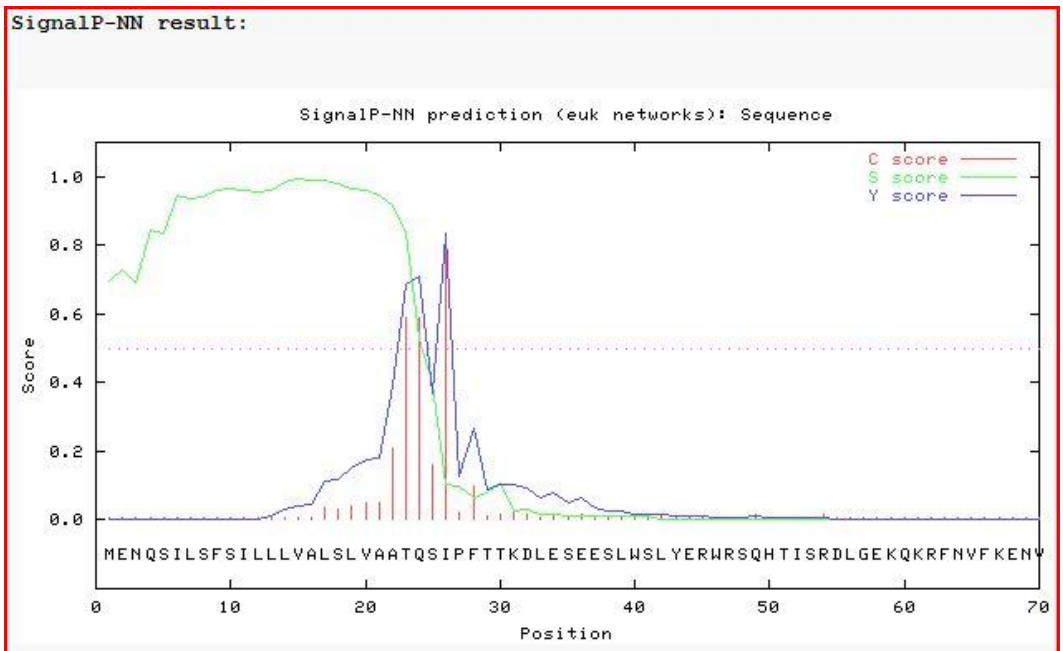

A

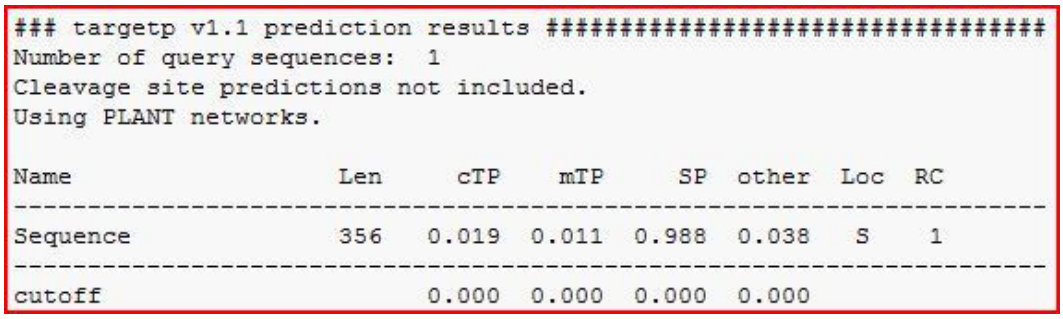

B

Figure 37. Analysis LlCyp aminoacid sequence using SignalP (A) and TargetP (B). SignalP incorporates a prediction of cleavage sites and a signal peptide/non-signal peptide prediction based on a combination of several artificial neural networks and hidden Markov models (Bendtsen *et al.*, 2004).

T0 T2 T3 T4 T5 T7 T10

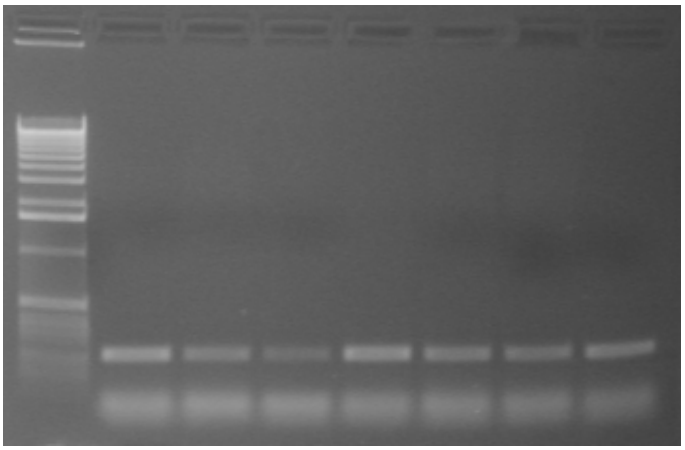

Figure 38. cDNA was checked with tubulin primers in order to ceck for genomic DNA contaminations. Primers should amplify a 230 bp fragment from cDNA and about 450bp from genomic DNA.

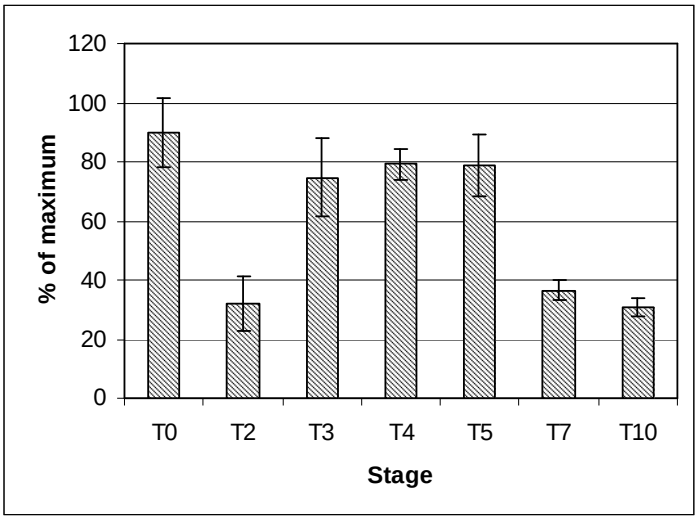

Figure 39. Semi-quantitative expression of LlCyp gene during tepal senescence. The expression level is expressed as percentage of maximum. Error bars represent ±SE (n=3).

Real-time quantitative RT-PCR was performed using another biological replicate in order to verify the results of the previous RT-PCR (Fig. 40A). LlCyp expression was high at stages of flower bud (T-2) and flower opening (T0, T2) and decreased at stage T3 (full bloom) where it reached the minimum value. A 6-fold increase in expression was measured during early senescence (T4, T5), while in advanced stages of senescence (T7, T10) the expression decreased dramatically. Expression was assessed in different flower organs using flowers at stage T4 (Fig. 40B). The expression was high in stamen and almost absent in the ovary. The expression in inner tepals at stage T4 was comparable to the expression in outer tepals at stage T3. In the style and stigma the expression was relatively low compared to stamens.

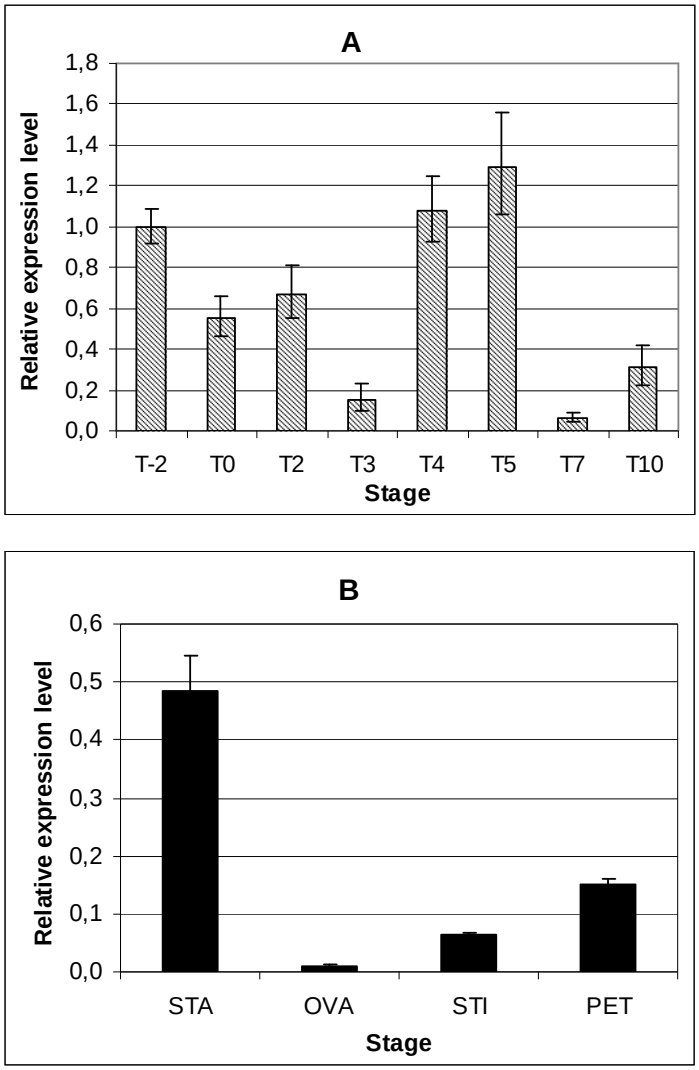

Figure 40. Quantitative expression of LlCyp gene measured through real-time RT-PCR. The expression level is expressed using T-2 as reference stage in outer tepals (A). The expression was assessed also in stamen (STA), ovary (OVA), style and stigma (STI), inner tepals (PET) (B). Error bars represent ±SE (n=3).

3.7. Sub-cellular localization of LlCyp KDEL-protease

I generated a YFP fusion with the LlCyp open reading frame (Clone 9) under the control of the 35S promoter to analyze the sub-cellular localization of LlCyp protease (35S-LlCyp-YFP). RFP fusions with the ctVSS of phaseolin, the tetrapeptide AFVY, appended to the C-terminus of RFP (spRFP-AFVY) were used as a vacuolar marker (Hunter *et al.*, 2007). Protoplasts were produced from *Arabidopsis* leaves expressing the YFP-based construct, and expression analyzed with a confocal laser scanning microscope. Both the YFP-LlCyp

construct and the vacuolar marker were exclusively detected in the endoplasmic reticulum (Fig. 41A). No fluorescent signals were detected within the vacuole or other cell compartments. Transient expression of the YFP-based construct was also performed in tobacco leaves by means of agro-infiltration (These experiments were performed by Dr Lorenzo Frigerio at Warwick HRI, University of Warwick). This technique allowed a longer incubation, necessary for protein maturation and transport to the target organelle. Confocal microscopy images clearly confirmed the endoplasmic reticulum localization (Fig. 41B). It is clearly evident the cortical endoplasmic reticulum containing the LlCyp protein and no fluorescence was detected within the vacuole.

An antibody raised against the SlCypEP KDEL-tailed protease from tomato anthers was used for immunogold localization of the LlCyp protease in lily tepals. The analysis of LlCyp and SlCypEP sequences showed 63% identity, potentially sufficient for LlCyp to be recognized by SlCypEP antibody (Fig. 42). Recombinant SlCysEP lacking 22 N-terminal amino acids was used for the antibody production (Senatore *et al.*, 2009). Tepals from opening flowers (T0), from flowers at full bloom (T3) and undergoing senescence (T5) were used. During flower senescence (T5) small electron-dense structures appeared within the vacuole or in diluted cytoplasm after vacuole rupture (Fig. 43, indicated by arrows). Using transmission electron microscopy, immunogold particles were detected on electron-dense structures similar to those observed previously within the vacuole (Fig. 44). A control experiment with preimmune serum showed no gold particles on the electron-dense structures (data not shown). The electron-dense structures seemed to derive directly from the cytoplasm (Fig. 44B) and in some cases seemed to possess membranous layers and to release their content into the vacuole (Fig. 44C and D). Similar structures and immunogold labelling were not detected in tissues at stage T0 and T3.

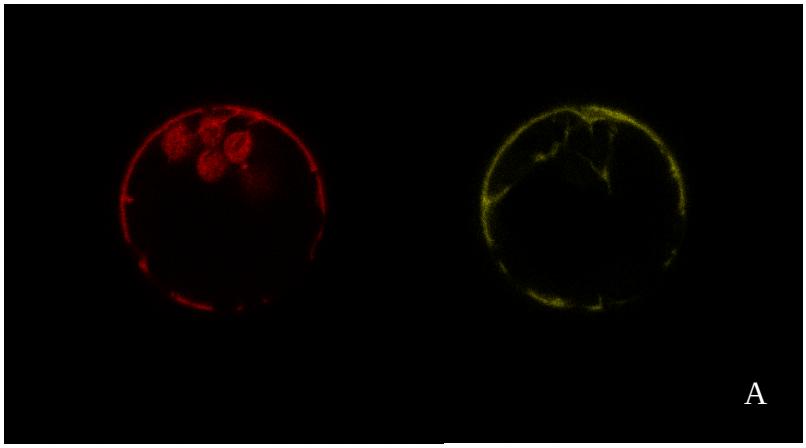

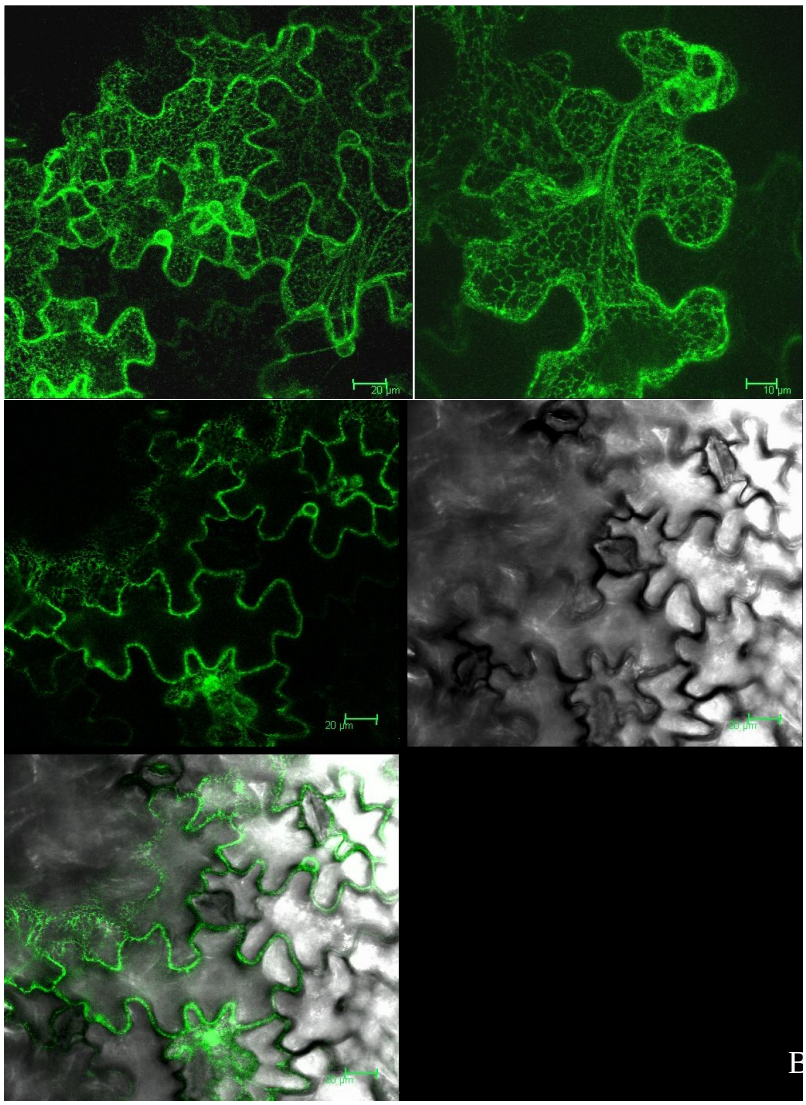

Figure 41. Transient expression of RFP and YFP fusions in Arabidopsis protoplasts (A) and tobacco leaves (B). RFP and YFP fusions label the endoplasmic reticulum of leaf protoplasts (A). Protoplast from Arabidopsis plants expressing the fluorescent reporter proteins were analyzed by confocal microscopy using YFP excited at 514 nm and RFP exited at 543 nm. YFP fluorescence is shown in yellow, chlorophyll autofluorescence and RFP fluorescence in red. YFP fusion labels the endoplasmic reticulum of tobacco leaves (B). Tobacco leaves expressing the fluorescent reporter protein were analyzed by confocal microscopy using YFP excited at 514 nm. YFP fluorescence is shown in green.

```
                10        20        30        40        50        60        70        80        90       100
                ....|....|....|....|....|....|....|....|....|....|....|....|....|....|....|....|....|....|
Clone 9    MENQSILSFSILLLVALSLVAATQSIPFTTKDLESEESLWSLYERWRSQHTISRDLGEKQKRFNVFKENVKFIHEFNQQDQPYKLALNKFADLTNQEFRS
Clone 20   MENQSILSFSILLLVTLSLVAATQSIPFTTKDLESEESLWSLYERWRSQHTISRDLGEKQKRFNVFKQNVKFIHEFNQQDQPYKLALNKFADLTNQEFRS
SlCyp      MKKLFLVLFTLALVLRLG-----ESFDFHEKELETEEKFWELYERWRSHHTVSRSLDEKHKRFNVFKANVHYVINFNKKDKPYKLKLNKFADMTNHEFRQ

                110       120       130       140       150       160       170       180       190       200
                ....|....|....|....|....|....|....|....|....|....|....|....|....|....|....|....|....|....|
Clone 9    KYAGSRHDHHRALRGNDHATSEFMYEK-AIAPPSVDWRQKGAVTAVKNQGQCGSCWAFSTIAAVEGINQIKTKNLVSLSEQELIDCDTEVNQGCNGGLMA
Clone 20   KYAGSRHDHHRALRRNHHATSEFMYEK-AIAPPSVDWRQKGAVTAVKNQGQCGSCWAFSTIAAVEGINQIKTKNLVSLSEQELIDCDTEVNQGCNGGLMA
SlCyp      HYAGSKHKHHRTLLGASRANGTFMYANEDNVPPSIDWRKKGAVTPVKDQGQCGSCWAFSTVVAVEGINQIKTKKLVSLSEQELVDCDTTENQGCNGGLMD

                210       220       230       240       250       260       270       280       290       300
                ....|....|....|....|....|....|....|....|....|....|....|....|....|....|....|....|....|....|
Clone 9    YAFEFIKKNGGITSEDAYPYAEVDQTCQS-KMNSPVVTVDGHQNVPLNNENALMKAVANQPVSVAIEASGYAFQFYSEGVFTGSCGTDLDHGVAIVGYGT
Clone 20   YAFEFIKKNGGITSEDAYPYAEVDQTCQS-KMNSPVVTVDGHQNVPLNNENALMKAVANQPVSVAIEASGYAFQFYSEGVFTGSCGTDLDHGVAIVGYGT
SlCyp      PAFDFIKKRGGITTEERYPYKAEDDKCDIQKRNTPVVSIDGHEDVPPNDEDALLKAVANQPISVAIDASGSQFQFYSEGVFTGECGTELDHGVAIVGYGT
```

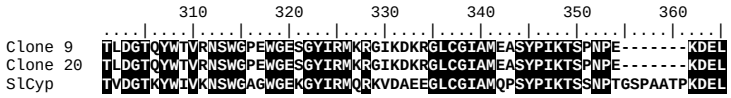

Figure 42. Alignment of LlCyp clones from lily tepals and SlCyp from tomato anthers using clustal analysis in BioEdit. Matching nucleotides are shaded.

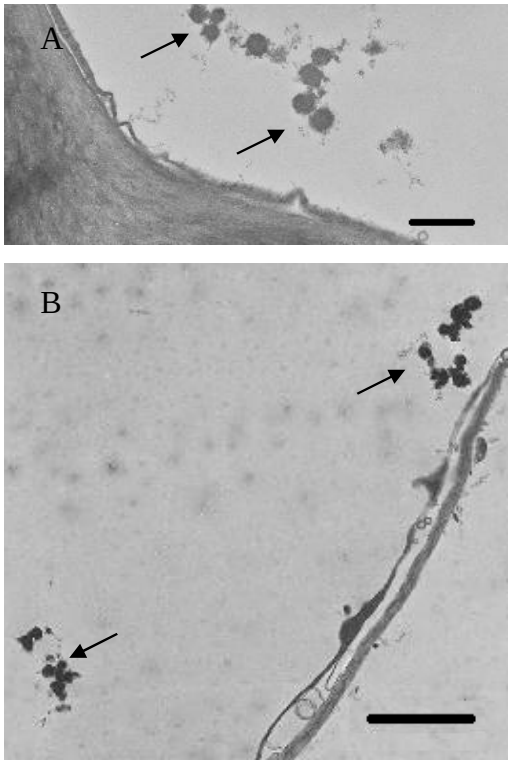

Figure 43. Transmission electron micrographs of cells of lily tepals at stage T5. Electron dense structures appear within the vacuole (A and B) of cells at stage T5. (A) Magnification 2.5 K, scale bar, 3 µm; (B) Magnification 6.3 K, scale bar, 1 µm;

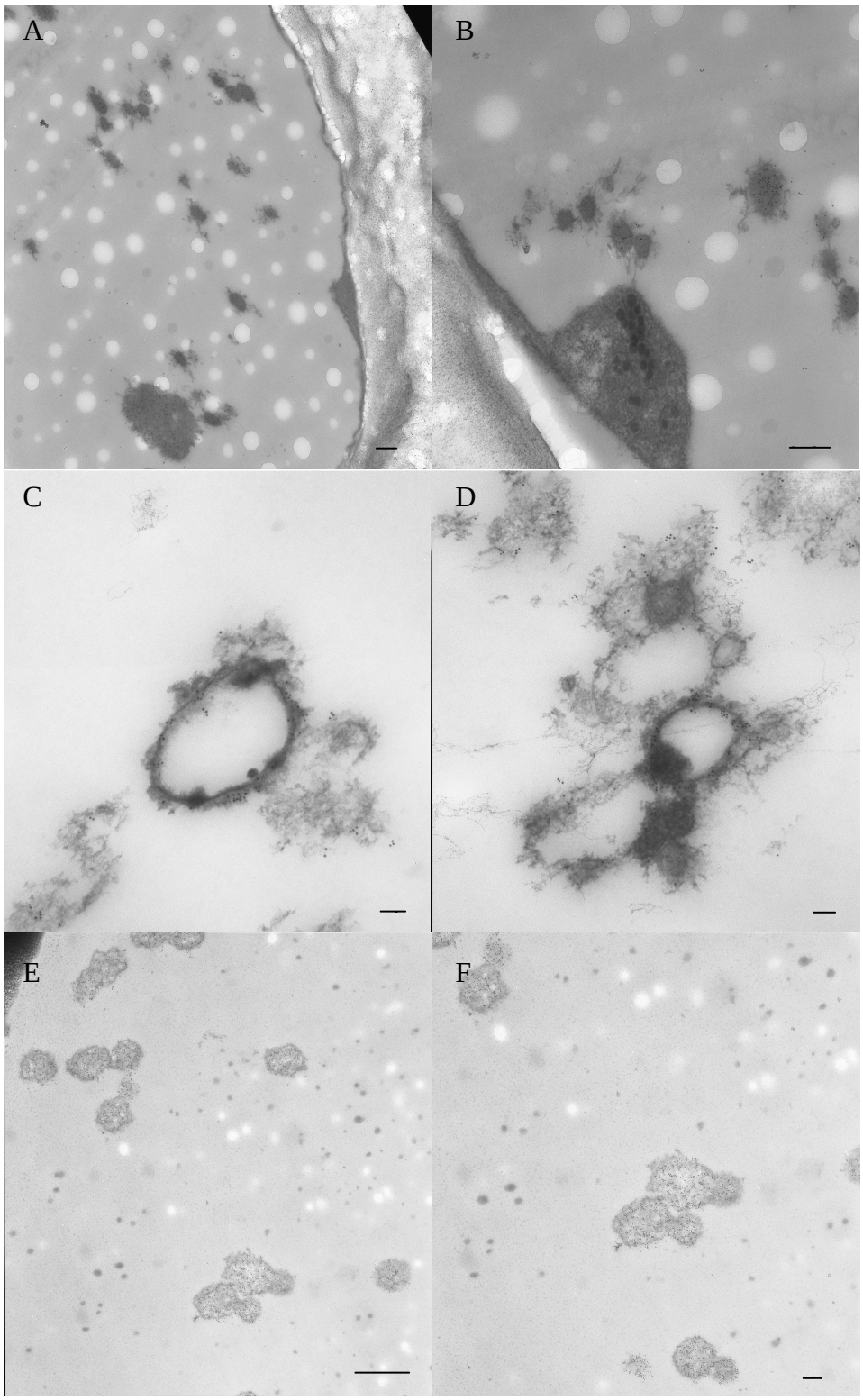

Figure 44. Immunolocalization of LlCyp in cells of lily tepal at stage T5. (A) Magnification 13 K, scale bar, 300 nm; (B) Magnification 25 K, scale bar, 300 µm; (C) Magnification 50 K, scale bar, 100 nm; (D) Magnification 40 K, scale bar, 100 nm; (E) Magnification 10 K, scale bar, 1 µm. (F) Magnification 13 K, scale bar, 300 nm.

3.8. Heterologous expression of LlCyp and western blotting

Full length LlCyp protease (clone 9) was over-expressed using pET21b vector in *E. coli* BL21 cells. After induction, 1 mL of culture was used in a western blotting assay to verify the expression and size of the protease (Fig. 45). SlCysEP purified protein was used as a positive control and samples from induced and non-induced *E. coli* cultures were analyzed. SlCysEP antibody was able to detect LlCyp that was shown to be a KDEL-tailed cysteine protease of about 45 KDa.

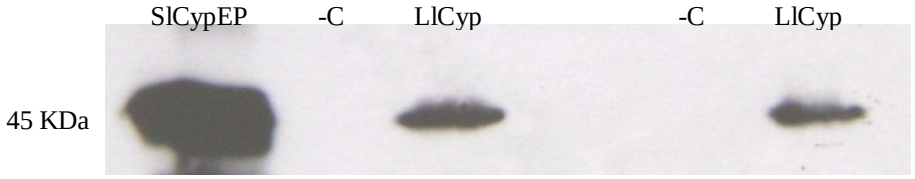

Figure 45. Western blotting after LlCyp over-expression. SlCypEP from Solanum lycopersicum was used as a positive control. Non-induced *E. coli* culture was used as negative control (-C). The experiment was done in duplicate using two different colonies of the same clone.

Proteins were extracted from lily tepals at each stage and used for western blotting. SlCypEP antibody cross-reacted with proteins in lily extracts and at least three bands were detected for each lane probably derived from the multi-step processing of KDEL-cysteine proteases (Fig. 46). A strong unspecific 70 KDa band was detected that increased by stage T3 and was no longer visible at stage T10. The polyclonal antibody could cross-react with unspecific proteins and the expected size for the unprocessed LlCyp was 45 KDa. The abundance of the 45, 43, and 35 KDa proteins increased by stage T4. At stage T5 and T6 the proteins were present at low levels until T10 in which they became more abundant. In lane T4 a 40 KDa protein was present which may represent a processing intermediate.

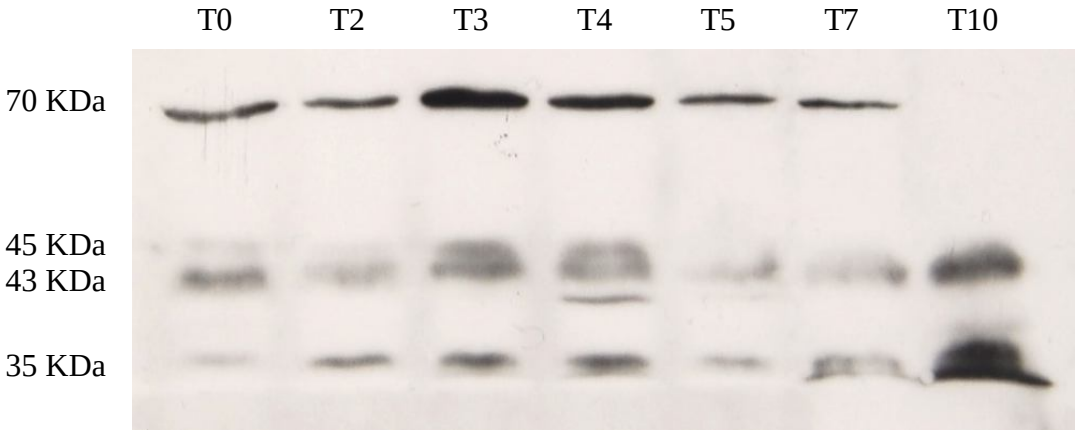

Figure 46. Western blot of protein extracts from lily tepals held in water. Blots were incubated with a primary antibody raised against SlCypEP.

3.9. Cloning and expression of VPE genes

Degenerate primers VegF2 and VegR2 were used to isolate partial VPE cDNAs from lily tepal tissues at stage T4. Two clones were identified differing in nucleotide and aminoacid sequence (Fig. 47 and 48).

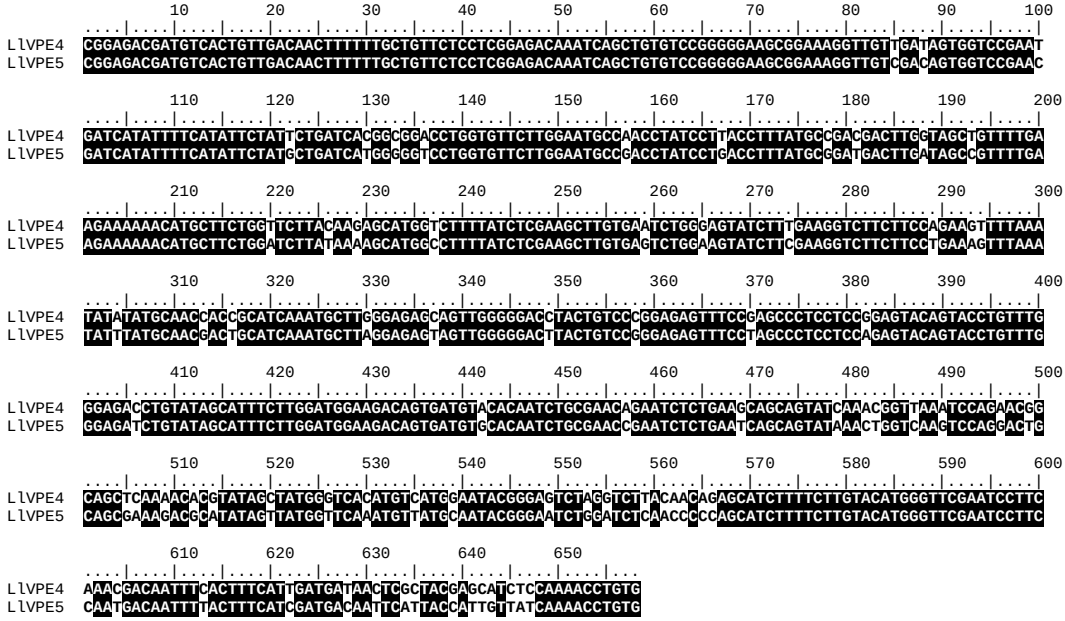

Figure 47. Alignment of LlCyp clones from lily tepal using clustal analysis in BioEdit. Matching nucleotides are shaded.

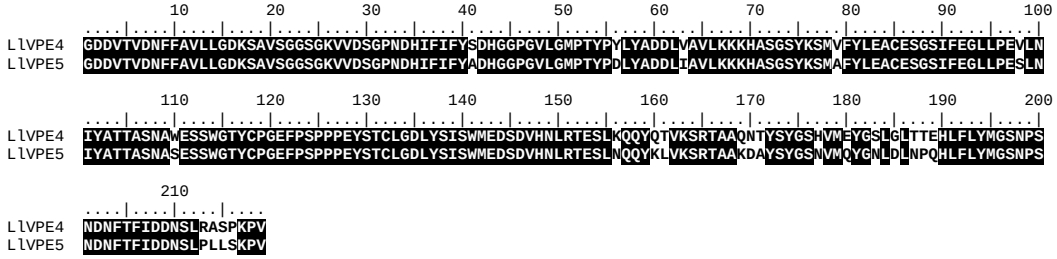

Figure 48. Alignment of LlCyp clones from lily tepal. Alignment was conduced using clustal analysis in BioEdit. Matching amino acids are shaded.

A BLAST search of the National Center for Biotechnology Information database was conducted using the 658 bp fragments (http://www.ncbi.nlm.nih.gov/), revealing an high similarity with legumain-like peptidades present in the database (Fig. 49 and 50). The alignment of the putative protein sequence deduced from the partial LlVPE4 cDNA showed 53-79% homology with the same region of See2B (*Zea mays*), Leg-4 (*Hordeum vulgare*), VPE-1 (*Saccarum officinarum*), NtVPE-1b (*Nicotiana tabacum*), GAMMA-VPE (Arabidopsis thaliana), VmPE-1 (Vigna mungo) and DELTA-VPE (*Arabidopsis thaliana*). The alignment of the putative protein sequence deduced from the partial LlVPE5 cDNA showed similar homology.

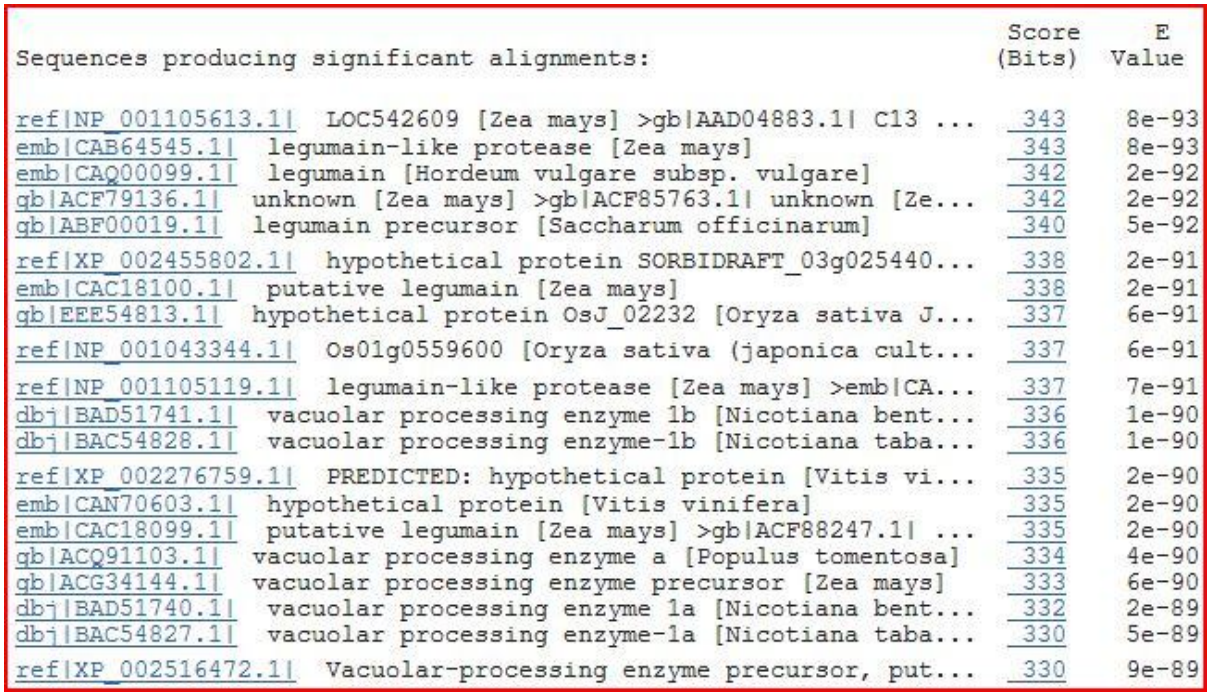

Sequences producing significant alignments:	Score (Bits)	E Value
ref|NP_001105613.1| LOC542609 [Zea mays] >gb|AAD04883.1| C13 ...	343	8e-93
emb|CAB64545.1| legumain-like protease [Zea mays]	343	8e-93
emb|CAQ00099.1| legumain [Hordeum vulgare subsp. vulgare]	342	2e-92
gb|ACF79136.1| unknown [Zea mays] >gb|ACF85763.1| unknown [Ze...	342	2e-92
gb|ABF00019.1| legumain precursor [Saccharum officinarum]	340	5e-92
ref|XP_002455802.1| hypothetical protein SORBIDRAFT_03g025440...	338	2e-91
emb|CAC18100.1| putative legumain [Zea mays]	338	2e-91
gb|EEE54813.1| hypothetical protein OsJ_02232 [Oryza sativa J...	337	6e-91
ref|NP_001043344.1| Os01g0559600 [Oryza sativa (japonica cult...	337	6e-91
ref|NP_001105119.1| legumain-like protease [Zea mays] >emb|CA...	337	7e-91
dbj|BAD51741.1| vacuolar processing enzyme 1b [Nicotiana bent...	336	1e-90
dbj|BAC54828.1| vacuolar processing enzyme-1b [Nicotiana taba...	336	1e-90
ref|XP_002276759.1| PREDICTED: hypothetical protein [Vitis vi...	335	2e-90
emb|CAN70603.1| hypothetical protein [Vitis vinifera]	335	2e-90
emb|CAC18099.1| putative legumain [Zea mays] >gb|ACF88247.1| ...	335	2e-90
gb|ACQ91103.1| vacuolar processing enzyme a [Populus tomentosa]	334	4e-90
gb|ACG34144.1| vacuolar processing enzyme precursor [Zea mays]	333	6e-90
dbj|BAD51740.1| vacuolar processing enzyme 1a [Nicotiana bent...	332	2e-89
dbj|BAC54827.1| vacuolar processing enzyme-1a [Nicotiana taba...	330	5e-89
ref|XP_002516472.1| Vacuolar-processing enzyme precursor, put...	330	9e-89

Figure 49. BLAST database search using the 658 bp LlVPE4 fragment. The first 20 sequences producing significant alignments are shown.

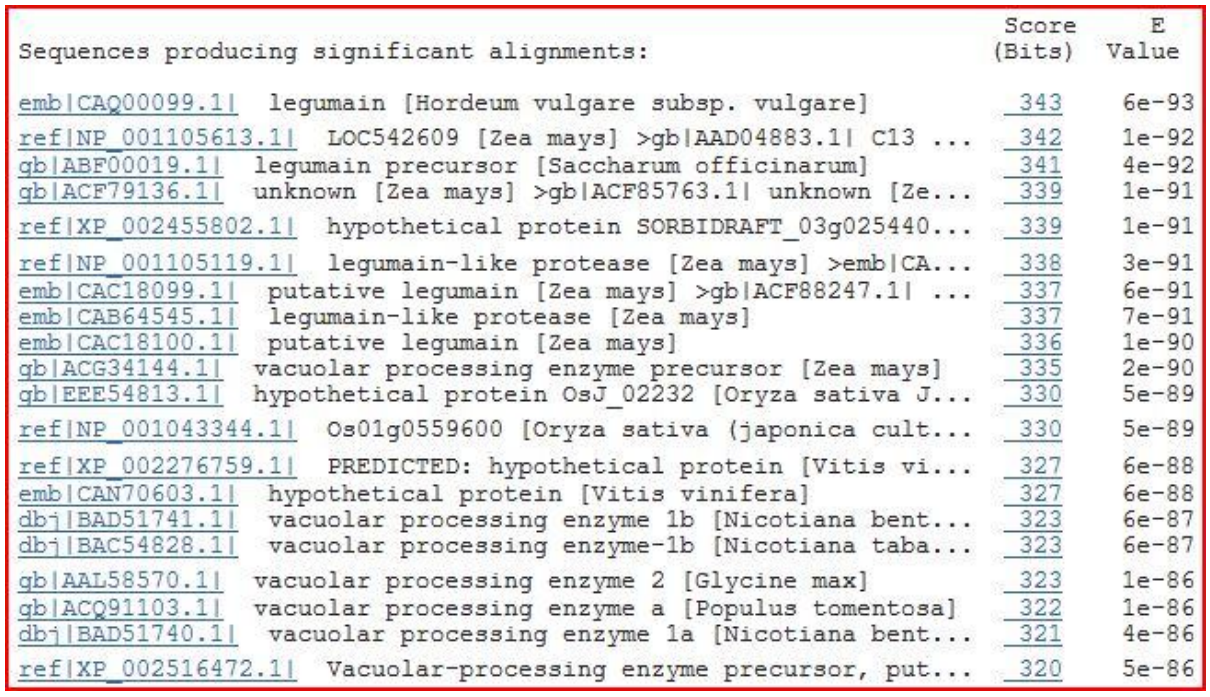

Sequences producing significant alignments:	Score (Bits)	E Value
emb|CAQ00099.1| legumain [Hordeum vulgare subsp. vulgare]	343	6e-93
ref|NP_001105613.1| LOC542609 [Zea mays] >gb|AAD04883.1| C13 ...	342	1e-92
gb|ABF00019.1| legumain precursor [Saccharum officinarum]	341	4e-92
gb|ACF79136.1| unknown [Zea mays] >gb|ACF85763.1| unknown [Ze...	339	1e-91
ref|XP_002455802.1| hypothetical protein SORBIDRAFT_03g025440...	339	1e-91
ref|NP_001105119.1| legumain-like protease [Zea mays] >emb|CA...	338	3e-91
emb|CAC18099.1| putative legumain [Zea mays] >gb|ACF88247.1| ...	337	6e-91
emb|CAB64545.1| legumain-like protease [Zea mays]	337	7e-91
emb|CAC18100.1| putative legumain [Zea mays]	336	1e-90
gb|ACG34144.1| vacuolar processing enzyme precursor [Zea mays]	335	2e-90
gb|EEE54813.1| hypothetical protein OsJ_02232 [Oryza sativa J...	330	5e-89
ref|NP_001043344.1| Os01g0559600 [Oryza sativa (japonica cult...	330	5e-89
ref|XP_002276759.1| PREDICTED: hypothetical protein [Vitis vi...	327	6e-88
emb|CAN70603.1| hypothetical protein [Vitis vinifera]	327	6e-88
dbj|BAD51741.1| vacuolar processing enzyme 1b [Nicotiana bent...	323	6e-87
dbj|BAC54828.1| vacuolar processing enzyme-1b [Nicotiana taba...	323	6e-87
gb|AAL58570.1| vacuolar processing enzyme 2 [Glycine max]	323	1e-86
gb|ACQ91103.1| vacuolar processing enzyme a [Populus tomentosa]	322	1e-86
dbj|BAD51740.1| vacuolar processing enzyme 1a [Nicotiana bent...	321	4e-86
ref|XP_002516472.1| Vacuolar-processing enzyme precursor, put...	320	5e-86

Figure 50. BLAST database search using the 658 bp LlVPE5 fragment. The first 20 sequences producing significant alignments are shown.

The predicted aminoacid sequence of LlVPEs was shown to begin 124 amino acids from the N-terminus of Leg-4 protease of *Hordeum vulgare* and it did not extend to the C-terminal region supposed to possess the conserved tetra-peptide GFSA (Fig. 51). However, LlVPEs

contained some elements characteristic of cysteine proteases such as the Cys and His forming a catalytic dyad (Fig. 51).

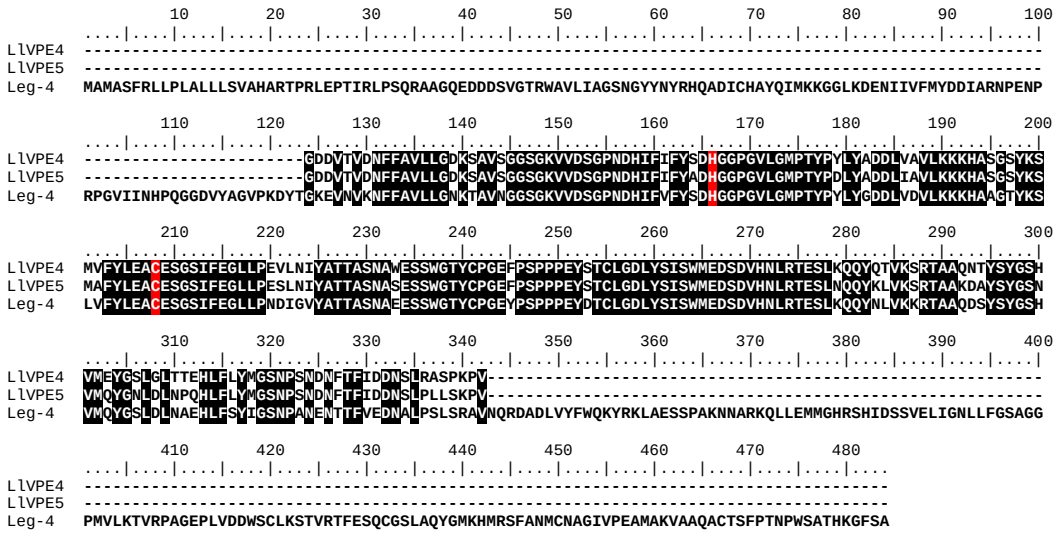

Figure 51. Alignment of LlVPE clones from with Leg-4 from *Hordeum vulgare*. Alignment was conduced using clustal analysis in BioEdit. Aminoacids matching the consensus are shaded. The Cys and His forming the catalytic dyad of the active site are also shown (in red).

The LlVPE4 fragment was used to obtain the full length open reading frame. RACE was performed using GSPF and GSPR primers. Using WinStar (DNASTAR Inc., US), 3' and 5' ends were assembled with the LlVPE5 fragment to get the 1440 bp consensus sequence from the starting Met to the stop codon.

Several aminoacids characteristic of legumain-like peptidases are conserved, such as the GFSA tetrapeptide at the C-terminus of the consensus sequence. The catalytic residues of legumain-type peptidases cysteine-204 and histidine-162 are also conserved (Fig. 52).

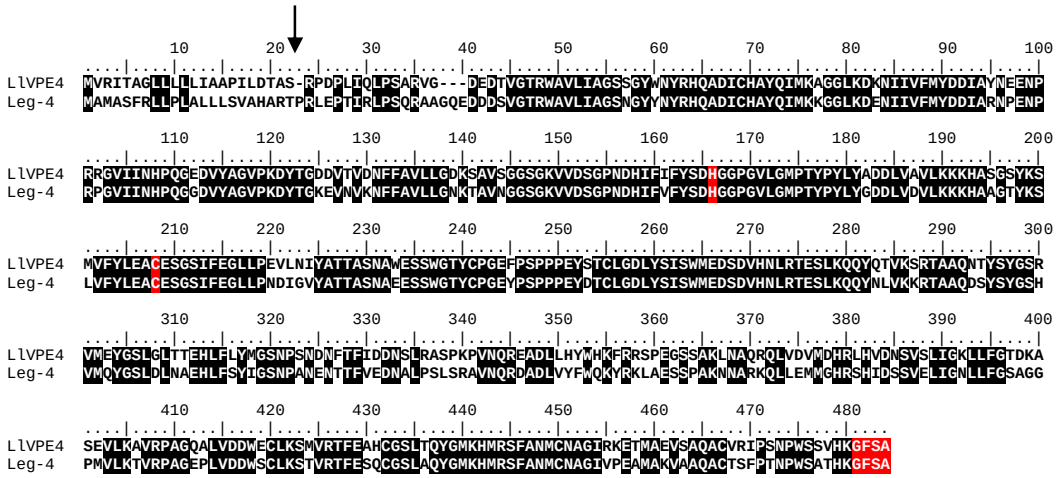

Fig. 52. Alignment of LlVPE4 consensus sequence with Leg-4 (*Hordeum vulgaris*) using clustal analysis in BioEdit. Matching aminoacids are shaded. Amino acids belonging to the catalytic pocket (Cys-204 and His-162) and the C-terminal GFSA motif are in red. The arrow represents the predicted cleavage site of the N-terminal signal peptide.

VPEs are synthesised with a signal peptide (pre-sequences), an N-terminal pro-peptide intercalated between the signal peptide and the N-terminus of the mature enzyme, and a C-terminal pro-peptide (Kuroyanagi *et al.*, 2002). Using SignalP and TargetP the cleavage site of the signal peptide and the subcellular localization of the protein were predicted (Emanuelsson *et al.*, 2000; Bendtsen *et al.*, 2004) (Fig. 53). LlVPE protease possesses a 22 aa signal peptide and is not predicted to be localised to chloroplasts or mitochondria but is probably secreted. It was not possible to predict the cleavage site of the N- and C-terminal pro-peptides by the aligment of LlVPE4 with VPEs in the database.

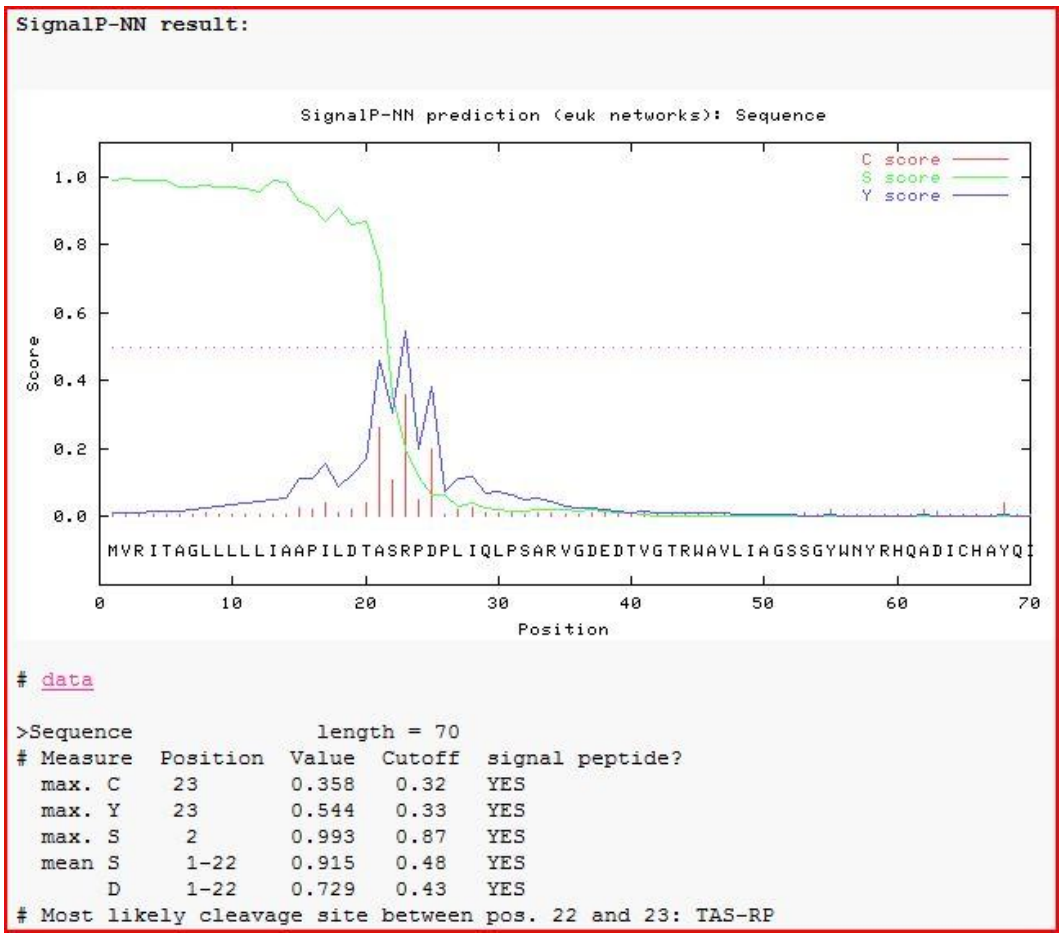

A

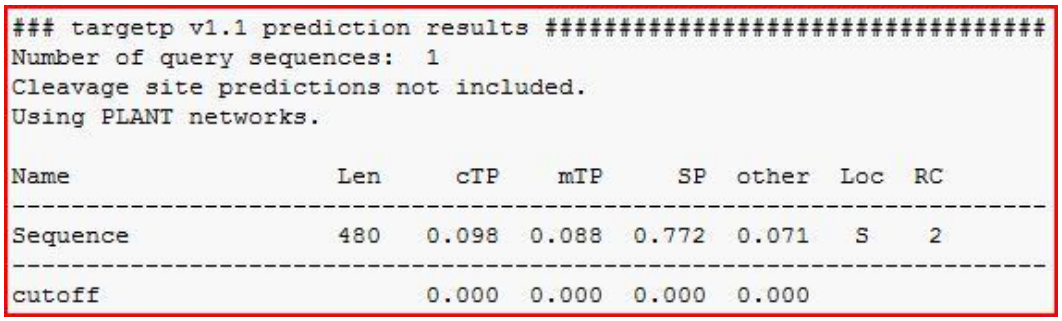

B

Figure 53. Analysis LlVPE4 aminoacid sequence using SignalP (A) and TargetP (B).

Real-time quantitative RT-PCR was performed to analyse the expression pattern of LlVPE4 during lily flower senescence. (Fig. 54A). LlVPE4 expression was high at stages of flower bud (T-2) and significantly decreased during flower opening. In senescing stages expression of LlVPE4 remained at low levels. The analysis of the expression in flower organs revealed a high expression level in stylo and stigma (Fig. 54B). In the ovary the expression was almost absent and very low in stamen and inner tepals.

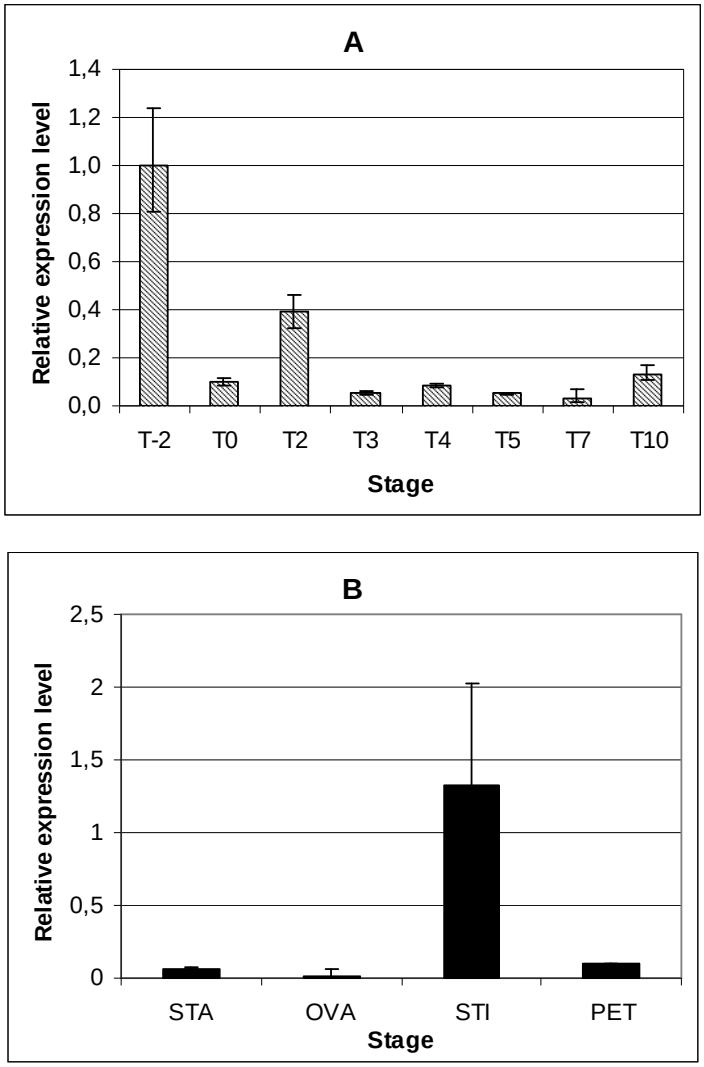

Figure 54. Quantitative expression of LlVPE4 gene measured through real-time RT-PCR. The expression level is expressed using T-2 as reference stage. The expression was assessed also in stamen (STA), ovary (OVA), style and stigma (STI), inner tepals (PET) (B). Error bars represent ±SE (n=3).

4. DISCUSSION

4.1. Timing of tepal senescence

The life span of flowers is generally determined by the time to petal abscission or wilting and in many species it is regulated by ethylene. Conversely, many species exist in which ethylene does not appear to play a major role (van Doorn, 2001). The genus *Lilium* includes almost 100 species distributed in Asia, North America and Europe. Numerous hybrids and cultivars exist differing in colour, shape, size and fragrance, and are grown as garden perennials, potted flowering plants or cut flowers (Wilkins and Dole, 1997). Commercial lilies are generally considered as ethylene insensitive species due their low sensitivity to applied ethylene and ethylene inhibitors. Moreover, ethylene production of lily flowers is very low and often below the detectable level (Elgar *et al.*, 1999; Celikel *et al.*, 2002; Han and Miller, 2003). The different morphological, physiological and genetic parameters analyzed in the present study allowed us to determine the timing and localization of the onset of corolla senescence and to identify key elements possibly involved in senescence initiation and progression in the ethylene-insensitive *Lilium longiflorum*.

Easter lily (*Lilium longiflorum*) is a long-lived flower with a life span of 12 d from harvest time to complete wilting, which occurs without petal abscission. The vase life of cut flowers is not affected by the presence of the stem and leaves leading to the conclusion that the opening flower is completely autonomous and that it may not require nutrients from the stem. The involvement of gynoecium and stamen in mediating senescence induction is still a matter of debate. In many flowers pollination initiates a sequence of precisely regulated developmental events that include senescence of the perianth and development of the ovary in which the hormone ethylene plays a regulatory role while in others the pattern of flower senescence is not affected (Stead, 1992). In carnation the removal of the gynoecium by hand prevented the evolution of ethylene production and prolonged the vase life of the flower, demonstrating a key role of the gynoecium in controlling flower senescence (Shibuya *et al.*, 2000). In lily the removal of gynoecium and stamen does not affect the progression of flower senescence and vase life. Thus tepal senescence in lily may be independent of pollination and the gynoecium, although it was demonstrated in carnation that the effect is strictly dependent on the technique used for gynoecium removal (Shibuya *et al.*, 2000). Thus, further work may be required to confirm this finding.

Chemicals have been extensively used for improving postharvest quality and flower longevity of ornamental plants. Calcium chloride was successfully used for delaying flower

senescence in cut rose. It was suggested that the calcium-induced delay in rose petal senescence involves the protection of membrane proteins and the reduction of ethylene production (Torrea *et al.,* 1999). Calcium applications also improved postharvest quality of cut gerberas (Gerasopulos and Chebli, 1999). In our experiments, applications of 1 mM $CaCl_2$ did not affect vase life of lily flowers while application of 5 mM $CaCl_2$ slightly reduced flower longevity. Zinc chloride significantly reduced flower senescence in isolated *Iris* tepals, while the protease inhibitor E-64 had no effect (Pak and van Doorn, 2004). E-64 and 1 mM zinc chloride were not effective in delaying lily flower senescence but the experiments were carried out using only intact flowers. Lanthanum chloride was successfully used in lily as an inhibitor of PCD induced by the fungal pathogen *Botrytis elliptica* (van Baarlen *et al.,* 2004), while it was not effective in delaying lily flower senescence in the present study. The positive effect of sucrose on postharvest quality of cut flowers has been extensively demonstrated in both ethylene-sensitive and –insensitive species (van Doorn, 2004). Also the addition of other sugars to the vase solution may delay senescence. Research has indicated that trehalose, a non-reducing disaccharide composed of two glucose units, may also be effective in extending flower longevity in cut stems of gladiolus (Otsubo and Iwaya-Inoue, 2000; Yamada *et al.,* 2003) and tulip flowers (Iwaya-Inoue and Takata, 2001). In gladiolus treahlose was reported to be more effective than sucrose in reducing PCD-associated events also at a concentration of 50 mM. In our experiments, 300 mM sucrose or trehalose solution delayed flower senescence by about 12% and there was no difference between the two treatments, whereas, 30 mM solutions did not affect the time to petal wilting.

One of the first signs of flower senescence is membrane degradation and the loss of petal fresh weight. In lily, tepal fresh weight increased by flower opening and then dramatically decreased to 15% of maximum reflecting a strong loss of water and probably an intensive rate of remobilization. This pattern is in accordance with data from other species such as *Petunia* (Jones *et al.,* 2005), *Narcissus* (Hunter *et al.,* 2004), *Hemerocallis* (Panavas *et al.,* 2004) and *Gladiolus* (Hossain *et al.,* 2006). The decrease in dry weight at stage T2 was in accordance with the onset of tepal senescence. However, during flower senescence the dry weight remained constant. Increased tepal dry weight observed following sucrose feeding is well known from previous studies on other flowers, such as *Sandersonia* (Eason *et al.,* 1997) and tulip (Ranwala and Miller, 2009). In lily held in water, dry weight-fresh weight ratio slightly decreased during flower opening and then increased in senescing tepals due to water loss. At stage T10 the ratio was 1.5-fold higher in outer tepals than in inner tepals, reflecting

the different timing of petal wilting. In sucrose treated flowers, the difference at stage T10 was less evident suggesting a delaying effect of sucrose on water loss.

A predominant feature of senescence in many systems is the loss of membrane permeability that leads to the release of electrolytes from the tissues. Ion leakage is a commonly used method for determining the extent of tissue damage indicative of the loss of membrane semi-permeability (Panavas and Rubinstein, 1998; Leverenz *et al.*, 2002). This was shown clearly in lily where leakage rate increased in tepals undergoing senescence. Differences were found in leakage rate and timing between inner and outer tepals, which confirm the different behaviour of the two whorls as previously observed. The increase in conductivity was in accordance with the decrease in fresh weight due to water loss and with the membrane degradation observed at stage T3 through transmission electron microscopy.

4.3. Flower structure

In lily tepals, physiological and biochemical changes take place before visible signs of petal wilting which are presumably correlated to mesophyll collapse. The complexity of tepal structure, comprising different cell types, makes the process of senescence not spatially homogeneous throughout the cross-section. In lily tepals, cell collapse is demonstrated to occur earlier in the mesophyll layer and this correlates well with the onset of visible senescence, as observed also in other species such as *Sandersonia* (O'Donoghue *et al.*, 2002), *Iris* (van Doorn *et al.*, 2003) and *Alstroemeria* (Wagstaff *et al.*, 2003). In senescing flower (stage T5), only vascular bundle and epidermal cells are still intact, in accordance with the observations previously made in *Ipomea* and *Alstroemeria* (Matile and Winkenbach, 1971; Wagstaff *et al.*, 2003). Tepal margins at stage T3 seem to be in an advanced stage of senescence compared to inner tissues, with mesophyll cells and the lower epidermis almost totally collapsed. A different timing of senescence through the petal plane was observed in *Alstroemeria* and tobacco flowers, in which senescence was reported to occur before in the petal margin or close to the abscission zone respectively (Serafini-Fracassini *et al.*, 2002; Wagstaff *et al.*, 2003).

Autophagy during senescence seems to be an important process responsible for cell dismantling and remobilization of compounds that can be used in other parts of the plant, and the vacuole is likely to play a crucial role (van Doorn and Woltering, 2008). The lysosomal nature of the vacuole and the autophagic activity in plant cells were hypothesized for the first time by Matile (Matile, 1968), and autolysing cells were observed in *Ipomea* corolla during senescence (Matile and Winkenbach, 1971). In lily tepals, cells began to show signs of

degradation at full bloom (T3) in which the intense vesiculaton was associated with the dilution of the cytoplasm, presumably due to the increase in tonoplast permeability, and the presence of dense structure within the vacuole. Afterwards, vacuolar rupture and protoplast shrinkage were the last events indicating the vacuole as a key executioner of cell death in lily tepals. Autophagy by sequestration of small portions of the cytoplasm at the vacuolar surface (micro-autophagy) or by permeabilization or rupture of the vacuole (mega-autophagy) appear to be common in plant PCD (van Doorn and Woltering, 2005 and references therein). In lily tepals there was no evidence for macro-autophagy in which the formation of a unique double-membrane structure, the autophagosome, engulfs part of the cytoplasm. In an advanced stage of senescence (stage T5), cells surrounding vascular tissues were still functional while mesophyll cells appeared completely collapsed as observed with light microscopy.

4.4. Proteolytic activity

Selective protein breakdown is involved in the maintenance of cell homeostasis and it prevents deleterious effects due to the presence of abnormal and non-functional proteins, regulates the activity of metabolic pathways through the modulation of key enzymes and regulates the levels of receptors (Callis, 1995). Proteolytic enzymes are known to have a principal role in remobilization processes during senescence of plant organs and may be involved as executioners or regulators of cell death. During flower senescence the decrease in protein level has been widely documented using different species (van Doorn and Woltering, 2008 and references therein). In *Lilium longiflorum* overall protein level decreased during tepal senescence and this could be due to a decrease in synthesis as well as an increase in degradation. Moreover, sucrose feeding had no effect on the protein level. The decrease in protein content observed in senescing leaves of lily coincided with chlorophyll degradation as observed in other species, such as wallflower (Prince *et al.,* 2008) and in accordance with the strong degradation of chloroplast proteins observed in senescing leaves (Hörtensteiner and Feller, 2002). An increase in protease activity has been reported to be correlated with a decrease in protein content and inhibitor studies suggest that several classes of proteolytic enzymes could be involved during flower senescence (Stephenson and Rubinstein, 1998; Wagstaff *et al.,* 2002; Jones *et al.,* 2005; Pak and van Doorn, 2005). The effect of sucrose in delaying protease activity was previously observed also in senescing flowers of *Sandersonia aurandica* (Eason *et al.,* 2002). Protease activity detected in lily during flower senescence had an optimum pH of 5.5, indicating the acidic nature of proteolytic enzymes. This in accordance with the hypothesis that vacuole plays a crucial role in executing cell death by

releasing hydrolases, upon rupture or permeabilization of the tonoplast (van Doorn and Woltering, 2005 and references therein).

Proteolytic enzymes possibly involved in flower senescence include cysteine-, serine-, aspartic-, and metallo-proteases, termed after the amino acid residues or metals required for the cleavage reactions. Several proteases have been cloned from floral tissues and a role in flower senescence and cell death has been hypothesized (Guerrero *et al.*, 1998; Eason *et al.*, 2002; Hunter *et al.*, 2002; Wagstaff *et al.*, 2002; Eason *et al.*, 2005; Jones *et al.*, 2005; Yamada *et al.*, 2009). The most representative cysteine proteases implicated in animal PCD are caspases. In spite of a lack of orthologous caspase sequences in plants, caspase-like activities have been detected in plants using synthetic tetrapeptides for specific mammalian caspases (Bonneau *et al.* 2008 and references therein). We report for the first time the induction of caspase-like activities in senescing tepals and leaves of *Lilium longiflorum*. YVADase, DEVDase and VEIDase activities were induced in senescing stages of tepals and leaves held in water, suggesting that they could be involved in executing cell death during senescence. Sucrose treatment resulted in increased caspase-like activities, but the mechanism by which this took place is not known. Caspase-like activities detected in lily are active at acidic pH, in contrast with what was observed for animal cytoplasmic caspases (Stennicke and Salvesen, 1997), and for most of the caspase-like activities detected in plant PCD systems which are active at neutral or basic pH. However, many authors have recently reported plant caspase-1, 3 and 6-like preference for acidic pH (He and Kermode, 2003; Danon *et al.*, 2004; Rotari *et al.*, 2005; Lombardi *et al.*, 2007). The pH requirement indicated again the vacuole as a key element in lily tepal senescence and may suggest that caspase-like proteases are possibly localized in the vacuole or are activated upon acidification of the cytosol following tonoplast degradation. VPE in *Nicotiana benthamiana* has been demonstrated to have YVADase activity and to be required for cell death in tobacco infected by TMV (Hatsugai *et al.*, 2004). Experiments using biotinylated inhibitors and *in vitro* assays suggested that also δ-VPE and γVPE have caspase-1 activity (Nakaune *et al.*, 2005; Kurojanagi *et al.*, 2005). In oats (*Avena sativa*), serine proteinases exhibit caspase-like activities, and the activities increase during fungal toxin victorin-induced PCD (Coeffeen and Wolpert, 2004). These results lead to the hypothesis that acidic hydrolytic enzymes are involved in tepal senescence and that caspase-like activities may participate in cell death in floral tissues, maybe through a series of events culminating in autophagic cell death.

VPEs are vacuolar peptidases also responsible for the maturation or activation of various vacuolar proteins (Shimada *et al.*, 2003; Yamada *et al.*, 2005). Moreover, αVPE and γVPE

mRNAs accumulated in rosette leaves of *Arabidopsis* in association with senescence (Kinoshita *et al.* 1999). VPE could be also involved in senescence of flower organs. Recently, the expression of a VPE gene from *Ipomea nil* petals was shown to increase significantly, suggesting a function for VPE peptidases in flower senescence (Yamada *et al.*, 2009).

In vitro VPE activity was detected using fluorogenic substrates in seed extracts (Shimada *et al.*, 2003; Nakaune *et al.*, 2005), leaf extracts (Hatsugai *et al.*, 2004) and using purified VPEs. In the VPE-null mutant of *Arabidopsis* VPE activity was completely abolished, indicating that there are no other proteases responsible for substrate cleavage and that the assay is specific (Kuroyanagi *et al.*, 2005). We used a fluorogenic substrate to measure VPE activity in extracts from lily tepals and leaves. A peak of activity was observed at full bloom (T2), suggesting the involvement of VPEs in a preliminary phase, at the beginning or before flower senescence. A weak peak was observed late in senescence (stage T7). In sucrose treated flowers, a dramatic increase in VPE activity was measured during flower opening. It could be hypothesized that VPEs are involved as an anti-senescent factor during flower development, but no evidence arose from our experiments and there are no data in the literature supporting this statement. VPE activity increased in lily leaves undergoing senescence in accordance with data reported for *Arabidopsis* (Kinoshita *et al.* 1999).

4.5. DNA degradation

Nuclear DNA fragmentation is considered one of the typical hallmarks of PCD and it has been reported to occur during petal senescence in a *Gladiolus* hybrid (Yamada *et al.* 2003), *Alstroemeria peruviensis* (Wagstaff *et al.* 2003) and *Pisum sativum* (Orzaez and Granell, 1997). In lily tepals, the decrease in DNA content is accompanied by DNA degradation, even though a true DNA laddering was not observed. This does not, however, rule out the hypothesis that cell death in tepals may be a form of PCD. DNA fragmentation into oligonucleosomal units is usually difficult to demonstrate in tissues in which a variable percentage of cells is undergoing PCD. Lily tepals are characterized by the presence of several tissues that undergo cell death following a different timing. Moreover, the appearance of laddering should not be considered an indicator of PCD without parallel evaluation of morphological changes and other PCD hallmarks, especially in quickly dying cells (Kuthanova *et al.*, 2008).

The TUNEL assay has been considered a better diagnostic feature of apoptotic cell death (Danon *et al.*, 2000), and has been widely used to detect DNA fragmentation in several plant

systems (Orzaez and Granell, 1997; Lee and Chen, 2002; Gunawardena *et al.*, 2004; Hoeberichts *et al.*, 2005; Lombardi *et al.*, 2007). In lily tepals the appearance of positive nuclei was an early event occurring at full bloom in flowers without signs of senescence, even if a rapid increase in the number of labelled nuclei took place at the beginning of the senescence process, coinciding with protein degradation and an increase in ion leakage. In *Pisum sativum*, petals TUNEL positive nuclei were observed during physiological senescence and were not detected in petals treated with ethylene inhibitors (Orzaez and Granell, 1997). In *Gypsophyla paniculata* the appearance of positive nuclei was an early event preceding the rise in ethylene production, and was not prevented by treatment with STS (Hoberichts *et al.*, 2005).

4.6. KDEL-protease involvement in flower senescence

The wilting of petals is related to the expression of genes encoding for enzymes such as cysteine proteases, which are probably responsible for the hydrolytic degradation of cell components leading to cell death during flower senescence. Papain-like proteases have been extensively studied in different plant systems and have been identified as key elements in regulating development and cell death (Beers *et al.*, 2000; Beers *et al.*, 2004; Schaller, 2004; Trobacher *et al.*, 2006). Cysteine proteases belonging to the papain family have been isolated from flowers belonging to different genera such as *Hemerocallis* (Guerrero *et al.*, 1998), *Sandersonia* (Eason *et al.*, 2002), *Narcissus* (Hunter *et al.*, 2002), *Alstroemeria* (Wagstaff *et al.*, 2002) and *Petunia* (Jones *et al.*, 2005). Some of these genes were up-regulated in senescing flowers and were proposed to be involved in the execution of senescence.

Two full length cDNAs encoding cysteine peptidase genes (LlCyp clone 9 and 20) were isolated from senescing tepals of *Lilum longiflorum*. The two peptidases differ in only four amino acids located in the pre- and pro-sequence of the enzyme, which are removed for the activation of the enzyme. The predicted amino acid sequence revealed the presence of a C-terminal ER retention signal (KDEL). The KDEL motif functions as a retrieval signal for soluble proteins of the endoplasmic reticulum and vesicles that are derived from the ER. The latter include vesicles that transport proteins to vacuoles (Schmid *et al.*, 2001; Okamoto *et al.*, 2003). LlCyp is homologous to other cysteine peptidase putatively involved in flower senescence, such as PRT5 from *Sandersonia* (Eason *et al.*, 2002) and ALSCYP1 from *Alstroemeria* (Wagstaff *et al.*, 2002). PRT5 codes for a KDEL-tailed cysteine peptidase which was shown to be highly expressed during flower senescence. ALSCYP1 codes for a

papain-like cysteine protease and its expression continuously increased during flower vase life.

Analysing the expression of LlCyp9 gene showed two main peaks, during flower opening and senescence. Differences in expression patterns between real-time and semi-quantitative PCR could be explained by the use of biological replicates grown in different environmental conditions. The expression pattern of LlCyp differs from PRT5 and ALCYP1 but is quite similar to the expression pattern of a thiolprotease gene (SEN102) form *Hemerocallis*, in which there is a first peak at full bloom and a second peak before flower collapse (Guerrero *et al.*, 1998). The high expression of LlCyp in stamen and the low expression in the ovary is in accordance with the results obtained by Guerrero *et al.* (1998) for SEN102. Moreover, Greenwood *et al.* (2009) isolated a KDEL-cysteine peptidase gene (SlCysEP) from tomato and suggested that the accumulation of SlCysEP and the appearance of ricinosomes act as very early predictors of cell death in anthers.

4.7. Sub-cellular localization of LlCyp

The pre-sequence of KDEL-cysteine peptidases directs the enzyme to the lumen of the ER. Subsequently, the protein is secreted by the ER bypassing the Golgi apparatus through a vesicular system that may differ among species. In *Vigna mungo* a KDEL cysteine peptidase (SH-EP) is first accumulated into the ER and afterwards is packed into KDEL-vesicles (KV) that fuse with the vacuole releasing their content (Toyooka *et al.*, 2000; Okamoto *et al.*, 2003). In *Ricinus communis* seeds and in tomato anthers, ricinosomes containing KDEL-peptidases bud from the ER but do not fuse with the vacuole; instead, they lyse upon the collapse of the central vacuole at death, releasing their contents as suicide bombs (Schmid *et al.*, 2001; Senatore *et al.*, 2009). Ricinosome-like structures have been found also in *Hemerocallis* tepals (Schmid *et al.*, 1999). Okamoto *et al.* (2003) showed that when SP-GFP-SHEP was expressed in BY-2 cells, strong fluorescence could be detected in small vesicles, similar to KV-vesicles observed with the immunogold assay. We over-expressed LlCyp under the 35S promoter, fused with the YFP fluorescent reporter in *Arabidopsis* protoplasts and tobacco leaves. In both experiments fluorescence was localized within the ER. It is interesting to note that also the vacuolar marker based on the RFP reporter that was used in the experiments with leaf protoplasts localised within the ER. This could be explained with the short incubation time that was not enough for the proper maturation of the fusion protein. Agroinfiltration of tobacco leaves allowed to increase the incubation time, but LlCyp was still localized within the ER. Because of the complexity of LlCyp proteases, having pro-

sequences and the KDEL motif, it would be useful to test other constructs, different from the construct with the YFP reporter fused at the C-terminus of LlCyp. Moreover, it would be more appropriate to use an RFP reporter because YFP is not stable in acidic compartments and could compromise the visualization of vacuolar localized products.

Immunogold in *Ricinus communis*, *Vigna mungo* and tomato localised KDEL-proteases in small vesicles that bud from the ER (Toyooka *et al.,* 2000; Schmid *et al.,* 2001; Senatore *et al.,* 2009). Using an antibody raised against tomato SlCypEP, we performed an immunogold assay in tissues from tepals at stage T0, T3, and T5. We did not localize gold particles in ricinosome-like or KV vesicles. Gold particles were, however, localised on electron dense structures within the vacuole in tepals at stage T5. We hypothesize that LlCyp is localised within the vacuole and gold particles can be visualised only when a substrate, in this case the electron dense structures, enter into the vacuole. Nevertheless, Toyooka *et al.* (2000) showed that KDEL-proteases are released within protein storage vacuoles, but gold particles where less numerous and sometimes not visible within the storage compartment compared to KV-vesicles. Similarly, VPEs are typically accumulated within the vacuole, but gold particles were only found in electron dense structures outside cell walls or within the vacuole (Kinoshita *et al.,* 1999; Nakaune *et al.,* 2005).

4.8. Heterologous expression and western blotting

Plant papain-like proteases are synthesized as pre-pro-enzymes (40-50 KDa) that are processed through the removal of the pre- and pro-sequences to yield the mature and fully active form (22-35 KDa) (Beers *et al.,* 2000; Trobacher *et al.,* 2006). Based on results from other species (Okamoto *et al.,* 1994; Schmid *et al.,* 1998; Senatore *et al.,* 2009), the predicted molecular masses of unprocessed LlCyp, the proprotein, and mature enzyme are about 45, 43, and 30 kDa, respectively. We over-expressed the full length LlCyp in *E. coli* and we compared it with the SlCyp KDEL-cysteine protease from tomato anthers. The antibody raised against SlCypEP recognized LlCyp protein that was shown to have a molecular mass of about 45 KDa.

We used the SlCysEP antibody to detect cysteine proteases in lily extracts. The antibody cross-reacted with bands at 45, 43 and 35 KDa. An additional band was detected at 40 KDa in extracts from stage T4. At stage T0, the strong 43 KDa band indicates that the enzyme is prevalently accumulated as pro-peptide. At stage T2 the decrease in 43 KDa band and the increase in 35 KDa band suggests an increase in protease processing and also a decrease in protein synthesis because the 43 KDa form is not replaced. From stage T3 the strong bands at

45, 43 and 35 KDa suggest an increase in protein synthesis and processing. This is in accordance with the results obtained with RT-PCR in which the expression of LlCyp gene decreased at full bloom (stage T2) and increased again at stage T3. In extracts from *Sandersonia* flowers, western analysis using an antibody raised against a castor bean cysteine protease (CysEP) identified three immunoreactive peptides, one of which represented the active form of putative KDEL-peptidases and its abundance increased during senescence (Eason *et al.*, 2002).

4.9. VPE involvement in flower senescence

VPEs are synthesized as large precursors and transferred to the vacuole, where they are converted into their mature form through the removal of the pre- and pro-sequences. The VPEs then apparently convert other proteins into mature forms. We isolated two cDNA fragments from senescing lily tepals showing high homology with other VPEs in the database such as See2B (*Zea mays*), Leg-4 (*Hordeum vulgare*), VPE-1 (*Saccarum officinarum*), NtVPE-1b (*Nicotiana tabacum*). The predicted aminoacid sequence of the full length LlVPE4 showed the highest homology with NtVPE-1b and a good homology with other VPEs such as NtVPE-1a, NtVPE-3 from tobacco, γVPE, αVPE, δVPE from *Arabidopsis* and VmPE-1 from *Vigna mungo*. In *Arabidopsis*, genes encoding αVPE and γVPE were up-regulated in association with PCD and in senescing leaves (Kinoshita *et al.*, 1999). We expected an involvement of VPEs in senescence of *Lilium longiflorum* flower. However, in lily tepals LlVPE4 was highly expressed before flower opening (stage T-2) and subsequently the expression level decreased. Based on this result LlVPE4 does not seem to be directly involved in senescence or, at least, in the executioner phase of tepal senescence. The expression profile matches with the VPE activity that showed a peak at stage T2 and then decreased during senescence, suggesting a role for VPEs in late flower development or early senescence. Our data are not in agreement with the results obtained by van Doorn *et al.* (2009) during *Ipomea* flower senescence. Moreover, during carnation petal senescence, an EST (accession DT214767) was up-regulated which showed high homology to an *Arabidopsis* γVPE (Hoeberichts *et al.*, 2007). LlVPE4 was highly expressed also in the style and stigma but no putative functions for such enzymes can be hypothesized in this organs.

5.0. Endogenous hormones

In contrast to ethylene-sensitive species in which ethylene plays a regulatory role in mediating flower senescence, in ethylene-insensitive species the involvement of hormones as inducers or regulators of senescence has not been demonstrated yet.

Our results from lily tepals show a decrease in free indoleacetic acid after flower opening and a steep increase during late senescence. Thus IAA does not appear to be an early regulator of lily flower senescence and further investigations will be necessary to establish the role of IAA during senescence. The increase shown in late senescence could be correlated to the substantial increase in hydrolytic activity possibly releasing indolic compounds. Because a substantial quantity of auxins has been reported to be present in the pollen of several flowers such as orchids (Stead, 1992), and auxin can mimic the post-pollination effects of induction of ethylene production and fading of flowers in *Phalaenopsis* spp. and *Vanda* spp. orchids (Bui and O'Nill, 1998), they have been identified as possible candidates in mediating flower senescence. Moreover, exogenous auxin may promote petal senescence in carnation through a stimulation of ethylene production (Wulster *at al.*, 1982; Shibuya *et al.*, 2000). However, in ethylene-insensitive species, the required signal for the rise of senescence might be endogenous, from the petal cells themselves, and may not require hormones as an intermediate signal (van Doorn and Woltering, 2008).

Abscisic acid was demonstrated to be involved in flower senescence of ethylene-sensitive flowers, probably by a stimulation of ethylene production. The senescing effect of ABA was demonstrated in carnation (Shibuya *et al.*, 2000; Nukui *et al.*, 2004), Petunia (Chang *et al.*, 2003), cocoa (Aneja *et al.*, 1999), rose (Müller *et al.*, 1999) and it was therefore concluded that exogenous ABA acts through induction of ethylene synthesis in the gynoecium. ABA was also reported to stimulate flower senescence and endogenous levels increased in senescing tepals of ethylene-insensitive species (Panavas *et al.*, 1998; Hunter *et al.*, 2004). In lily tepals, the pattern of endogenous ABA was significantly different by expressing the data per fresh weight, dry weight or tepal. However, ABA content increased during flower senescence and it could be hypothesized that it has a role in flower senescence, even if not as an early regulator. We did not analyze endogenous levels in the ovary even though, in carnation, it was concluded that exogenous ABA acts through induction of ethylene synthesis in the gynoecium (Shibuya *et al.*, 2000; Nukui *et al.*, 2004).

GAs are generally considered anti-senescing molecules both in ethylene-sensitive and -insensitive species. Gibberellic acid delayed senescence in carnation flowers (Saks *et al.*, 1992), GA_4+GA_7 was reported to delay leaf senescence and petal fall in *Alstroemeria* (Mutui

et al., 2006), and GA_3 extended the vase life of daylily suggesting an anti-senescing action of GAs (Hunter *et al.,* 2004). However, few data are available on endogenous level of GAs during senescence. In *Alstroemeria* the biologically active GA_1 and GA_4 were shown to decrease with senescence in leaves (Kappers *et al.,* 1997). Our results on endogenous GAs are in accordance with data from *Alstroemeria* leaves. We demonstrated that in lily the 13-non-hydroxylated pathway is prevalent and that there is a gradual reduction of bioactive forms. The reduction in GAs does not seem to be the cause of flower senescence but rather a physiological feature accompanying tepal senescence. We did not perform experiments with exogenous applications of GAs, thus we cannot suggest a role for GAs as anti-senescing molecules in lily.

5. CONCLUSIONS

Petal senescence is a genetically controlled and irreversible process leading to cell death and occurs relatively quickly throughout the tissue. It makes the flower a useful system for studying programmed cell death of plant organs. On the other hand, the whole petal comprises cells at various stage of senescence, and often petal wilting and other symptoms start at the petal tips or petal margins making difficult the interpretation of data. However, petal senescence has been widely studied using both ethylene-sensitive and –insensitive species and some of the key components involved in senescence initiation or progression have been identified. Nevertheless, primary signals initiating senescence and the basic mechanisms leading to cell death in flower organs have not been fully understood so far.

Lilium longiflorum is an ethylene insensitive species in which senescence takes place in a highly predictable fashion. Lily flowers are formed by two tepal whorls that display a different behaviour probably reflecting the different ontogenetic origin. Tepals undergo senescence without abscission and are characterized by severe dehydration, probably preceded by an intense remobilization of nutrients. Visible signs of senescence are preceded by biochemical and physiological alterations, and are probably associated with the dismantling of the mesophyll layer. As observed in other flowers and other plant organs, the autophagic machinery seems to be implicated in cell death and the vacuole plays a prominent role working as a lytic compartment and releasing hydrolytic enzymes after vacuole permeabilization or rupture. Large-scale degradation of macromolecules, such as proteins, precedes visible signs of senescence and is associated with an increase in proteolytic activity. The presence of caspase-like activities and their up-regulation during senescence and the early detection of VPE activity suggest proteases as key elements in the regulation and

execution of cell death. The same activity has been detected also in leaves suggesting a correlation with senescing organs. We tried to identify key components of the cell death machinery involved in protein degradation and protease processing. KDEL-tailed cysteine proteases, known to be responsible for protein degradation in other forms of PCD, are involved in lily flower senescence even though further experiments are necessary to fully clarify their exact role. VPE genes isolated from tepals are strong candidates to be regulators in flower senescence and VPEs could potentially possess a caspase-like activity as demonstrated in other species.

Although lily flower senescence could be affected by hormones, endogenous levels of IAA, ABA and GAs in tepals do not seem to be strictly correlated with the onset of flower senescence. Rather, changes in endogenous hormones seem to follow the senescence process, being physiologically correlated to it. Nevertheless, endogenous level of other hormones, such as cytokinins, and the levels of bioactive molecules in other flower organs such as the ovary were not measured here and should also be taken into account.

Postharvest senescence of flowers is under genetic control and future identification of the key genes controlling this process may help to elucidate the signalling cascade for better understanding flower senescence mechanisms and allow the enhancement of postharvest quality characteristics. Moreover, it would be extremely useful to understand how various external or internal stimuli and developmental factors control flower senescence.

ACKNOWLEDGMENTS

I wish to thank Dr. Barend de Graaf (Cardiff University) and Dr. Dennis Francis for helpful advices and for stimulating exchanges of ideas during my stay at School of Biosciences at Cardiff University. I also thank Dr. de Graaf for providing the binary plasmid carrying 35S-YFP. I am grateful to Dr. Lorenzo Frigerio (University of Warwick) for providing 35S-RFP-AFVY plasmid and for doing agroinfiltration experiments. I am grateful to Prof. Ikuko Hara-Nishimura (Tokyo University), Dr. Takashi Okamoto (Tokyo Metropolitan University) and Dr. John Greenwood (Guelph University) for the gift of anti-VPE and anti-SlCysEP antibodies. I also thank Dr. Anthony Hann (Cardiff University) for helping me with TEM and immunogold assay. I am grateful to Dr. Lara Lombardi (University of Pisa) for her invaluable suggestions and great contribution to the work, and to Dr. Lorenzo Mariotti (University of Pisa) for his assistance and for teaching me HPLC and GC/MS techniques.

I wish to thank wholeheartedly my friends and colleagues Lara, Lorenzo and Francesco for their continuous support and for the memorable days spent in the laboratory. I am also deeply grateful to all my colleagues/friends at Cardiff University, particularly to Faezah and Danilo for their help during my stay at Cardiff and for spending unforgettable moments as lab mates and friends.

REFERENCES

Alonso JM, Stepanova AN. 2004. The ethylene signaling pathway. *Science* 306, 1513-1515.

Altschul SF, Madden TL, Schäffer AA, Zhang J, Zhang Z, Miller W, Lipman DJ. 1997. Gapped BLAST and PSI-BLAST: a new generation of protein database search programs, *Nucleic Acids Res.* 25, 3389-3402.

Aneja M, Gianfagna T, Ng E. The role of abscisic acid and ethylene in the abscission and senescence of cocoa flowers. *Plant Growth Regulation* 27, 149-155.

Arora A, Watanabe S, Ma B, Takada K, Ezura H. 2006. A novel ethylene receptor homolog gene isolated from ethylene-insensitive flowers of gladiolus (*Gladiolus grandiflora* hort.). *Biochemical and Biophysical Research Communication* 351, 739-744.

Ashman T-L, Schoen DJ. 1994. How long should flowers live? *Nature* 371, 788-791.

Azad AK, Ishikawa T, Ishikawa T, Sawa Y, Shibata H. 2008, Intracellular energy depletion triggers programmed cell death during petal senescence in tulip. *Journal of Experimental Botany* 59, 2085-2095.

Azeez A, Sane AP, Bhatnagar D, Nath P. 2007. Enhanced expression of serine proteases during flower senescence in *Gladiolus*. *Phytochemistry* 68, 1352-1357.

Bachmair A, Novatchkova M, Potuschak T, Eisenhaber F. 2001. Ubiquitylation in plants: a post-genomic look at a post-translational modification. *Trend in Plant Science* 6, 463-470.

Bailly C, Corbineau F, van Doorn WG. 2001. Free radical scavenging and senescence in *Iris* tepals. *Plant Physiology Biochem*. 39, 649-656.

Balk J, Chew SK, Leaver CJ, McCabe PF. 2003. The intermembrane space of plant mitochondria contains a DNase activity that may be involved in programmed cell death. *The Plant Journal* 34, 573-583.

Barrett AJ. 1994. Classification of peptidases. *Methods in Enzymology*. 244, 1-15.

Bartoli CG, Simontacchi M, Guiamet J, Montaldi E, Puntarulo S. 1995. Antioxidant enzyme and lipid peroxidation during aging of *Chrysanthemum morifolium* RAM petals. *Plant Science* 104, 161-168.

Bartoli CG, Simontacchi M, Montaldi ER, Puntarulo S. 1997. Oxidants and antioxidants during aging of chrysanthemum petals. *Plant Science* 129, 157-165.

Batoko H, Zheng HQ, Hawes C, Moore I. 2000. A Rab1 GTPase is required for transport between the endoplasmic reticulum and Golgi apparatus and for normal Golgi movement in plants. *The Plant Cell* 12, 2201-2217.

Belenghi B, Romero-Puertas MC, Vercammen D, Brackenier A, Inzé D, Delledonne M, Van Breusegem F. 2007. Metacaspase activity of *Arabidopsis thaliana* is regulated by S-nitrosylation of a critical cysteine residue. *Journal of Biological Chemistry* 282, 1352-1358.

Bendtsen JD, Nielsen H, von Heijne G, Brunak S. 2004. Improved prediction of signal peptides: SignalP 3.0. *J. Mol. Biol.* 340, 783-795.

Beers EP, Woffenden BJ, Zhao C. 2000. Plant proteolytic enzymes: possible role during programmed cell death. *Plant Molecular Biology* 44, 399-415.

Beers EP, Jones AM, Dickerman AW. 2004. The S8 serine, C1A cysteine and A1 aspartic protease families in *Arabidopsis*. *Phytochemistry* 65, 43-58.

Belknap WR, Garbarino JE. 1996. The role of ubiquitin in plant senescence and stress response. *Trends in Plant Science* 1, 331-335.

Bhalerao R, Keskitalo J, Sterky F, Erlandsson R, Björkbacka H, Birve SJ, Karlsson J, Gardestörm P, Gustafsson P, Lundenerg J, Jansson S. 2003. Gene expression in autumn leaves. *Plant Physiology* 131, 430-442.

Bieleski RL. 1995. Onset of phloem export from senescent petals of daylily. *Plant Physiology* 109, 557-565.

Bonneau L, Ge Y, Drury GE, Gallois P. 2008. What happened to plant caspases ? *Journal of Experimental Botany* 59, 491-499.

Boren M, Höglund AS, Bozhkov P, Jansson C. 2006. Developmental regulation of a VEIDase caspase-like proteolytic activity in barley caryopsis. *Journal of Experimental Botany* 57, 3747-3753.

Bosch M, Franklin-Tong VE. 2007. Temporal and spatial activation of caspase-like enzymes induced by self-incompatibility in *Papaver* pollen. *Proc. Natl. Acad. Sci*. USA 104, 18327-18332.

Bosch M, Poulter NS, Vatovec S, Franklin-Tong VE. 2008. Initiation of programmed cell death in self-incompatibility: role of cytoskeleton modifications and several caspase-like activities. *Molecular Plant* 1, 879-887.

Bozhkov PV, Filonova LH, Suarez MF, Helmersson A, Smertenko AP, Zhivotovsky B, von Arnold S. 2004. VEIDase is a principal caspase-like activity involved in plant programmed cell death and essential for embryonic pattern formation. *Cell Death and Differ*. 11, 175-182.

Bozhkov PV, Suarez MF, Filonova LH, Daniel G, Zamyatnin AA, Rodriguez-Nieto S, Zhivotovsky B, Smertenko A. 2005. Cysteine protease mcII-Pa executes programmed cell death during plant embryogenesis. *Proc. Natl. Acad. Sci.* USA 102, 14463-14468.

Bovy AG, Angenent GC, Dons HJM, Altvorst AC. 1999. Heterologous expression of the *Arabidopsis etr1-1* allele inhibits the senescence of carnation flowers. *Molecular Breeding* 5, 301-308.

Breeze E, Wagstaff C, Harrison E, Bramke I, Rogers H, Stead H, Thomas B, Buchanan-Wollaston V. 2004. Gene expression patterns to define stage of post-harvest senescence in *Alstroemeria* petals. *Plant Biotech Journal* 2, 155-168.

Buchanan-Wollaston V. 1997. The molecular biology of leaf senescence. *Journal of Experimental Botany* 48, 181-199.

Callis J. 1995. Regulation of protein degradation. *The Plant Cell* 7, 845-857.

Carimi F, Zottini M, Formentin E, Terzi M, Lo Schiavo F. 2003. Cytokinins: new apoptotic inducers in plants. *Planta* 216, 413-421

Celikel FG, Dodge LL, Reid MS. 2002. Efficacy of 1-MCP (1-methylcyclopropene) and Promalin for extending the postharvest life of Oriental lilies (*Lilium* x "Mona Lisa" and "Stargazer"). *Scientia Horticulturae* 93, 149-155.

Cervantes E, De Diego JG, Gomez MD, De las Rivas J, Igual JM, Velasquez E, Grappin P, Cercos M, Carbonell J. 2001. Expression of cysteine proteinase mRNA in chickpea (*Cicer arietinum* L.) is localized to provascular cells in the developing root. *Journal of Plant Physiol*. 158, 1463-1469.

Chang HS, Jones ML, Banowetz GM, Klark DG. 2003. Overproduction of cytokinins in petunia flowers transformed with P-$_{SAG12}$-IPT delays corolla senescence and decreases sensitivity to ethylene. *Plant Physiol*. 132, 2174-2183.

Chasanut U, Rogers HJ, Leverentz MK, Griffith G, Thomas B, Stead AD. Increasing flower longevity in *Alstroemeria*. *Postharvest Biology and Technology* 29, 325-333.

Chen S, Dickman MB. 2004. Bcl-2 family members localize to tobacco chloroplasts and inhibit programmed cell death induced by chloroplast-targeted herbicides. *Journal of Experimental Botany* 55, 2617-2623.

Chichkova NV, Kim SH, Titova ES, Kalkum M, Morozom VS, Rubtsov YP, Kalinina NO, Taliansky ME, Vartapetian AB. 2004. A plant caspase like protease activated during the hypersensitive response. *Plant Cell* 16, 157-171.

Coffeen WC, Wolpert TJ. 2004. Purification and characterization of serine proteases that exibit caspase-like activity and are associated with programmed cell death in *Avena sativa*. *The Plant Cell* 16, 857-873.

Courtney SE, Rider CC, Stead AD. 1994. Changes in protein ubiquitination and the expression of ubiquitin-encoding transcripts in daylily petals during flower development and senescence. *Physiology Plantarum* 91, 196-204.

Danon A, Delorme V, Mailhac N, Gallois P. 2000. Plant programmed cell death: a common way to die. *Plant Physiology Biochem*. 38, 647-655.

Danon A, Rotari VI, Gordon A, Maihac N, Gallois P. 2004. Ultraviolet-C overexposure induces programmed cell death in *Arabidopsis*, which is mediated by caspase-like activities and which can be suppressed by caspase inhibitors, p35 and Defender against Apoptotic Death. *Journal of Biological Chemistry* 279, 779-787.

De Jong AJ, Hoeberichts FA, Yakimova ET, Maximova E, Woltering EJ. 2000. Chemical-induced apoptotic cell death in tomato cells: involvement of caspase-like proteases. *Planta* 211, 656-662.

del Pozo O, Lam E. 1998. Caspases and programmed cell death in the hypersensitive response of plants to pathogens. *Current Biology* 8, 1129-1132.

del Pozo O, Lam E. 2003. Expression of the baculovirus p35 protein in tobacco affects cell death progression and compromises N gene-mediated disease resistance response to tobacco mosaic virus. *Molecular Plant-Microbe Interaction* 16, 485-494.

Dickman MB, Park YK, Oltersdorf T, Li W, Clemente T, French R. 2001. Abrogation of disease development in plants expressing animal antiapoptotic genes. *Proc. Natl. Acad. Sci.* USA 98, 6957-6962.

Dreher K, Callis J. 2007. Ubiquitin, hormones and biotic stressing plant. *Annals of Botany* 99, 787-822.

Eason JR, de Vré LA, Somerfield SD, Heyes JA. 1997. Physiological changes associated with *Sandersonia aurantica* flower senescence in response to sugar. *Postharvest Biology and Technology* 12, 43-50.

Eason JR, Ryan DJ, Pinkney TT, O'Donoghue EM. 2002. Programmed cell death during flower senescence: isolation and characterization of cysteine proteinases from *Sandersonia aurantica*. *Funct. Plant Biol*. 29, 1055-1064.

Eason JR, Ryan DJ, Watson LM, Hedderley D, Christey MC, Braun RH, Coupe SA. 2005. Suppression of the cysteine protease, aleurain, delays floret senescence in *Brassica oleracea*. *Plant Mol. Biol.* 57, 645-657.

Elgar HJ, Woolf AB, Bieleski RL. 1999. Ethylene production by three lily species and their responce to ethylene exposure. *Postharvest Biology and Technology* 16, 257-267.

Emanuelsson O, Nielsen H, Brunak S, von Heijne G. 2000. Predicting subcellular localization of proteins based on their N-terminal amino acid sequence. *Journal Molecular Biology* 300, 1005-1016.

Farage-Barhom S, Burd S, Sonego L, Perl-Treves R, Lers A. 2008. Expression analysis of the BFN1 nuclease gene promoter during senescence, abscission and programmed cell death-related processes. *Journal of Experimental Botany* 59, 3247-3258.

Fath A, Bethke PC, Jones RL. 1999. Barley aleurone cell death is non apoptotic: characterization of nuclease activities and DNA degradation. *The Plant Journal* 20, 305-315.

Feng XQ, Apelbaum A, Sisler EC, Goren R. 2004. Control of ethylene activity in various plant systems by structural analogous of 1-methylcyclopropene. *Plant Growth Regulation* 42, 29-38.

Fobel M, Lynch DV, Thompson JE. 1987. Membrane deterioration in senescing carnation flowers. *Plant Physiology* 85, 204-211.

Frigerio L, Pastres A, Prada A, Vitale A. 2001. Influence of KDEL on the fate of trimeric or assembly-defective phaseolin: selective use of an alternative route to vacuoles. *The Plant Cell* 13, 1109-1126.

Fukuchi-Mizutani M, Ishiguro K, Nakayama T, Utsunomiya Y, Tanaka Y, Kusumi T, Ueda T. 2000. Molecular and functional characterization of a rose lipoxygenase cDNA related to flower senescence. *Plant Science* 160, 129-137.

Gan S, Amasino RM. 1995. Inhibition of leaf senescence by autoregulated production of of cytokinin. *Science* 270, 1986-1988.

Gechev TS, Hille J. 2005. Hydrogen peroxide as a signal controlling plant programmed cell death. *The Journal of Cell Biology* 168, 17-20.

Gerasopoulos D, Chebli B. 1999. Effecet of pre- and postharvest calcium application an the vase life of cut gerberas. *JOURNAL Hort. Sci. & Biotech.* 74, 78-81.

Gladish DK, Xu J, Niki T. 2006. Apoptosis-like programmed cell death occurs in procambium and ground meristem of pea (*Pisum sativum*) root tips exposed to sudden flooding. *Annals of Botany* 97, 895-902.

Groover A, DeWitt N, Heidel A, Jones A. 1997. Programmed cell death of plant tracheary elements differentiating in vitro. *Protoplasma* 196, 197-211.

Guerrero FD, De la Calle M, Reid MS, Valpuesta V. 1998. Analysis of the expression of two thiolprotease genes from daylily (*Hemerocallis* spp.) during flower senescence. *Plant Mol. Biol*. 15, 11-26.

Gunawardena AHLAN, Greenwood JS, Dengler NG. 2004. Programmed cell death remodels lace plant leaf shape during development. *The Plant Cell* 16, 60-73.

Hall TA. 1999. BioEdit: a user-friendly biological sequence alignment editor and analysis program for Windows 95/98/NT. *Nucl. Acids. Symp. Ser.* 41, 95-98.

Halliwell B. 2006. Reactive species and antioxidants. Redox biology is a fundamental theme of aerobic life. *Plant Physiol*. 141, 312-322.

Han SS, Miller JA. 2003. Role of ethylene in postharvest quality of cut oriental lily "Stargazer". *Plant Growth Regulation* 40, 213-222.

Hansen G. 2000. Evidence for Agrobacterium-induced apoptosis in maize cells. *Molecular Plant-Microbe Interaction* 13, 649-657.

Hara-Nishimura I, Inoue K, Nishimura M. 1991. A unique vacuolar processing enzyme responsabile for conversion of several proprotein precursors into the mature form. *FEBS Lett.* 294, 89-93.

Hara-Nishimura I, Hatsugai N, Satoru N, Kuroyanagi M, Nishimura M. 2005. Vacuolar processing enzyme: an executor of plant cell death. *Curr. Opin. Plant Biol.* 8, 1-5.

Harrak H, Azelmat S, Baker EN, Tabaeizadeh Z. 2001. Isolation and characterization of a gene encoding a drought-induced cysteine protease in tomato (*Lycopersicon esculentum*). *Genome* 44, 368-374.

Hatsugai N, Kuroyanagi M, Yamada K, Meshi T, Tsuda S, Kondo M, Nishimura M, Hara-Nishimura I. 2004. A plant vacuolar protease, VPE, mediates virus-induced hypersensitive cell death. *Science* 305, 855-858.

Hatsugai N, Kuroyanagi M, Nishimura M, Hara-Nishimura I. 2006. A cellular suicide strategy of plants: vacuole mediated cell death. *Apoptosis* 11, 905-911.

Hayashi Y, Yanada K, Shimada T, Matsushima R, Nishizawa NK, Nishimura M, Hara-Nishimura I. 2001. A proteinase-storing body that prepares for cell death or stresses in the epidermal cells of *Arabidopsis*. *Plant Cell Physiol*. 42, 894-899.

He R, Drury GE, Rotari VI, Gordon A, Willer M, Farzaneh T, Woltering EJ, Gallois P. 2008. Metacaspase-8 modulate programmed cell death induced by ultraviolet light and H_2O_2 in Arabidopsis. *The Journal of Biological Chemistry* 283, 774-783.

He X, Kermode AR. 2003. Proteases associated with programmed cell death of megagametophyte cells after germination of white spruce (*Picea glauca*) seeds. *Plant Molecular Biology* 52, 729-744.

Hellens RP, Edwards EA, Leyland NR, Bean S, Mullineaux PM. 2000. pGreen: a versatile and flexible binary Ti vector for Agrobacterium mediated plant transformation. *Plant Mol Biol* 42, 819–832.

Hengartner MO. 2000. The biochemistry of apoptosis. *Nature* 407, 770-776.

Hoeberichts FA, ten Have A, Woltering EJ. 2003. A tomato metacaspase gene is up-regulated during programmed cell death in Botrytis cinerea-infected leaves. *Planta* 217, 517-522.

Hoeberichts FA, de Jong AJ, Woltering EJ. 2005. Apoptotic-like cell death marks the early stage of gypsophila (Gypsophila paniculata) petal senescence. *Postharvest Biology and Technology* 35, 229-236.

Hoeberichts FA, van Doorn WG, Vorst O, Hall RD, van Wordragen MF. 2007. Sucrose prevents up-regulation of senescence-associated genes in carnation petals. *Journal of Experimental Botany* 58, 2873-2875.

Hörtensteiner S, Feller U. 2002. Nitrogen metabolism and remobilization during senescence. *Journal of Experimental Botany* 53, 923-937.

Hossain Z, Mandal AKA, Datta SK, Biswas AK. 2006. Decline in ascorbate peroxidase activity – a prerequisite factor for tepal senescence in gladiolus. *Journal of Plant Physiology* 163, 186-194.

Huang LC, Lai UL, Yang SF, Chu MJ, Kuo CI, Tsai MF, Sun CW. 2007. Delayed flower senescence of Petunia hybrida plants transformed with antisense broccoli ACC synthase and ACC oxidase genes. *Postharvest Biology and Technology* 46, 47-53.

Huang YJ, To KY, Yap MN, Chiang WJ, Suen DF, Chen SCG. 2001. Cloning and characterization of leaf senescence up-regulated genes in sweet potato. *Physiology Plant*. 113, 384-391.

Hunter DA, Steele BC, Reid MS. 2002. Identification of genes associated with perianth senescence in daffodil (*Narcissus pseudonarcissus* L. "duch master"). *Plant Science* 163, 13-21.

Hunter DA, Ferrante A, Vernieri P, Reid MS. 2004. Role of abscisic acid in perianth senescence of daffodil (*Narcissus pseudonarcissus* 'Dutch Master'). *Physiologia Plantarum* 121, 313-321.

Hunter PR, Craddock CP, Di Benedetto S, Roberts LM, Frigerio L. 2007. Fluorescent reporter proteins for the tonoplast and the vacuolar lumen identify a single vacuolar compartment in Arabidopsis cells. *Plant Physiology* 145, 1371–1382.

Iwaya-Inoue M, Takata, M. 2001. Trehalose plus chloramphenicol prolong the vase life of tulip flowers. *HortScience* 36, 946–950.

Jones ML, Chaffin GS, Eason JR, Clark DG. 2005. Ethylene-sensitivity regulates proteolytic activity and cysteine protease gene expression in petunia corollas. *Journal of Experimental Botany* 56, 2733-2744.

Jones RB, Serek M, Kuo CL, Reid MS. 1994. The effect of protein synthesis inhibition on petal senescence in cut bulb flowers. *J. Amer. Soc. Hort. Sci*. 119, 1243-1247.

Kappers IF, Jordi W, Maas FM, van der Plas LHW. 1997. Gibberellins in leaves of *Alstroemeria hybrida*: identification and quantification in relation to leaf age. *Journal of Plant Growth Regulation* 16, 219-225.

Karrer KM, Peiffer SL, DiToms ME. 1993. Two distinct gene subfamily within the family of cysteine protease genes. *Proc. Natl. Acad. Sci.* USA 90, 3063-3067.

Kinoshita T, Yamada K, Hiraiwa N, Kondo M, Nishimura M, Hara-Nishimura I. 1999. Vacuolar processing enzyme is up-regulated in the lytic vacuoles of vegetative tissues during senescence and under various stress conditions. *The Plant Journal* 19, 43-53.

Kladnik A, Chamusco K, Dermastia M, Chourey P. 2004. Evidence of programmed cell death in post-phloem transport cells of the maternal pedicel tissue in developing caryopsis of maize. *Plant Physiology* 136, 3572-3581.

Kotchoni SO, Gachomo EW. 2006. The reactive oxygen species network pathway: an essential prerequisite for perception of pathogen attack and the acquired disease resistance in plant. *J. Biosci.* 31, 389-404.

Kuo A, Cappelluti S, Cervantes-Cervantes M, Rodriguez M, Bush DS. 1996. Okadaic acid, a protein phosphatase inhibitor, blocks calcium changes, gene expression, and cell death induced by gibberellin in wheat aleurone cells. *The Plant Cell* 8, 259-269.

Kuroyanagi M, Nishimura M, Hara-Nishimura I. 2002. Activation of Arabidopsis vacuolar processing enzyme by self-catalytic removal of an auto-inhibitory domain of the C-terminal propeptide. *Plant Cell Physiol.* 43, 143-151.

Kuroyanagi M, Yamada K, Hatsugai N, Kondo M, Nishimura M, Hara-Nishimura I. 2005. VPE is essential for mycotoxin-induced cell death in Arabidopsis thaliana. *Journal of Biological Chemistry* 280, 32914-32920.

Kuthanova A, Opatrny Z, Fischer L. 2008. Is internucleosomal DNA fragmentation of programmed deth in plant? *Journal of Experimental Botany* 59, 2233-2240.

Laloi C, Apel K, Danon A. 2004. Reactive oxygen signalling: the latest news. *Current Opinion in Plant Biology* 7, 323-328.

Lam E, del Pozo O. 2000. Caspase-like protease involvement in the control of plant cell death. *Plant Molecular Biology* 44, 417-428.

Langston BJ, Bai S, Jones ML. 2005. Increase in DNA fragmentation and induction of a senescence-specific nuclease are delayed during corolla senescence in ethylene-insensitive (*etr1-1*) transgenic petunias. *Journal of Experimental Botany* 56, 15-23.

Lay-Yee M, Stead AD, Reid MS. 1992. Flower senescence in daylily (*Hemerocallis*). *Physiologia Plantarum* 86, 308-314.

Ledford H. 2007. The flower of seduction. *Nature* 445, 816-817.

Lee RH, Chen SCG. 2002. Programmed cell death during rice leaf senescence is non apoptotic. *New Phytologist* 155, 25-32.

Leopold AC. 1961. Senescence in plant development. *Science* 134, 1727-1732.

Lerslerwong L, Ketsa S, van Doorn WG. 2009. Protein degradation and peptidase activity during petal senescence in *Dendrobium* cv. Khao Sanan. *Postharvest Biology and Technology* 52, 84-90.

Leverentz MK, Wagstaff C, Rogers HJ, Stead AD, Chanasut U, Silkowski H, Thomas B, Weichert H, Feussner I, Griffiths G. 2002. Characterization of a novel lipoxygenase-independent senescence mechanism in *Alstroemeria peruviana* floral tissue. *Plant Physiol*. 130, 273-283.

Lim PO, Kim HJ, Nam HG. 2007. Leaf senescence. *Ann. Rev. Plant. Biol.* 58, 115-136.

Lincoln JE, Richael C, Overduin B, Smith K, Bostock R, Gilchrist DG. 2002. Expression of the antiapoptotic baculovirus p35 gene in tomato blocks programmed cell death and provides broad-spectrum resistance to disease. *Proc. Natl. Acad. Sci*. USA 99, 15217-15221.

Llop-Tous I, Barry CS, Grierson D. 2000. Regulation of ethylene biosynthesis in response to pollination in tomato flowers. *Plant Physiol*. 123, 971-978.

Lombardi L, Ceccarelli N, Picciarelli P, Lorenzi R. 2007a. DNA degradation during programmed cell death in *Phaseolus coccineus* suspensor. *Plant Physiology and Biochemistry* 45, 221-227.

Lombardi L, Casani S, Ceccarelli N, Galleschi L, Picciarelli P, Lorenzi R. 2007b. Programmed cell death of the nucellus during *Sechium edule* Sw. seed development is associated with activation of caspase like proteases. *Journal of Experimental Biology* 58, 2949-2958.

Love AJ, Milner JJ, Sadanandom A. 2008. Timing is everithing: regulatory overlap in plant cell death. *Trends in Plant Science* 13, 589-595.

Matile P. 1968. Vacuole as lysosome of plant cells. *Biochemistry J.* 111, 7-26.

Martinez M, Cambra I, Carrillo L, Diaz-Mendoza M, Diaz I. 2009. Characterisation of the entire cystatin gene family in barley and their target cathepsin L-like cysteine-proteases, partners in the hordein mobilization during seed germination. *Plant Physiology* 151, 1531-1545.

Moon J, Parry G, Estelle M. 2004. The ubiquitin-proteasome pathway and plant development. *The Plant Cell* 16, 3181-3195.

Mukhopadhyay D, Riezman H. 2007. Protesome-indipendent functions of ubiquitin in endocytosis and signalling. *Science* 315, 200-205.

Müller R, Stummann BM, Andersen AS, Serek M. 1999. Involvement of ABA in postharvest life of miniature potted rose. *Plant Growth Regulation* 29, 143-150.

Münz K, Shutov AD. 2002. Legumains and their functions in plant. *Trends in Plant Science* 7, 340-344.

Mutui TM, Emongor VE, Hutchinson MJ. 2006. The effect of gibberellin $_{4+7}$ on the vase life and quality of *Alstroemeria* cut flowers. *Plant Growth Regulation* 48, 207-214.

Nadeau JA, Zhang XS, Nair H, O'Neill SD. 1993. Temporal and spatial regulation of 1-amynociclopropane-1-carboxylate oxidase in the pollination-induced senescence of orchid flowers. *Plant Physiology* 103, 31-39.

Nagata S, Nagase H, Kawane K, Mukae N, Fukuyama H. 2003. Degradation of chromosomal DNA during apoptosis. *Cell Death and Differentiation* 10, 108-116.

Nakaune S, Yamada K, Kondo M, Kato T, Tabata S, Nishimura M, Hara-Nishimura I. 2005. A vacuolar processing enzyme, {delta}VPE, is involved in seed coat formation at the early stage of seed development. *The Plant Cell* 17, 876-887.

Nukui H, Kudo S, Yamashita A, Satoh S. 2004. Repressed ethylene production in the gynoecium of long-lasting flowers of the carnation "White Candle": role of the gynoecium in carnation flower senescence. *Journal of Experimental Botany* 55, 641-650.

O'Donoghue EM, Somerfield SD, Heyes JA. 2002. Organization of cell walls in Sandersonia aurantiaca floral tissue. *Journal of Experimental Botany* 53, 513–523.

O'Donoghue EM, Somerfield SD, Watson LM, Brummell DA, Hunter DA. 2009. Galactose metabolism in cell walls of opening and senescing *Petunia* petals. *Planta* 229, 709-721.

Okamoto T, Nakayama H, Seta K, Isobe T, Minamikawa T. 1994. Posttranslational processing of a carboxy-terminal propeptide containing a KDEL sequence of plant vacuolar cysteine endopeptidase (SH-EP). *FEBS Letters* 351, 31-34.

Okamoto T, Minamikawa T. 1999. Molecular cloning and characterization of *Vigna mungo* processing enzyme 1 (VmPE-1) an asparaginyl endopeptidase possibly involved in post-translational processing of a vacuolar cysteine endopeptidase (SH-EP). *Plant Mol. Biol*. 39, 63-73.

Okamoto T, Shimada T, Hara-Nishimura I, Nishimura N, Minamikawa T. 2003. C-terminal KDEL sequence of a KDEL-tailed cysteine proteinasi (sulfhydryl-endopeptidase) is involved in formation of KDEL vescicle and in efficient vacuolar transport of sulfhydryl-endopeptidase. *Plant Physiol*. 132, 1892-1900.

Orzaez D, Granell A. 1997. The plant homologue of the defender against apoptotic death gene is down-regulated during senescence of flower petals. *FEBS Lettes* 404, 275-278.

Otsubo M, Iwaya-Inoue M. 2000. Trehalose delays senescence in cut gladiolus spikes. *HortScience* 36, 1107–1110.

Pak C, van Doorn WG. 2005. Delay of Iris flower senescence by protease inhibitors. *New Phytologist* 165, 473-480.

Panavas T, Walker ER, Rubinstein B. 1998. Possible role of abscisic acid in senescence of daylily petals. *Journal of Experimental Botany* 49, 1987-1997.

Panavas T, Rubinstein B. 1998b. Oxidative events during programmed cell death of daylily (*Hemerocallis hybrid*) petals. *Plant Science* 133, 125-138.

Panavas T, Pikula A, Reid PD, Rubinstein B, Walker EL. 1999. Identification of senescence-associated genes from daylily petals. *Plant Molecular Biology* 40, 237-248.

Panavas T, LeVangie R, Mistler J, Reid PD, Rubinstein B. 2000. Activities of nucleases in senescing daylily petals. *Plant Physiology Biochem*. 38, 837-843.

Pérez-Amador MA, Abler ML, De Rocher EJ, Thompson DM, van Hoof A, LeBrasseur LD, Lers A, Green PJ. 2000. Identification of BFN1, a bifunctional nuclease induces during leaf and steam senescence in Arabidopsis. *Plant Physiol*. 122, 169-179.

Phillips AR, Suttangkakul A, Vierstra RD. 2008. The ATG12-coniugating enzyme ATG10 is essential for autophagic vesicle formation in *Arabidopsis thaliana*. *Genetics* 178, 1339-1353.

Price AM, Orellana DFA, Salleh FM, Stevens R, Acock R, Buchanan-Wollaston V, Stead AD, Rogers HJ. 2008. A comparison of leaf and petal senescence in wallflower reveals common and distinct patterns of gene expression and physiology. *Plant Physiol*. 147, 1898-1912.

Qu GQ, Liu X, Zhang YL, Yao D, Ma QM, Yang MY, Zhu WH, Yu S, Luo YB. 2009. Evidence for programmed cell death and activation of specific caspase-like enzymes in the tomato fruit heat stress response. *Planta* 229, 1269-1279.

Quint M., Gray WM. 2006 Auxin signalling. *Current Opinion in Plant Biology* 9, 448-453.

Quirino BF, Noh Y-S, Himelblau E, Amasino RM. 2000. Molecular aspects of leaf senescence. *Trends in Plant Science* 5, 278-282.

Ranwala AP, Miller WB. 2009. Comparison of the dynamics of non-structural carbohydrate pools in cut tulip stems supplied with sucrose or trehalose. *Postharvest Biology and Technology* 52, 91-96.

Rawlings ND, Morton FR, Kok CY, Kong J, Barrett AJ. 2008. MEROPS: the peptidase database. *Nucleic Acids Res* 36, D320-D325.

Rawlings ND, Barrett AJ. 1994. Families of cysteine peptidases. *Methods Enzymol* 244, 461-486

Reape TJ, McCabe PF. 2008. Apoptotic-like programmed cell death in plants. *New Phytologist* 180, 13-26.

Reid MS, Chen JC. 2007. Flower senescence. In Senescence Processes in Plants. *Annual Plant Review* 26, Blackwell Publishing.

Rogers HJ. 2006. Programmed cell death in floral organs: how and why do flowers die? *Annals of Botany* 97, 309-315.

Rojo E, Martin R, Carter C, Zouhar J, Pan S, Plotnikova J, Jin H, Paneque M, Sánchez-Serrano JJ, Baker B, Ausubel FM, Raikhel NV. 2004. VPEγ exhibits a caspase-like activity that contributes to defence against pathogens. *Current Biol*. 14, 1897-1906.

Rolland F, Moore B, Sheen J. 2002. Sugar sensing and signalling in plants. *The Plant Cell* 14(Suppl.), S185-S205.

Rotari VI, He R, Gallois P. 2005. Death by proteases in plants: whodunit? *Physiologia Plantarum* 123, 376-385.

Rubinstein B. 2000. Regulation of cell death in flower petals. *Plant Molecular Biology* 44, 303-318.

Saks Y, Van Staden J, Smith MT. 1992. Effect of gibberellic acid on carnation flower senescence: evidence that the delay of carnation flower senescence by gibberellic acid depends on the stage of flower development. *Plant Growth Regulation* 11, 45-51.

Saks Y, Van Staden J. 1993. Evidence for the involvement of gibberellins in the developmental phenomena associated with carnation flower senescence. *Plant Growth Regulation* 12, 105-110.

Sanmartín M, Jaroszewski L, Raikhel NV, Rojo E. 2005. Caspases. Regulating death since the origin of life. *Plant Physiol*. 137, 841-847.

Schaller A. 2004. A cut above the rest: the regulatory function of plant proteases. *Planta* 220, 183-197.

Schmid M, Simpson D, Kalousek F, Gietl C. 1998. A cysteine endopeptidase with a C-terminal KDEL motif isolated from castor bean endosperm is a marker enzyme for the ricinosome, a putative lytic compartment. *Planta* 206, 466-475.

Schmid M, Simpson D, Gietl C. 1999. Programmed cell death in castor bean endosperm is associated with the accumulation and release of a cysteine endopeptidase from ricinosomes. *Proc. Natl. Acad. Sci*. USA 96, 14159-14164.

Schmid M, Simpson DJ, Sarioglu H, Lottspeich F, Gietl C. 2001. The ricinosome of senescencing plant tissue buds from the endoplasmic reticulum. *Proc. Natl. Acad. Sci*. USA 98, 5353-5358.

Senatore A, Trobacher CP, Greenwood JS. 2009. Ricinosomes predict programmed cell death leading to anther dehiscence in tomato. *Plant Physiol*. 149, 775-790.

Serafini-Fracassini D, Del Duca S, Monti F, Poli F, Sacchetti G, Bregoli AM, Biondi S, Della Mea M. Transglutaminase activity during senescence and programmed cell death in the corolla of tobacco (*Nicotiana tabacum*) flowers. *Cell Death and Diff*. 9, 309-321.

Serek M, Sisler EC, Reid MS. 1995. Effects of 1-MCP on the vase life and ethylene response of cut flowers. *Plant Growth Regulation* 16, 93-97.

Sheokand S, Dahiya P, Vincent JL, Brewin NJ. 2005. Modified expression of cysteine protease affects seed germination, vegetative growth and nodule development in transgenic lines of *Medicago trunculata*. *Plant Science* 169, 966-975.

Shibuya K, Yoshioka T, Hashiba T, Satoh S. 2000. Role of the gynoecium in natural senescence of carnation (*Dianthus caryophyllus* L.) flowers. *Journal of Experimental Botany* 51, 2067-2073.

Shibuya K, Nagata M, Tanikawa N, Yoshioka T, Hashiba T, Satoh S. 2002. Comparison of mRNA levels of three ethylene receptors in senescing flowers of carnation (*Dianthus caryophyllus* L). *Journal of Experimental Botany* 53, 399-406.

Shibuya K, Yamada T, Suzuki T, Shimizu K, Ichimira K. 2009a. InPSR26, a putative membrane protein, regulates programmed cell death during petal senescence in Japanese morning glory. *Plant Physiology* 149, 816-824.

Shibuya K, Yamada T, Ichimira K. 2009b. Autophagy regulates progression of programmed cell death during petal senescence in Japanese morning glory. *Autophagy* 5, 546-547.

Shimada T, Yamada K, Kataoka M, Nakaune S, Koumoto Y, Kuroyanagi M, Tabata S, Kata T, Shinozaki K, Seki M, Kobayashi M, Kondo M, Nishimura M, Hara-Nishimura I. 2003. Vacuolar processing enzymes are essential for proper processing of seed storage proteins in *Arabidopsis thaliana*. *The Journal of Biol. Chem*. 278, 32292-32299.

Singh A, Evensen KB, Kao TH. 1992. Ethylene synthesis and floral senescence following compatible and incompatible pollinations in *Petunia inflata*. *Plant Physiol* 99, 38–45.

Singh A, Kumar J, Kumar P. 2008. Effects of plant growth regulators and sucrose on post harvest physiology, membrane stability and vase life of cut spikes of gladiolus. *Plant Growth Regulation* 55, 221-229.

Sisler EC, Serek M. 1997. Inhibitors of ethylene responses in plants at the receptor level: recent developments. *Physiologia Plantarum* 100, 577-582.

Smith MT, Saks Y, van Staden. 1992. Ultrastructural changes in the petal of senescing flowers of Dianthus caryophyllus L. *Annals of Botany* 69, 277-285.

Sriskandarajah S, Mibus H, Serek M. 2007. Transgenic Campanula carpatica plants with reduced ethylene sensitivity. *Plant Cell Rep*. 26, 805-813.

Stead AD. 1992. Pollination-induced flower senescence: a review. *Plant Growth Regulation* 11, 13-20.

Stein JC, Hansen G. 1999. Mannose induces an endonuclease responsible for DNA laddering in plant cells. *Plant Physiol*. 121, 71-79.

Stennicke HR, Salvesen GS. 1997. Biochemical characteristics of caspase -3, -6, -7, and -8. *Journal of Biological Chemistry* 272, 25719-25723.

Stephenson P, Rubinstein B. 1998. Characterization of proteolytic activity during senescence in daylily. *Physiologia Plantarum* 104, 463-473.

Sundström JF, Vaculova A, Smertenko AP, Savenkov EI, Golovko A, Minina E, Tiwari BS, Rodriguez-Nieso S, Zamyatnin Jr AA, Välineva T, Saarikettu J, Frilander MJ, Suarez MF, Zavialov A, Stahl U, Hussey PJ, Silvennoinen O, Sundberg E, Zhivotovsky B, Bozhkov PV. 2009. Tudor staphylococcal nuclease is an evolutionarily conserved component of the programmed cell death degradome. *Nature Cell Biology* 11, 1347-1354.

Taverner EA, Letham DS, Wang J, Cornish E. 2000. Inhibition of carnation petal inrolling by growth retardants and cytokinins. *Australian journal of Plant Physiology* 27, 357-362.

ten Have A, Woltering EJ. 1997. Ethylene biosynthetic genes are differentially expressed during carnation (*Dianthus caryophyllus* L.) flower senescence. *Plant Molecular Biology* 34, 89-97.

Than ME, Helm M, Simpson DJ, Lottspeich F, Huber R, Gietl C. 2004. The 2.0-Á crystal structure of the KDEL-tailed cysteine endopeptidase from germinating endosperm of *Ricinus communis* confirms its function in the final stage of programmed cell death. *Journal of Molecular Biology* 336, 1103-1116.

Thompson JE, Froese CD, Madey E, Smith MD, Hong Y. 1998. Lipid metabolism during plant senescence. *Prog. Lipid Res.* 37, 119-141.

Timmer JC, Salvesen GS. 2007. Caspase substrates. *Cell Death and Diff.* 14, 66-72.

Torrea S, Borochov A, Halevy AH. 1999. Calcium regulation of senescence in rose petals. *Physiologia Plantarum* 107, 214-219.

Toyooka K, Okamoto T, Minamikawa T. 2000. Mass transport of proform of a KDEL-tailed cysteine proteinase (SH-EP) to protein storage vacuoles by endoplasmic reticulum-derived vesicles is involved in protein mobilization in germinating seeds. *The Journal of Cell Biology* 148, 453-463.

Trobacher CP, Senatore A, Geenwood JS. 2006. Masterminds or minions? Cysteine proteinases in plant programmed cell death. *Canadian Journal of Botany* 84, 651-667.

Uren AG, O'Rourke K, Aravind L, Pisabarro MT, Seshagiri S, Koonin EV, Dixit VM. 2000. Identification of paracaspases and metacaspases: two ancient families of caspase-like proteins, one of which plays a key role in malt lymphoma. *Molecular Cell* 6, 961-967.

Valpuesta V, Lange NE, Guerrero C, Reid MS. 1995. Up-regulation of a cysteine protease accompanies the ethylene-insensitive senescence of daylily (*Hemerocallis*) flowers. *Plant Mol. Biol* 28, 575-582.

van Baarlen P, Staats M, van Kan JAL. 2004. Induction of programmed cell death in lily by the fungal pathogen *Botrytis elliptica*. *Molecular Plant Pathology* 5, 559-574.

van Baarlen P, Woltering EJ, Staats M, van Kan JAL. 2007. Histochemical and genetic analysis of host and non-host interactions of *Arabidopsis* with three *Botrytis* species: an important role for cell death control. *Molecular Plant Pathology* 8, 41-54.

van der Kop DAM, Ruys G, Dees D, van der Schoot C, de Boer AD, van Doorn WG. 2001 Expression of defender against apoptotic death (DAD-1) in Iris and Dianthus petals. *Physiologia Plantarum* 117, 256-263.

van Doorn WG. 1997. Effects of pollination on floral attraction and longevity. *Journal of Experimental Botany* 48, 1615-1622.

van Doorn WG. 2001. Categories of petal senescence and abscission: a re-evaluation. *Annals of Botany* 87, 447-456.

van Doorn WG, Balk PA, van Houwelingen AM, Hoeberichts FA, Hall RD, Vorst O, van der Schoot C, van Wordragen MF. 2003. Gene expression during anthesis and senescence in *Iris* flowers. *Plant Molecular Biology* 53, 885-903.

van Doorn and Woltering. 2004a. Senescence and programmed cell death: substance or semantics? *Journal of Experimental Botany* 55, 2147-2153.

van Doorn WG. 2004. Is senescence due to sugar starvation? *Plant Phisiol*. 134, 35-42.

van Doorn WG, Woltering EJ. 2005. Many way to exit? Cell death categories in plants. *Trends in Plant Science* 10, 117-122.

van Doorn WG, Woltering EJ. 2008. Physiology and molecular biology of petal senescence. *Journal of Experimental Botany* 59, 453-480.

van Doorn WG. 2008. Is the onset of senescence in leaf cells of intact plants due to low or high sugar levels? *Journal of Experimental Botany* 59, 1963-1972.

van Staden J, Featonby-Smith BC, Mayak S, Spiegelstein H, Halevy AH. 1987. Cytokinins in cut carnation flowers. II. Relation between endogenous ethylene and citokinins levels in the petals. *Plant Growth Regulation* 5, 75-86.

Vercammen D, van de Cotte B, De Jaeger G, Eeckhout D, Casteels P, Vandepoele K, Vandenberghe I, Van Beeumen J, Inzé D, Van Breusegem F. 2004. Type II metacaspases Atmc4 and Atmc9 of Arabidopsis thaliana cleave substrate after arginine and lysine. *The Journal of Biological Chemistry* 279, 45329-45336.

Vercammen D, Belenghi B, van de Cotte B, Beunens T, Gavigan JA, De Rycke R, Brackenier A, Inzé D, Harris JL, Van Breusegem F. 2006. Serpin1 of *Arabidopsis thaliana* is a suicide inhibitor for metacaspase 9. *Journal Mol. Biol*. 364, 625-636.

Vercammen D, Declercq W, Vandenabeele P, Van Breusegem. 2007. Are metacaspases caspases? *The Journal of Cell Biology* 179, 375-380.

Vierstra RD. 2003. The ubiquitin/26S proteasome pathway, the complex last chapter in the life of many plant proteins. *Trends in plant Science* 8, 135-142.

Wagstaff C, Leverentz MK, Griffiths G, Thomas B, Chanasut U, Stead AD, Rogers HJ. 2002. Cysteine protease gene expression and proteolytic activity during senescence of *Alstroemeria* petals. *Journal of Experimental Botany* 53, 233-240.

Wagstaff C, Malcolm P, Rafiq A, Leverentz M, Griffiths G, Thomas B, Stead A, Rogers HJ. 2003. Programmed cell death (PCD) processes begin extremely early in Alstroemeria petal senescence. *New Phytologist* 160, 49-59.

Wang KLC, Li H, Ecker JR. Ethylene biosynthesis and signaling networks. *The Plant Cell* 14, S131-S151.

Watanabe N, Lam E. 2005. Two Arabidopsis metacaspase AtMCP1b and AtMCP2b are arginine/lysine-specific cysteine proteases and activate apoptosis-like cell death in yeast. The *Journal of Biological Chemestry* 280, 14691-14699.

Wijayanto T, Barker SJ, Wylie SJ, Gilchrist DG, Cowling WA. 2009. Significant reduction of fungal disease symptoms in transgenic lupin (*Lupinus angustifolius*) expressing the antiapoptotic baculovirus gene p35. *Plant Biotechnology Journal* 7, 778-790.

Wilkins HF, Dole JM. 1997. The physiology of flowering in *Lilium*. *Acta Hort.* 430, 183-188.

Wingler A, Roitsch T. 2008. Metabolic regulation of leaf senescence: interaction of sugar signalling with biotic and abiotic stress responses. *Plant Biology* 10, 50-62.

Wingler A, Masclaux-Daubresse C, Fischer AM. 2009. Sugars, senescence, and ageing in plants and heterotrophic organisms. *Journal of Experimental Botany* 60, 1063-1066.

Woltering EJ, van Doorn WG. 1988. Role of ethylene in senescence of petals: morphological and taxonomical relationships. *Journal of Experimental Botany* 39, 1605-1616.

Woltering EJ, van der Bent A, Hoeberichts FA. 2002. Do plant caspases exist? *Plant Physiol*. 130, 1764-1769.

Woo HR, Chung KM, Park JH, Oh SA, Ahn T, Hong SH, Jang SK, Nam HG. 2001. ORE9, an F-box protein that regulates leaf senescence in Arabidopsis. *Plant Cell* 13, 1779-1790.

Woodson WR, Lawton KA. 1988. Ethylene induced gene expression in carnation petals. *Plant Physiol*. 87, 490-503.

Xu Y, Hanson MR. 2000. Programmed Cell Death during Pollination-Induced Petal Senescence in Petunia. *Plant Physiology* 122, 1323-1333.

Xu X, Gookin T, Jiang CZ, Reid M. 2007. Gene associated with opening and senescence of Mirabilis jalapa flowers. *Journal of Experimental Botany* 58, 2193-2201.

Xu X, Jiang CZ, Donnelly L, Reid MS. 2007. Functional analysis of a ring domain ankyrin repeat protein that is highly expressed during flower senescence. *Journal of Experimental Botany* 58, 3623-3630.

Xue JQ, Li YH, Tan H, Yang F, Ma N, Gao JP. 2008. Expression of ethylene biosynthetic and receptor genes in rose floral tissues during ethylene-enhanced flower opening. *Journal of Experimental Botany* 59, 2161-2169.

Yakimova ET, Kapchina-Toteva VM, Woltering EJ. 2007. Signal transduction events in aluminium-induced cell death in tomato suspension cells. *Journal of Plant Physiology* 164, 702-708.

Yakimova ET, Yordaniva ZP, Slavov S, Kapchina-Toteva VM, Woltering EJ. 2009. Alternaria alternaria AT toxin induces programmed cell death in tobacco. *Journal of Phytopathology* 157, 592-601.

Yamada K, Shimada T, Nishimura M, Hara-Nishimura I. 2005. A VPE family supporting various vacuolar functions in plant. *Physiologia Plantarum* 123, 369-375.

Yamada T, Takatsu Y, Manabe T, Kasumi M, Marubashi W. 2003. Suppressive effect of trehalose on apoptotic cell death leading to petal senescence in ethylene-insensitive flowers of gladiolus. *Plant Science* 164, 213-221.

Yamada T, Ichimura K, van Doorn WG. 2006a. DNA degradation and nuclear degeneration during programmed cell death in petals of *Antirrhinum, Argyranthemum,* and *Petunia*. *Journal of Experimental Botany* 57, 3543-3552.

Yamada T, Takatsu Y, Kasumi M, Ichimura K, van Doorn WG. 2006b. Nuclear fragmentation and DNA degradation during programmed cell death in petals of morning glory (*Ipomoea nil*). *Planta* 224, 1279-1290.

Yamada T, Ichimura K, Kanekatsu M, van Doorn WG. 2007. Gene expression in opening and senescing petals of morning glory (*Ipomea nil*) flowers. *Plant Cell Rep*. 26, 823-835.

Yamada T, Ichimura K, Kanekatsu N, van Doorn WG. 2009. Homologs of genes associated with programmed cell death in animal cells are differentially expressed during senescence of *Ipomea nil* petals. *Plant and Cell Physiol*. 50, 610-625.

Yang TF, Gonzales-Carranza ZH, Maunders MJ, Roberts JA. 2008. Ethylene and the regulation of senescence processes in transgenic *Nicotiana sylvestris* plants. *Annals of Botany* 101, 301-310.

Yoshida S. 2003. Molecular regulation of leaf senescence. *Current Opinion in Plant Biology* 6, 79-84.

Zhang L, Xu Q, Xing D, Gao C, Xiong H. 2009. Real time detection of caspase 3-like protease activation in vivo using fluorescence resonance energy transfer during plant programmed cell death induced by ultraviolet C overexposure. *Plant Physiology* 150, 1773-1783.

Zhou Y, Wang C-Y, Ge H, Hoeberichts FA, Visser PB. 2005. Programmed cell death in relation to petal senescence in ornamental plants. *Journal of Integrative Plant Biology* 47, 641-650.